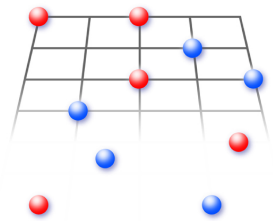


Quantum Monte Carlo simulations of ultracold fermions on optical lattices within dynamical mean-field theory

Nils Blümer and Elena Gorelik
Gutenberg University Mainz, Germany



Transregional Collaborative Research Centre SFB / TRR 49
Condensed matter systems with variable many-body interactions
Frankfurt / Kaiserslautern / Mainz

JOHANNES
GUTENBERG
UNIVERSITÄT
MAINZ

Outline

Introduction: SCES, cold atoms on lattices

Approaches for correlated lattice Fermi systems, multigrid HF-QMC

Paramagnetic Mott transitions in 3-flavor mixtures

[E. V. Gorelik and N. Blümer, Phys. Rev. A **80**, 051602(R) (2009)]

Néel transition of lattice fermions in a harmonic trap (RDMFT)

[N. Blümer and E. V. Gorelik, CPC, in press, doi:10.1016/j.cpc.2010.07.011]

[E. V. Gorelik, I. Titvinidze, W. Hofstetter, M. Snoek, N. Blümer, PRL **105**, 065301 (2010)]

Outline

Introduction: SCES, cold atoms on lattices

Approaches for correlated lattice Fermi systems, multigrid HF-QMC

Paramagnetic Mott transitions in 3-flavor mixtures

[E. V. Gorelik and N. Blümer, Phys. Rev. A **80**, 051602(R) (2009)]

Néel transition of lattice fermions in a harmonic trap (RDMFT)

[N. Blümer and E. V. Gorelik, CPC, in press, doi:10.1016/j.cpc.2010.07.011]

[E. V. Gorelik, I. Titvinidze, W. Hofstetter, M. Snoek, N. Blümer, PRL **105**, 065301 (2010)]

Effect of nonlocal correlations? Comparisons with direct QMC

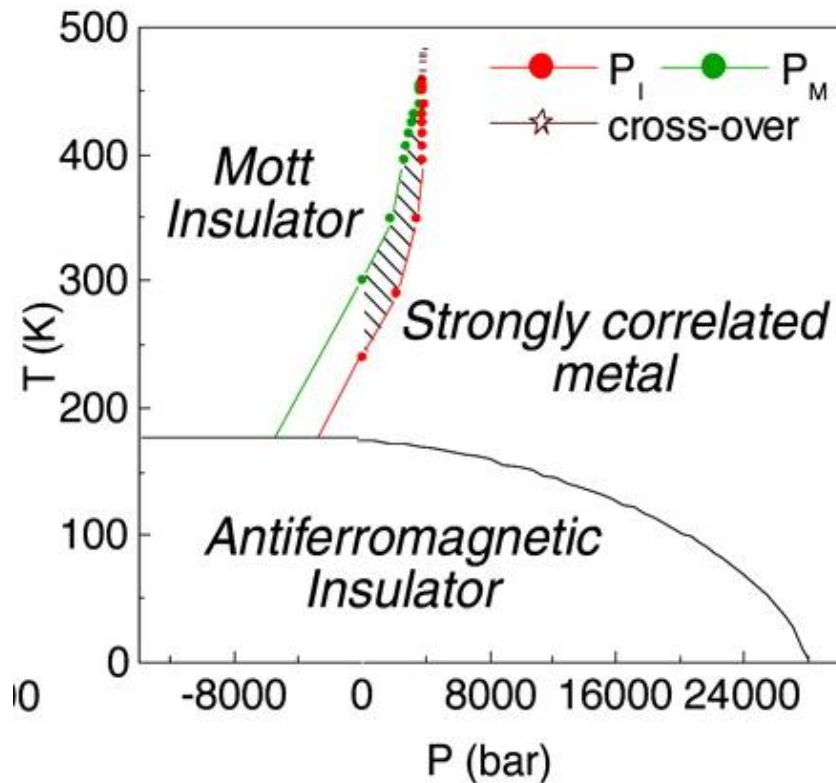
[ongoing collaboration with T. Paiva and R. Scalettar]

Summary and outlook

Introduction: Systems with strong electronic/fermionic correlations

Prototype example: V_2O_3 doped with Cr/Ti and/or under pressure

Phase diagram



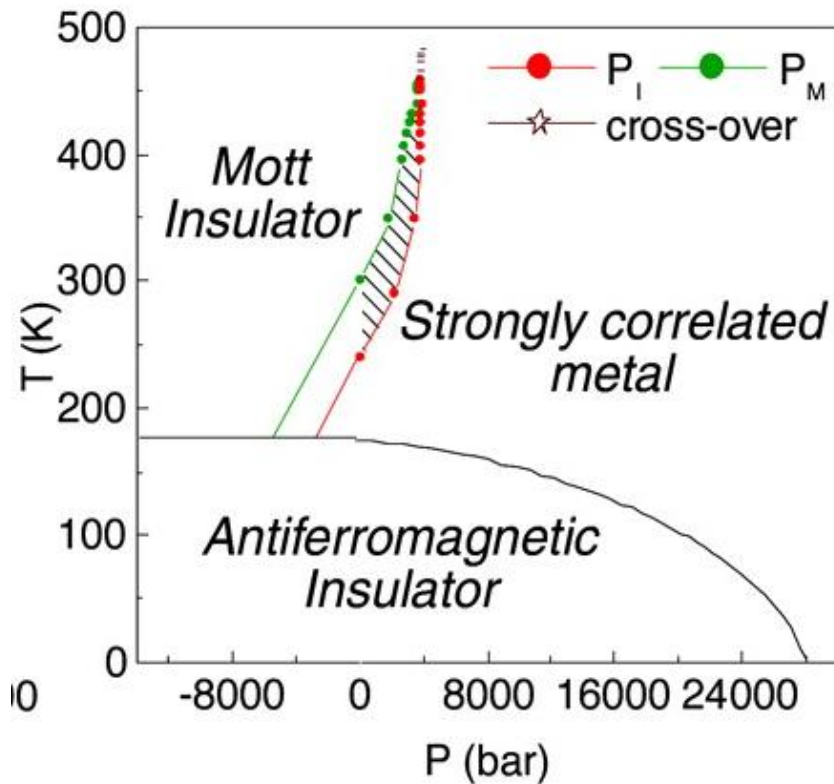
[Limelette et al., Science 302, 89 (2003)]

Introduction: Systems with strong electronic/fermionic correlations

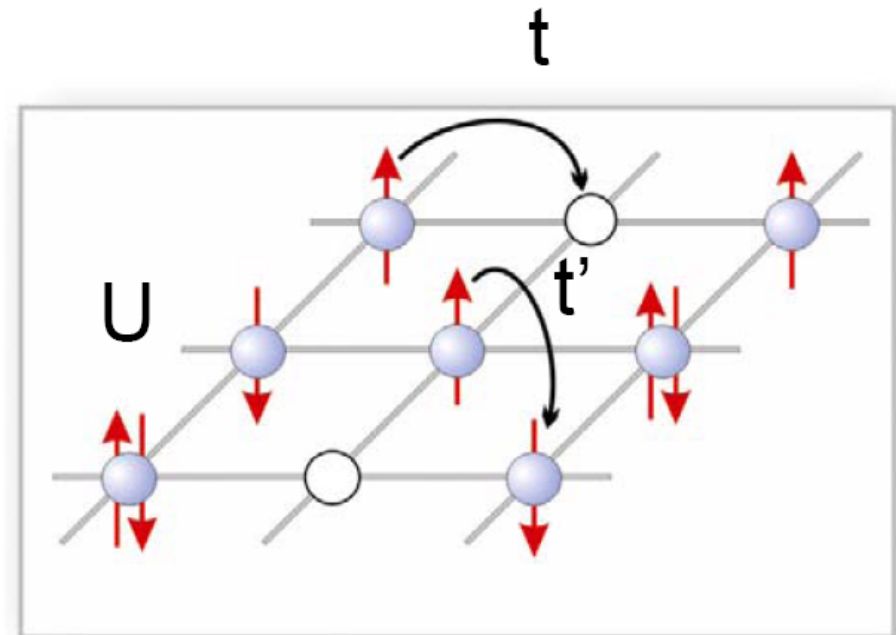
Prototype example: V_2O_3 doped with Cr/Ti and/or under pressure

Mott metal-insulator transition and AF:
generic physics of 1-band Hubbard model

Phase diagram



[Limelette et al., Science 302, 89 (2003)]

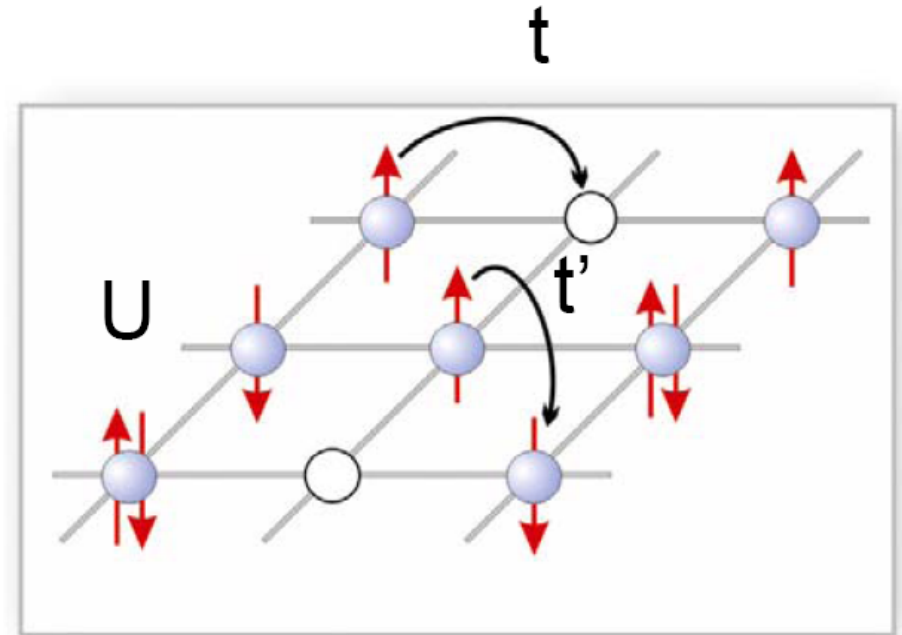
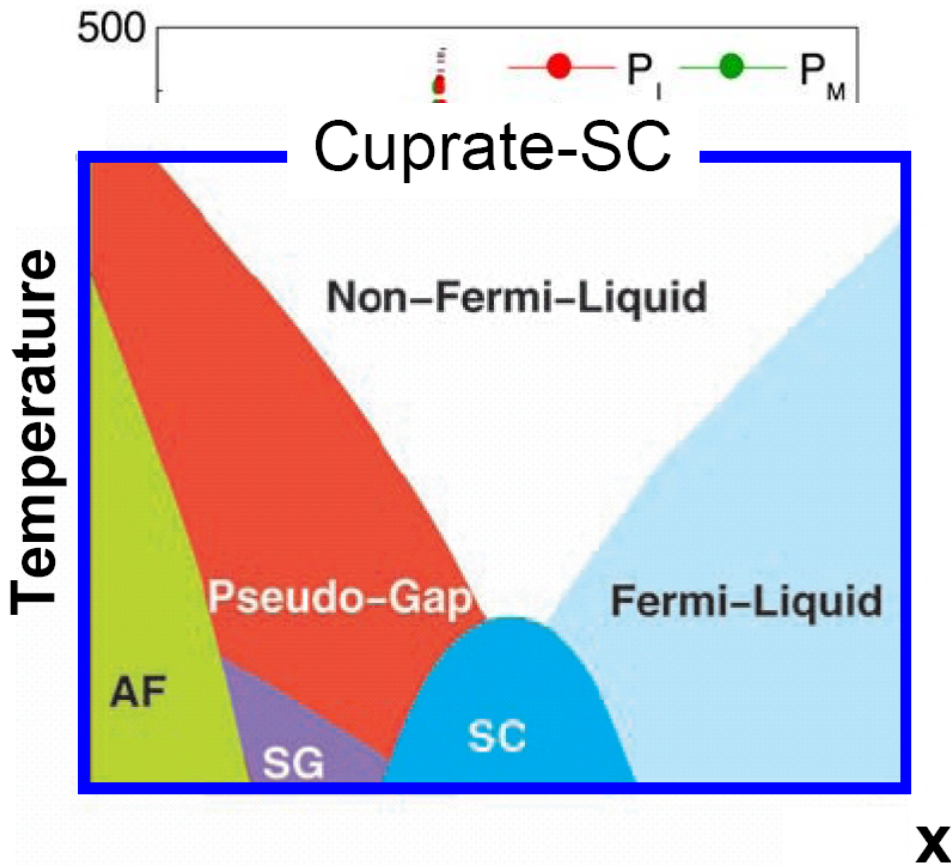


Introduction: Systems with strong electronic/fermionic correlations

Prototype example: V_2O_3 doped with Cr/Ti and/or under pressure

Mott metal-insulator transition and AF:
generic physics of 1-band Hubbard model

Phase diagram

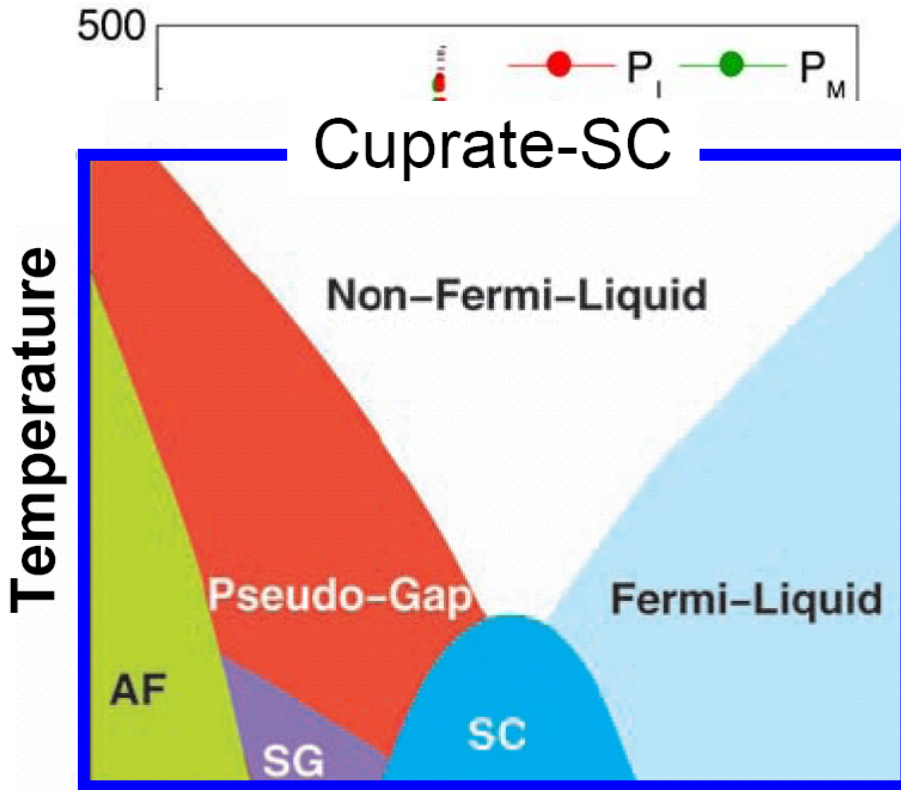


Are AF and Mott phases essential for superconductivity?

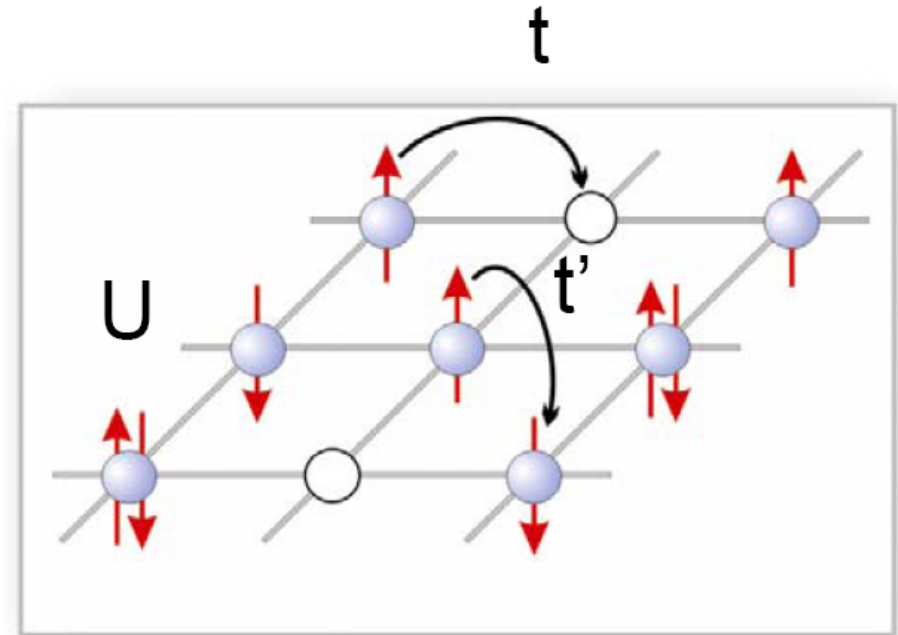
Introduction: Systems with strong electronic/fermionic correlations

Prototype example: V_2O_3 doped with Cr/Ti and/or under pressure

Phase diagram



Mott metal-insulator transition and AF:
generic physics of 1-band Hubbard model



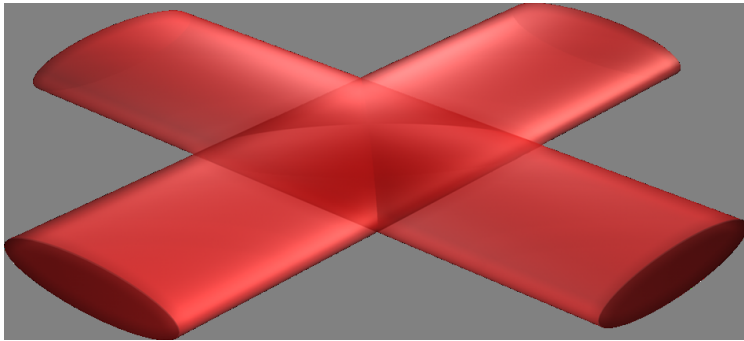
Are AF and Mott phases essential for superconductivity?

x Claim: cold atoms \rightsquigarrow quantum simulators

Correlated ultracold quantum gases on optical lattices: basics

Experimental systems: small dilute clouds of about 10^6 ultracold atoms \rightsquigarrow need trap

Optical dipole trap (2 beams)



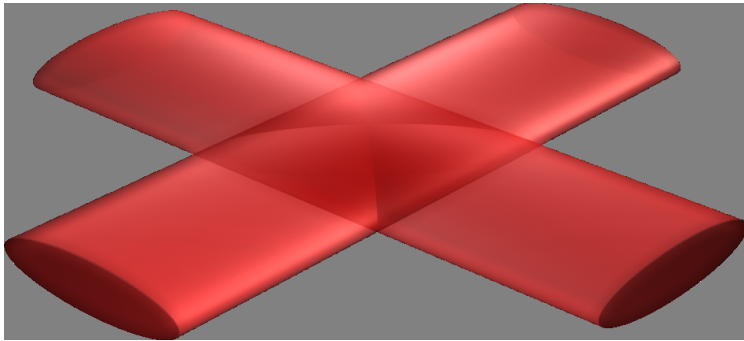
$$V_{\text{dipole}}(\mathbf{r}) = -\mathbf{d} \cdot \mathbf{E}(\mathbf{r}) \propto \alpha(\omega_L) |\mathbf{E}(\mathbf{r})|^2$$

time-averaged
intensity $|\mathbf{E}(\mathbf{r})|^2$

Correlated ultracold quantum gases on optical lattices: basics

Experimental systems: small dilute clouds of about 10^6 ultracold atoms \rightsquigarrow need trap

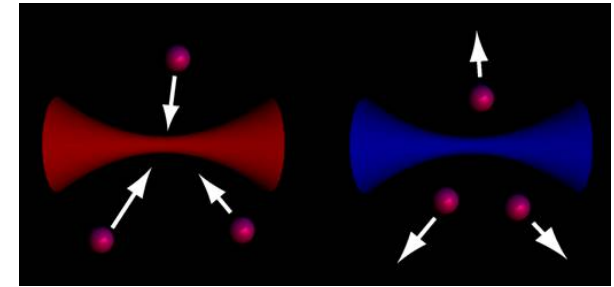
Optical dipole trap (2 beams)



$$V_{\text{dipole}}(\mathbf{r}) = -\mathbf{d} \cdot \mathbf{E}(\mathbf{r}) \propto \alpha(\omega_L) |\mathbf{E}(\mathbf{r})|^2$$

time-averaged
intensity $|\mathbf{E}(\mathbf{r})|^2$

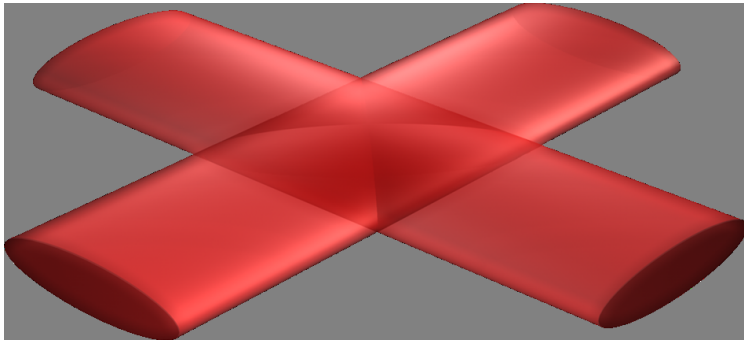
polarizability $\alpha(\omega_L)$
changes sign at ω_0



Correlated ultracold quantum gases on optical lattices: basics

Experimental systems: small dilute clouds of about 10^6 ultracold atoms \rightsquigarrow need trap

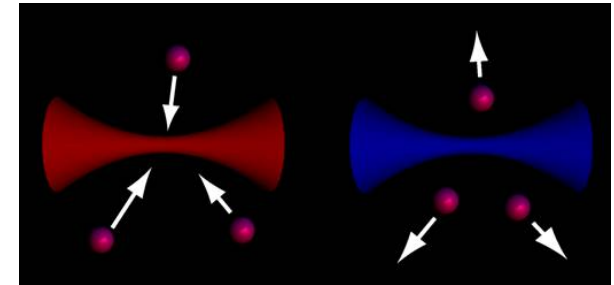
Optical dipole trap (2 beams)



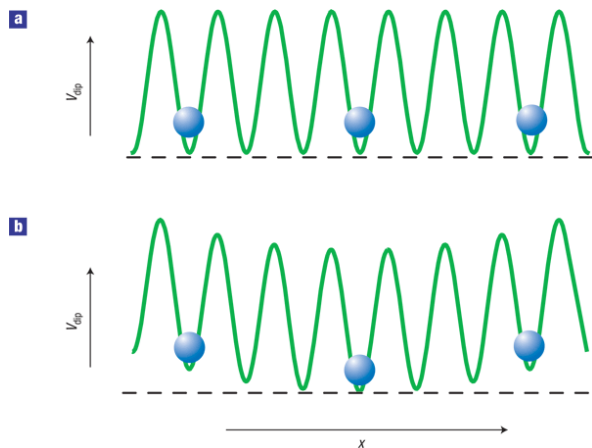
$$V_{\text{dipole}}(\mathbf{r}) = -\mathbf{d} \cdot \mathbf{E}(\mathbf{r}) \propto \alpha(\omega_L) |\mathbf{E}(\mathbf{r})|^2$$

time-averaged
intensity $|\mathbf{E}(\mathbf{r})|^2$

polarizability $\alpha(\omega_L)$
changes sign at ω_0



Standing wave (from coherent counterpropagating beams) \rightsquigarrow modulated potential

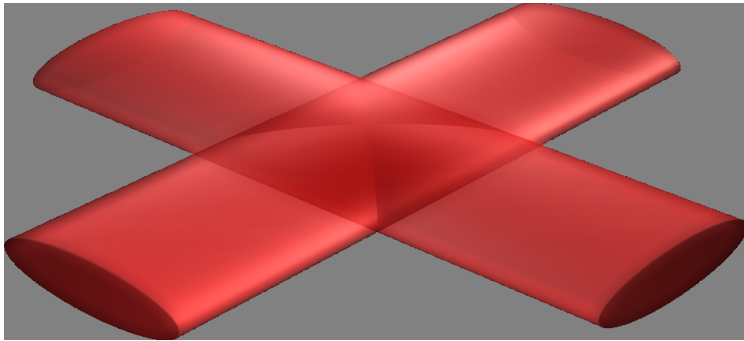


Beam profile: (anti) trapping

Correlated ultracold quantum gases on optical lattices: basics

Experimental systems: small dilute clouds of about 10^6 ultracold atoms \rightsquigarrow need trap

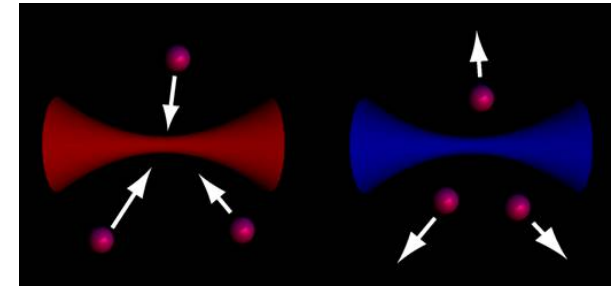
Optical dipole trap (2 beams)



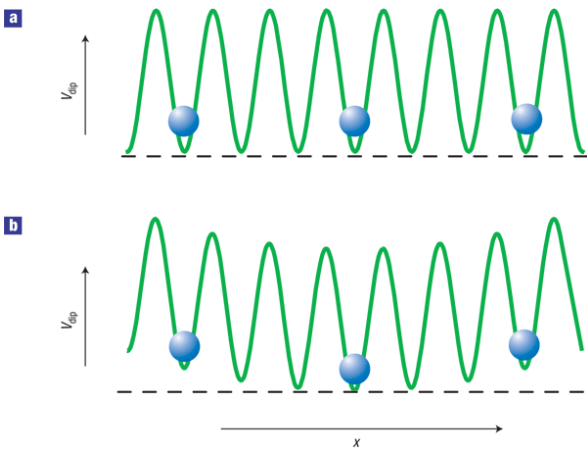
$$V_{\text{dipole}}(\mathbf{r}) = -\mathbf{d} \cdot \mathbf{E}(\mathbf{r}) \propto \alpha(\omega_L) |\mathbf{E}(\mathbf{r})|^2$$

time-averaged
intensity $|\mathbf{E}(\mathbf{r})|^2$

polarizability $\alpha(\omega_L)$
changes sign at ω_0



Standing wave (from coherent counterpropagating beams) \rightsquigarrow modulated potential



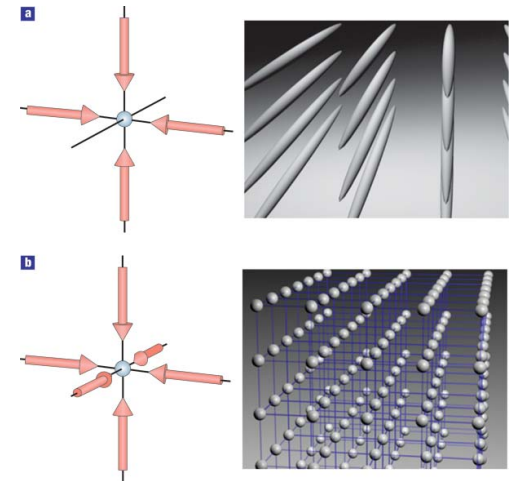
Beam profile: (anti) trapping

1 pair of lasers \rightsquigarrow pancakes

2 pairs of lasers \rightsquigarrow tubes

3 pairs of lasers \rightsquigarrow 3D lattice

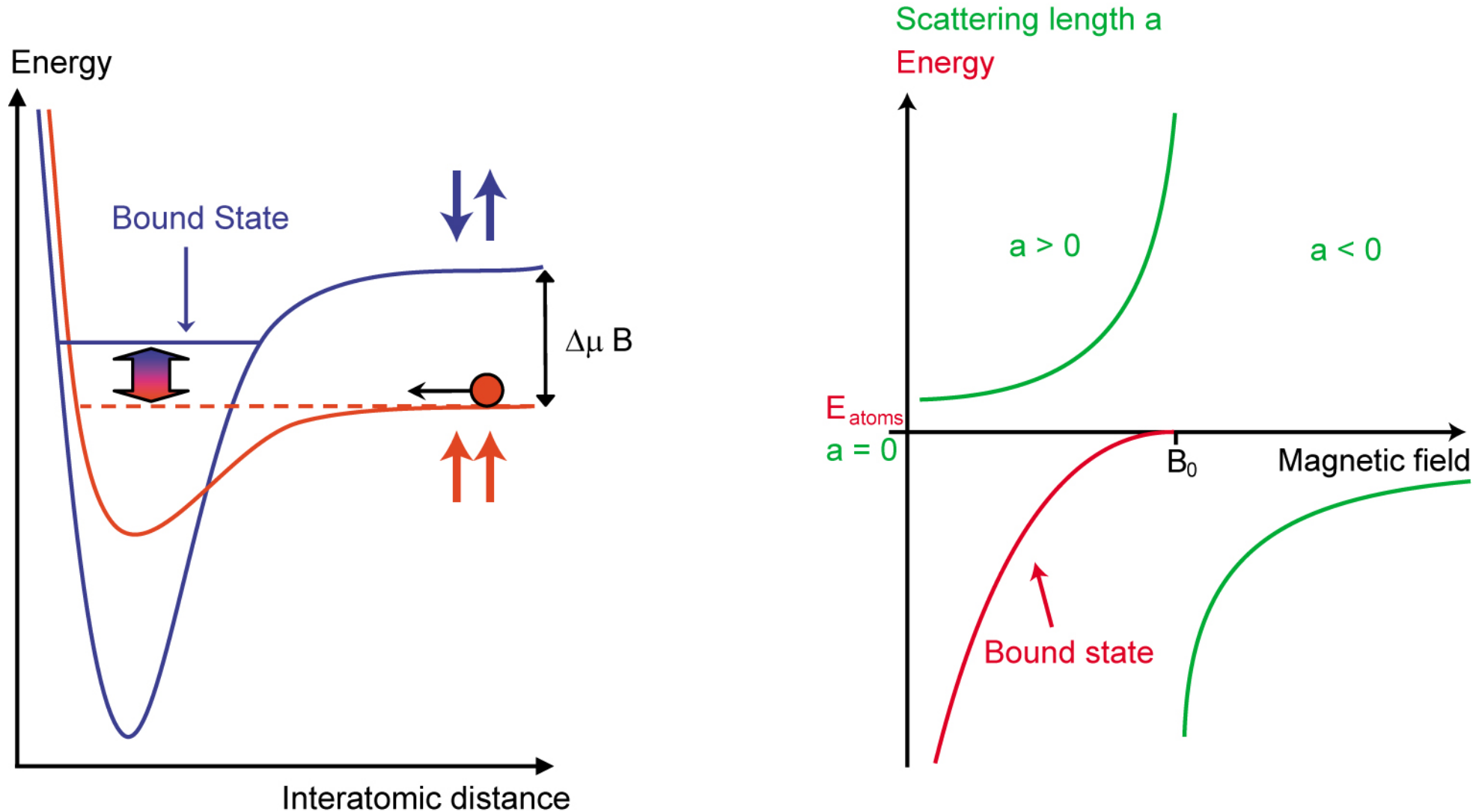
hopping t tunable by laser



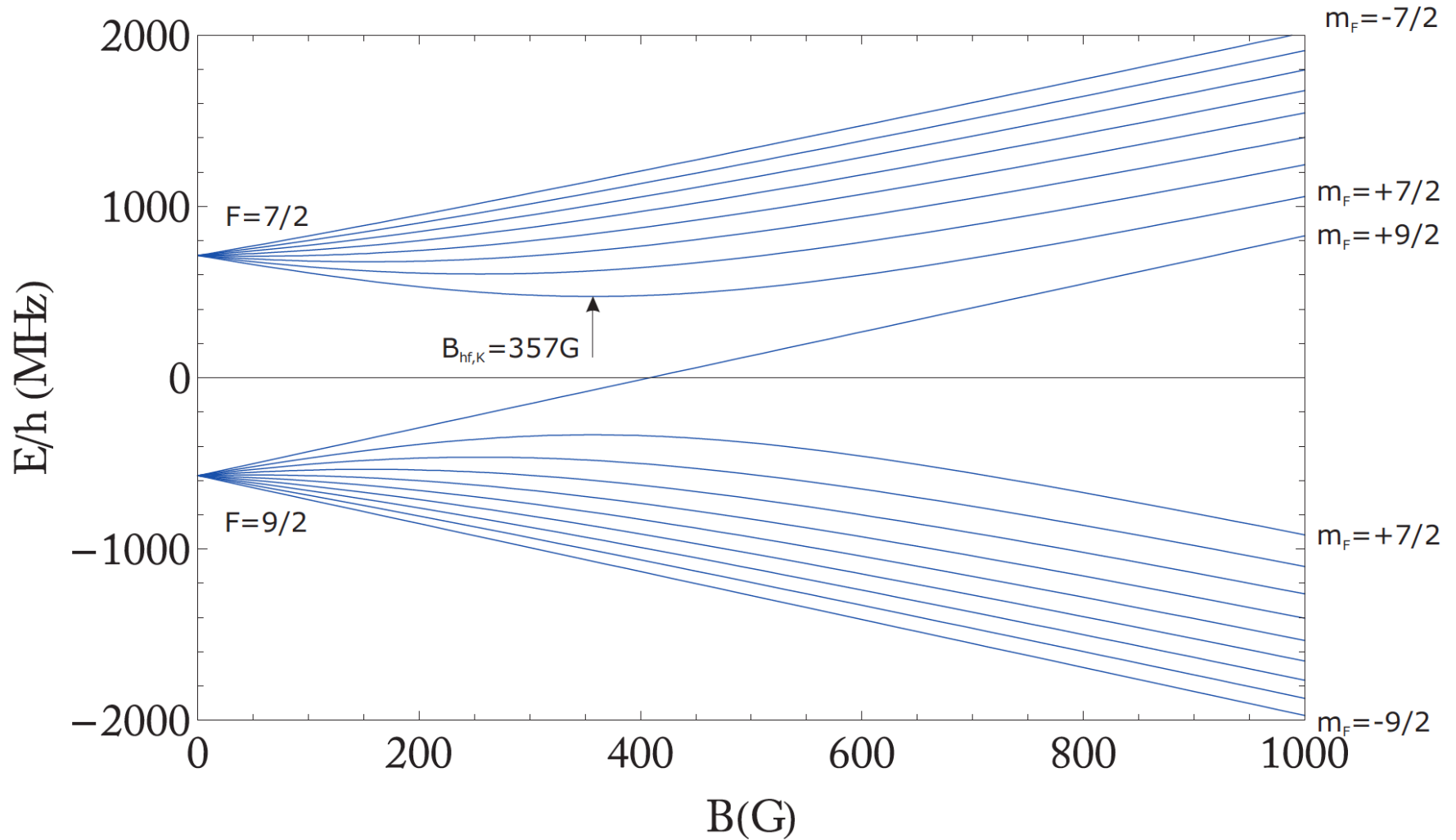
Interactions can be tuned via Feshbach resonances

Interactions can be tuned via Feshbach resonances (here in magnetic field \mathbf{B})

short ranged: characterized by scattering length a – both signs possible!



Large multiplets: reservoir of “flavors”



Hyperfine structure of the $^2S_{1/2}$ ground state of ^{40}K (Breit-Rabi formula)

[Tiecke, unpublished]

Main measurement technique: column density distribution, TOF

Send resonant parallel light through atomic cloud, detect by CCD

\rightsquigarrow shadows \propto column density (integrated over line of sight)

Use flavor sensitivity \rightsquigarrow partial densities, “magnetization” profiles

In situ atomic (site) resolution only for 2-dimensional lattice systems:

large-aperture lens [Kuhr, Greiner], electron microscopy [Ott]

Main measurement technique: column density distribution, TOF

Send resonant parallel light through atomic cloud, detect by CCD

↪ shadows \propto column density (integrated over line of sight)

Use flavor sensitivity ↪ partial densities, “magnetization” profiles

In situ atomic (site) resolution only for 2-dimensional lattice systems:

large-aperture lens [Kuhr, Greiner], electron microscopy [Ott]

Main application: use time of flight (TOF) for measuring in \mathbf{k} space
switch off trap (and strong interactions), let atoms fall freely

$$\text{assume } \hbar \mathbf{k}_j = m \mathbf{v}_j(0) \quad ; \quad \mathbf{r}_j(t) = \mathbf{r}_j(0) + \mathbf{v}_j(0)t - \frac{1}{2}g\hat{\mathbf{e}}_z t^2$$

Main measurement technique: column density distribution, TOF

Send resonant parallel light through atomic cloud, detect by CCD

→ shadows \propto column density (integrated over line of sight)

Use flavor sensitivity → partial densities, “magnetization” profiles

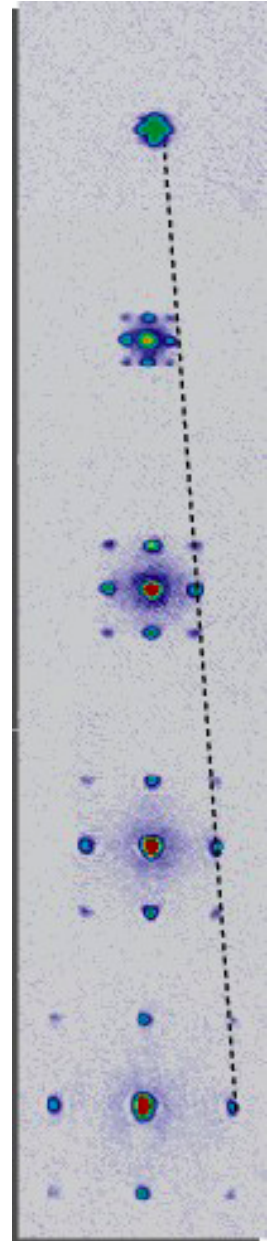
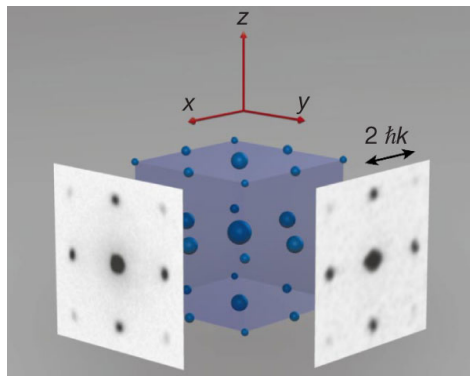
In situ atomic (site) resolution only for 2-dimensional lattice systems:

large-aperture lens [Kuhr, Greiner], electron microscopy [Ott]

Main application: use time of flight (TOF) for measuring in \mathbf{k} space
switch off trap (and strong interactions), let atoms fall freely

$$\text{assume } \hbar \mathbf{k}_i = m \mathbf{v}_i(0) \quad ; \quad \mathbf{r}_i(t) = \mathbf{r}_i(0) + \mathbf{v}_i(0)t - \frac{1}{2}g\hat{\mathbf{e}}_z t^2$$

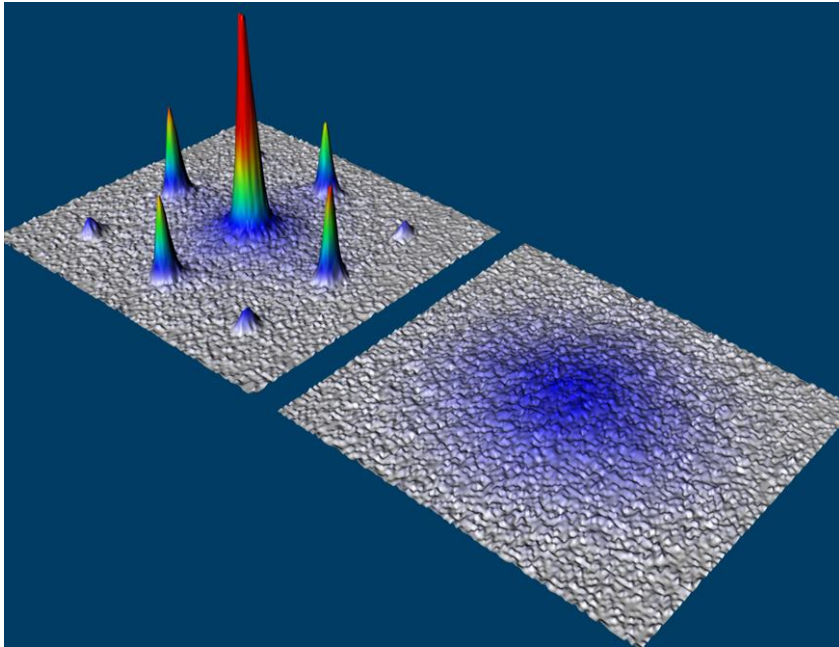
$$\rightsquigarrow (\mathbf{r}_i(T) + \frac{1}{2}g\hat{\mathbf{e}}_z T^2) \frac{m}{\hbar T} \approx \mathbf{k}_i \quad \text{for } T\sqrt{\langle \mathbf{v}^2 \rangle} \gg \sqrt{\langle r^2 \rangle}$$



Correlated ultracold quantum gases on optical lattices: bosons

First evidence of strongly correlations in cold atoms: bosonic Mott transition

Time-of-flight image – \mathbf{k} distribution

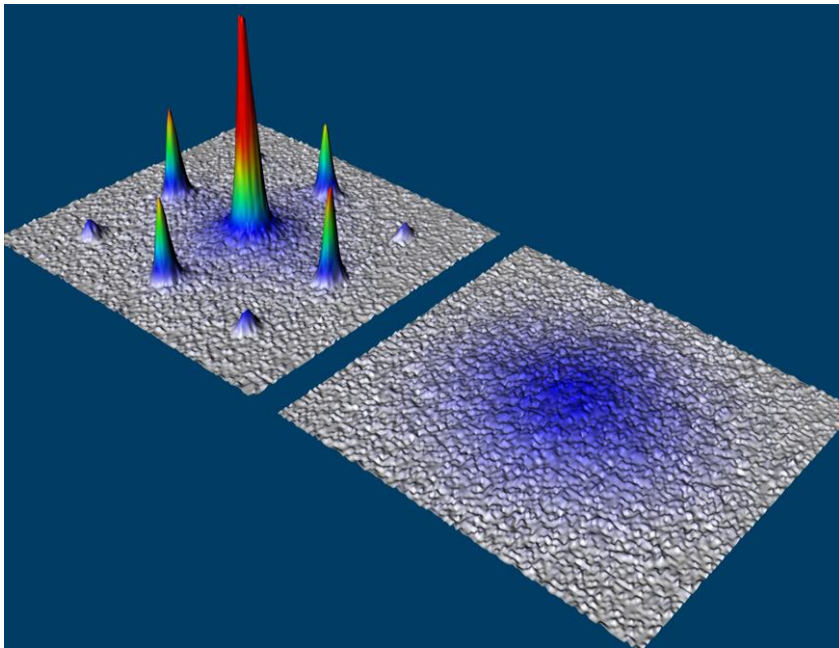


[Bloch group, 2002]

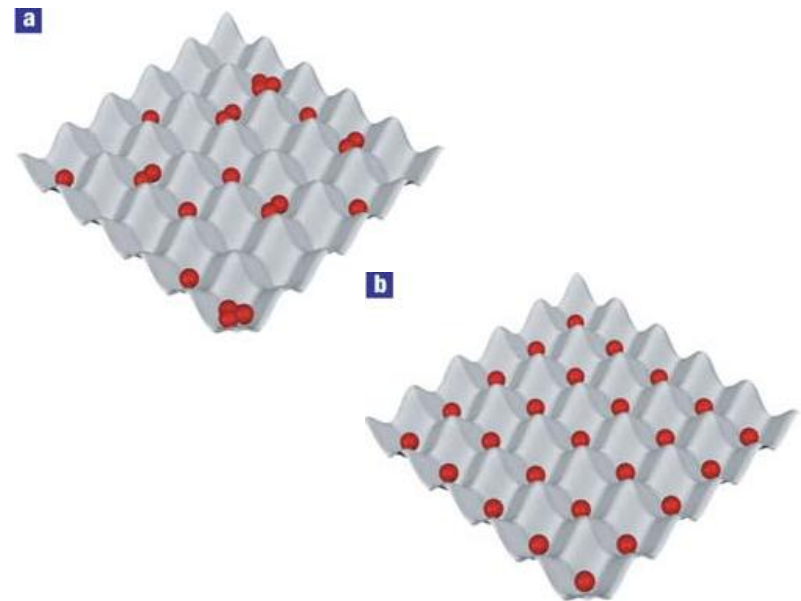
Correlated ultracold quantum gases on optical lattices: bosons

First evidence of strongly correlations in cold atoms: bosonic Mott transition

Time-of-flight image – \mathbf{k} distribution



corresponding real-space picture



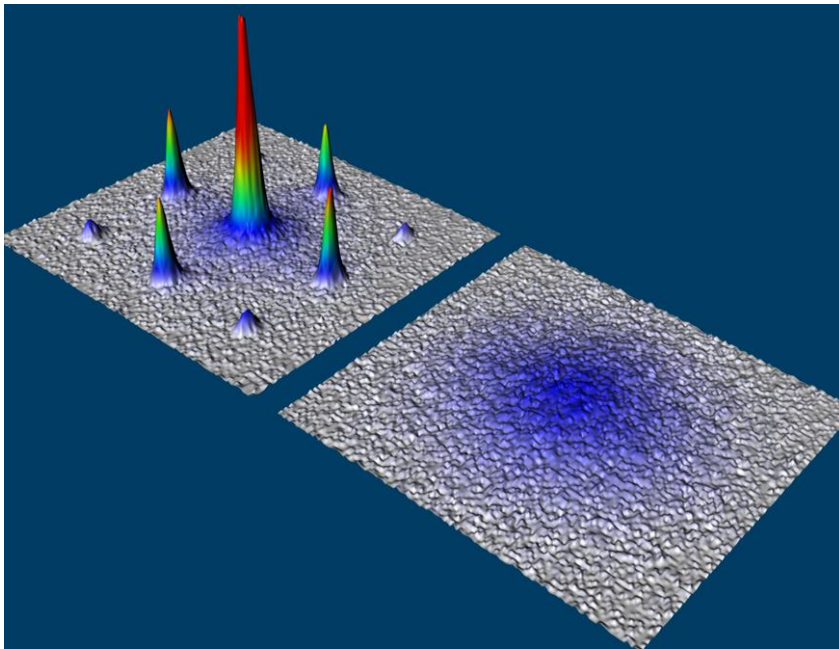
[Bloch group, 2002]

Superfluidity destroyed by density constraint at large U

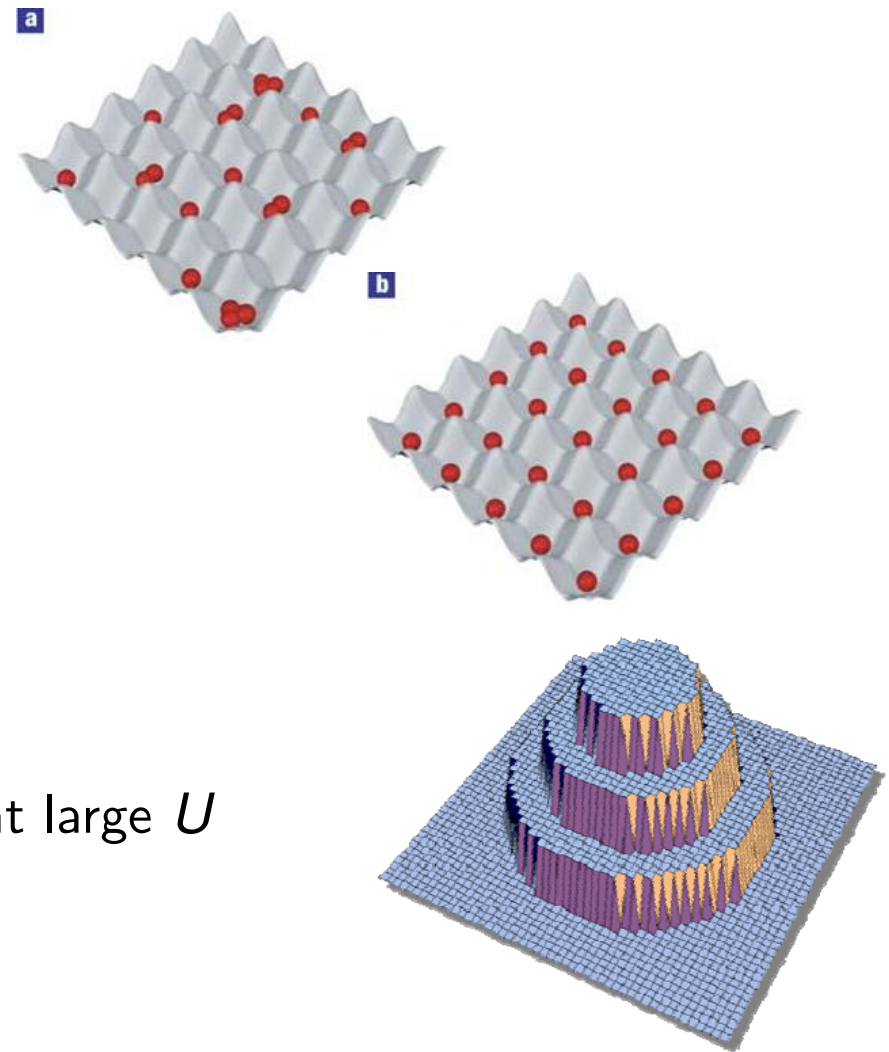
Correlated ultracold quantum gases on optical lattices: bosons

First evidence of strongly correlations in cold atoms: bosonic Mott transition

Time-of-flight image – \mathbf{k} distribution



corresponding real-space picture

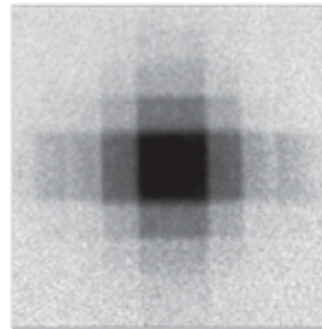
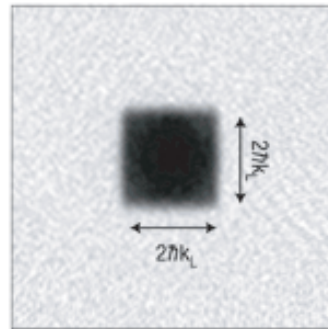
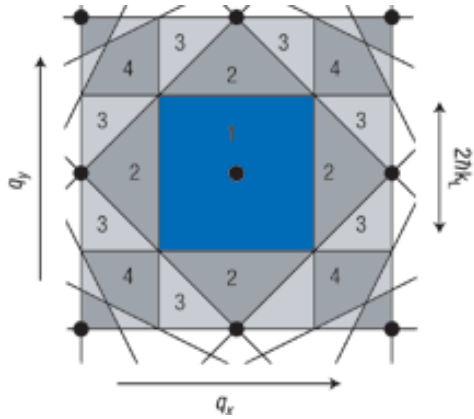


[Bloch group, 2002]

Superfluidity destroyed by density constraint at large U

Trapping potential \rightsquigarrow wedding cake structure

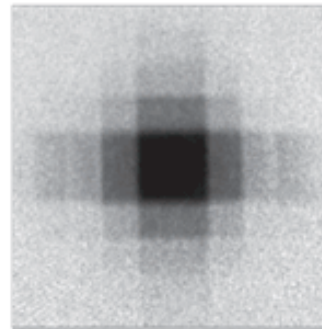
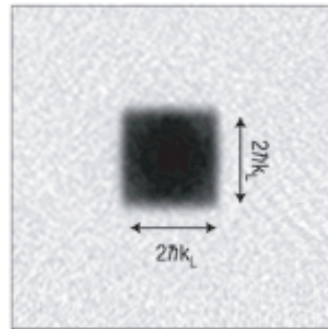
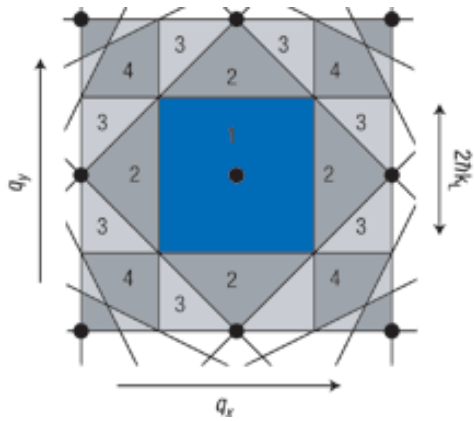
Correlated ultracold quantum gases on optical lattices: fermions



1 species: band insulator for filled 1st Brillouin zone:

[Köhl et al, PRL (2005)]

Correlated ultracold quantum gases on optical lattices: fermions



1 species: band insulator for filled 1st Brillouin zone:

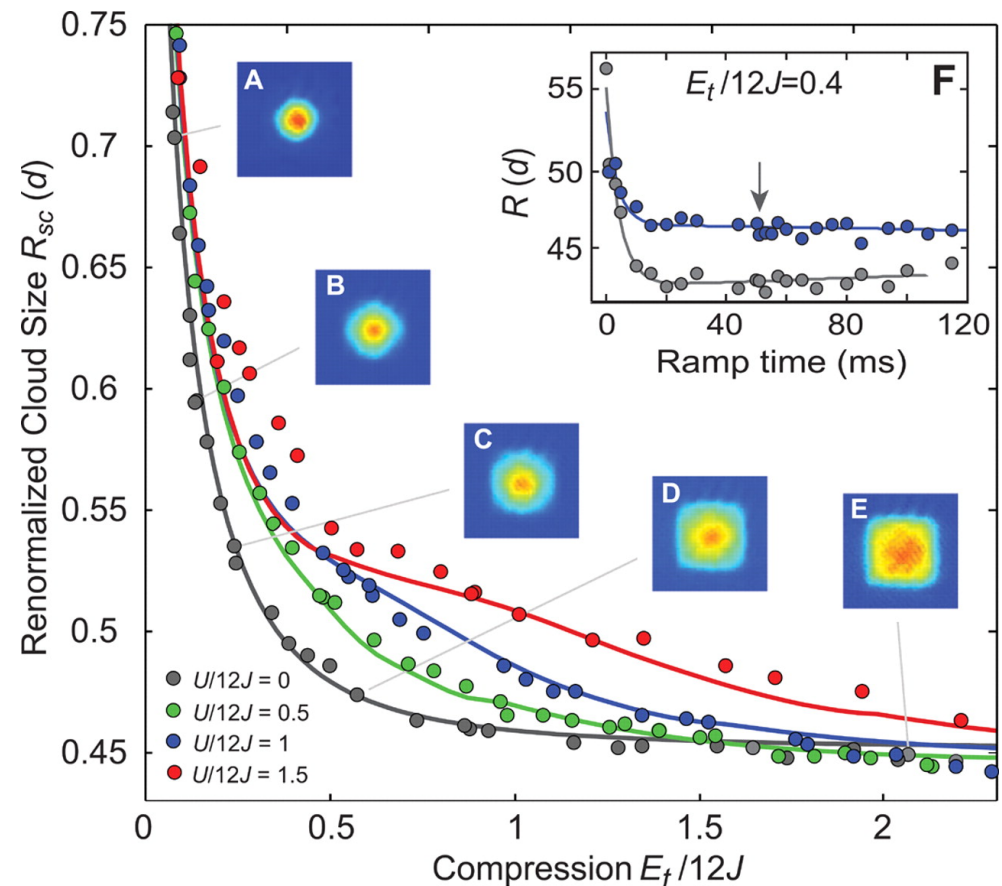
[Köhl et al, PRL (2005)]

Recent breakthrough: paramagnetic Mott transition in 2-flavor mixtures

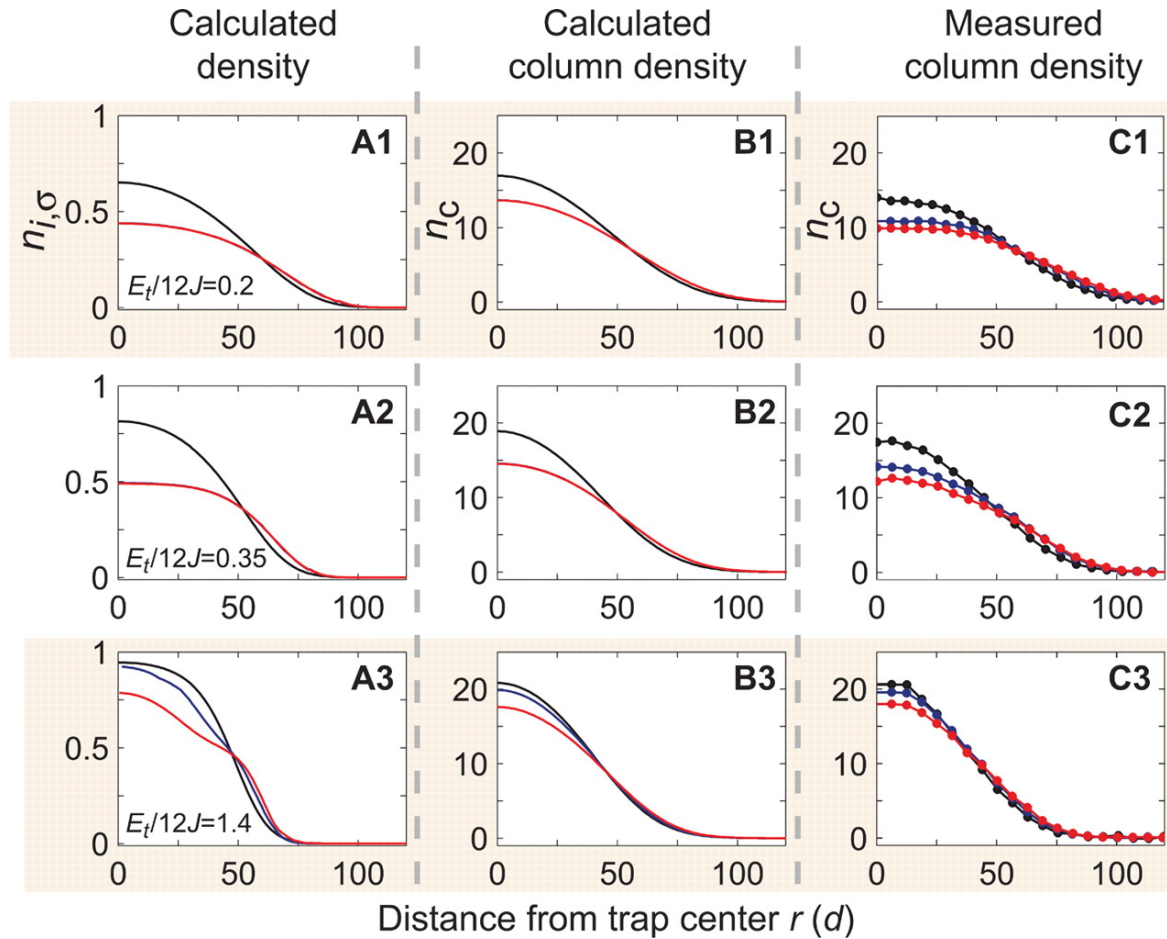
Detection method: measure cloud diameter vs. trap strength

Simulations (here DMFT+NRG) essential for interpretation of data!

[Schneider et al, Science 322, 1520 (2008)]

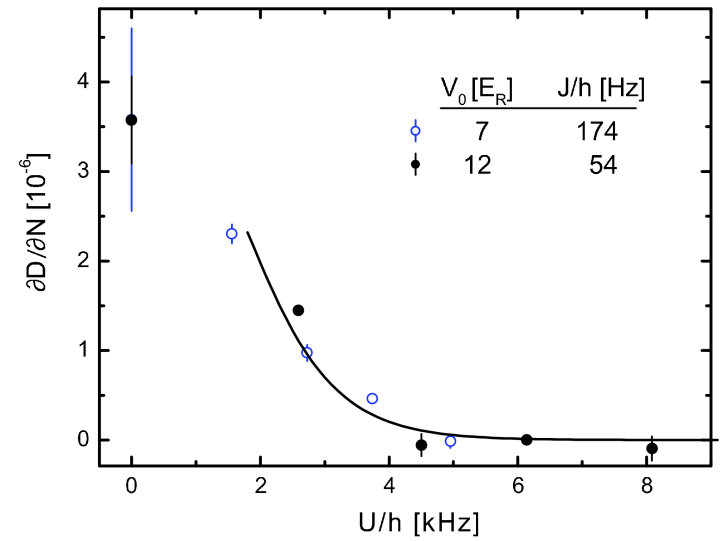
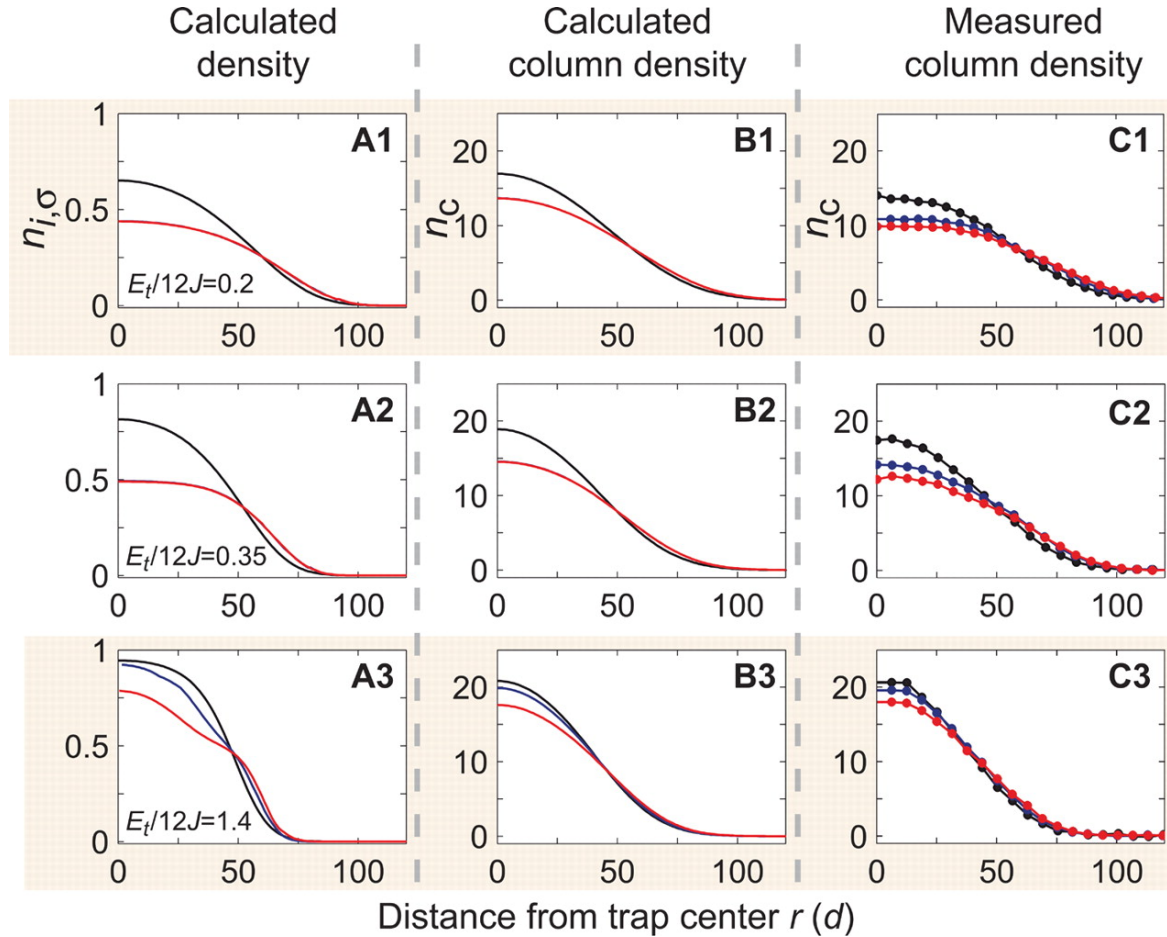


Further MIT observables: **column density**, fraction of atoms with **double occupations**



[Schneider et al, Science **322**, 1520 (2008)]

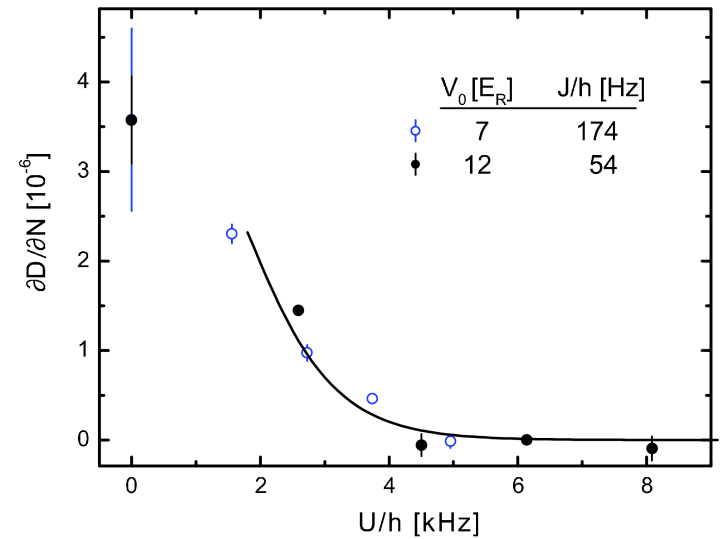
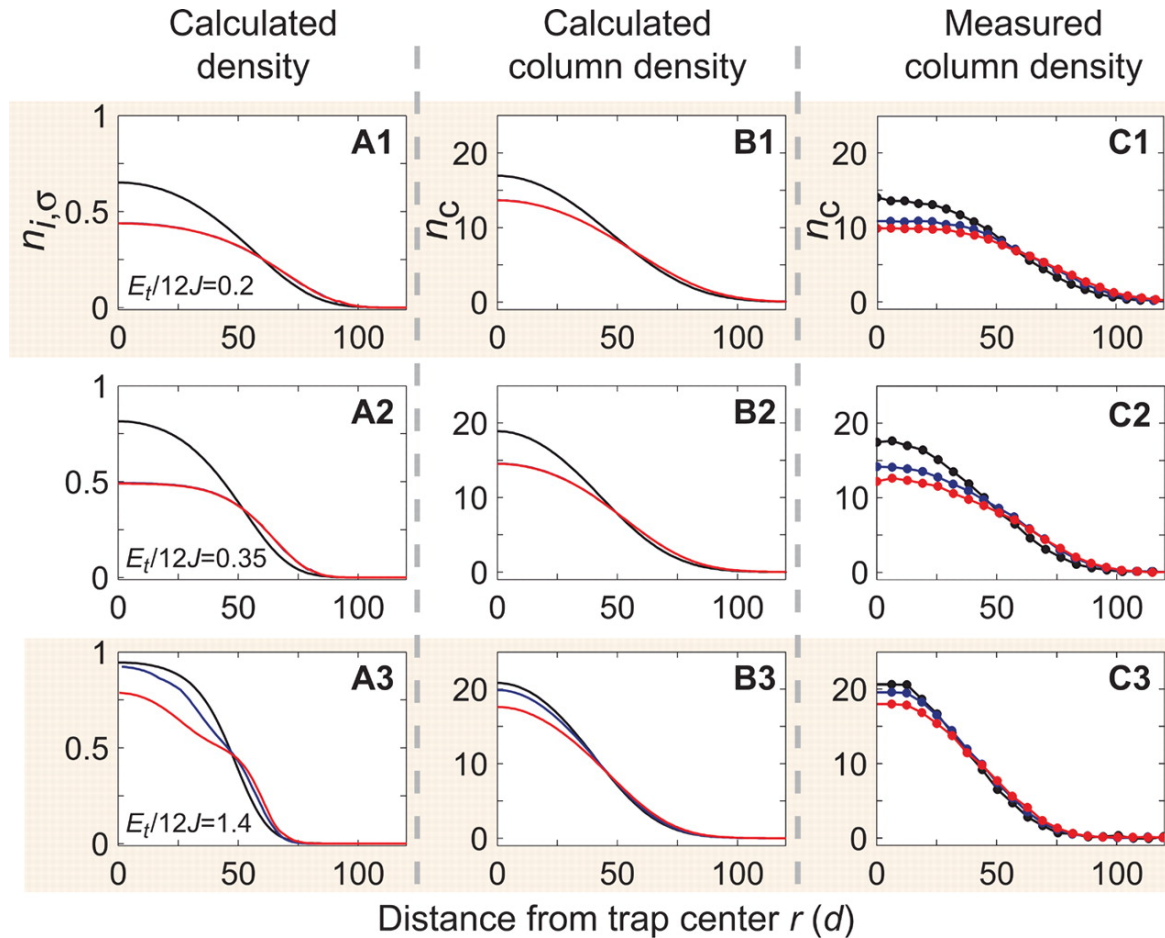
Further MIT observables: **column density**, fraction of atoms with **double occupations**



[Jördens et al., Nature (2008)]

[Schneider et al, Science **322**, 1520 (2008)]

Further MIT observables: **column density**, fraction of atoms with **double occupations**



[Jördens et al., Nature (2008)]

[Schneider et al, Science **322**, 1520 (2008)]

Many other phenomena seen: **superconductivity**, **vortices**, **BEC-BCS crossover**, ...

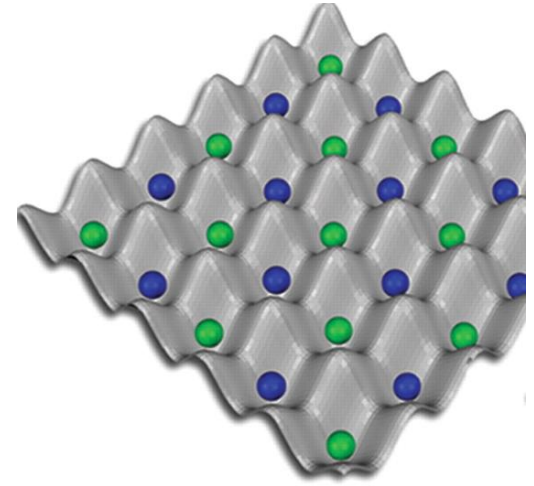
Next grand challenges:

Antiferromagnetism (staggered order) in ultracold fermions

Problems:

- (i) difficult to reach sufficiently low temperatures/entropies
- (ii) detection of order parameter is not straightforward

Realization of quantum magnetism: prerequisite for quantum simulation!

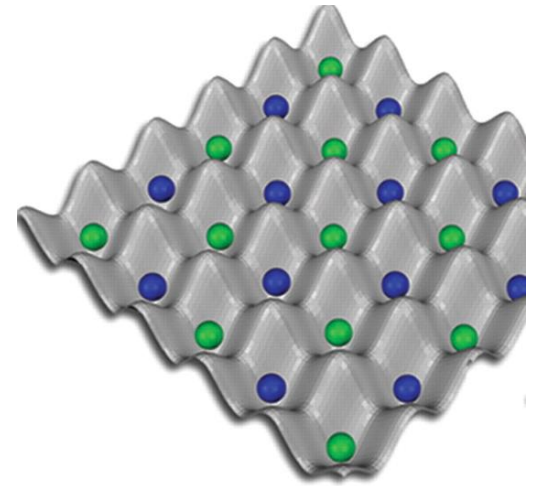


Next grand challenges:

Antiferromagnetism (staggered order) in ultracold fermions

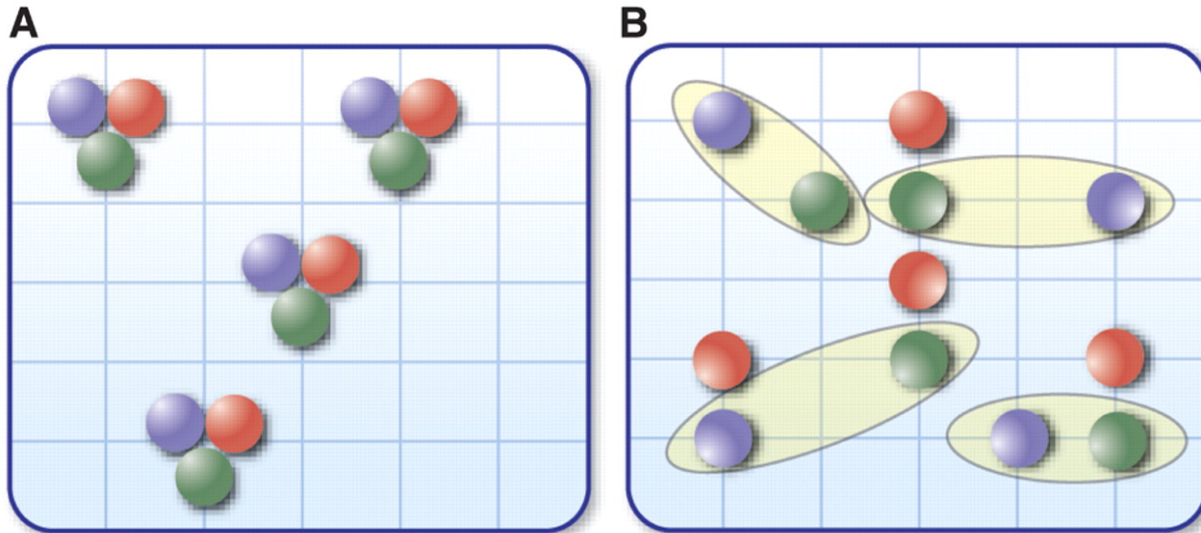
Problems:

- (i) difficult to reach sufficiently low temperatures/entropies
- (ii) detection of order parameter is not straightforward



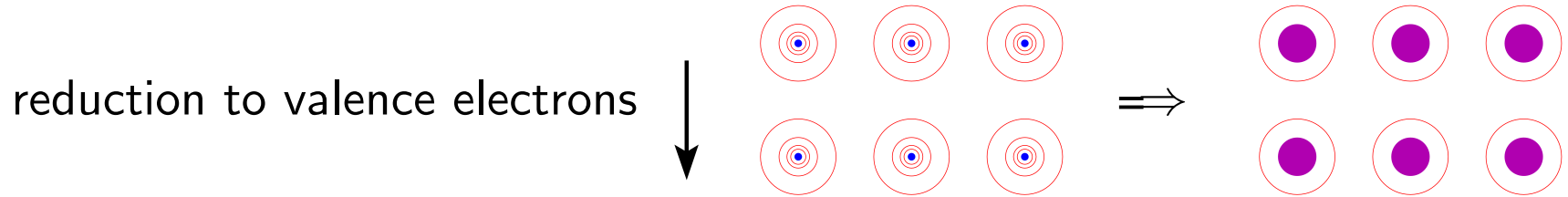
Realization of quantum magnetism: prerequisite for quantum simulation!

Multiflavor phenomena, e.g. trions versus color superconductivity



Approaches for correlated lattice Fermi systems

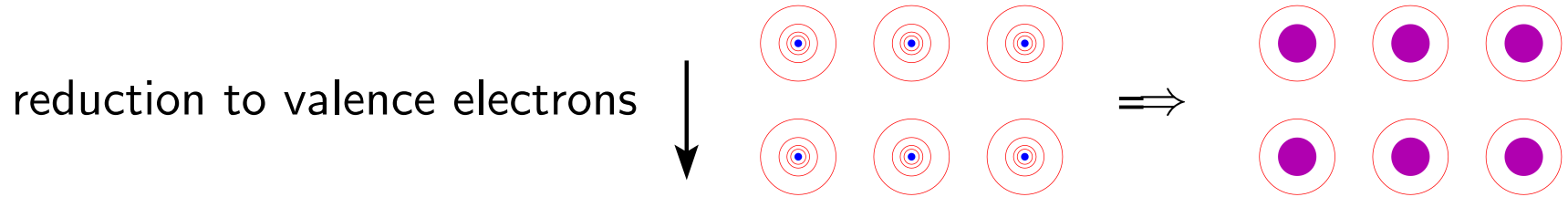
$$H = \sum_{i=1}^{N_e} \frac{\mathbf{p}_i^2}{2m} + \sum_i V(\mathbf{r}_i) + \sum_{i < j} \frac{e^2}{|\mathbf{r}_i - \mathbf{r}_j|}$$



$$H = \sum_{i=1}^{N_v} \frac{\mathbf{p}_i^2}{2m} + \sum_{i=1}^{N_v} V^{\text{ion}}(\mathbf{r}_i) + \sum_{i=1}^{N_v-1} \sum_{j=i+1}^{N_v} V^{ee}(\mathbf{r}_i, \mathbf{r}_j)$$

Approaches for correlated lattice Fermi systems

$$H = \sum_{i=1}^{N_e} \frac{\mathbf{p}_i^2}{2m} + \sum_i V(\mathbf{r}_i) + \sum_{i < j} \frac{e^2}{|\mathbf{r}_i - \mathbf{r}_j|}$$



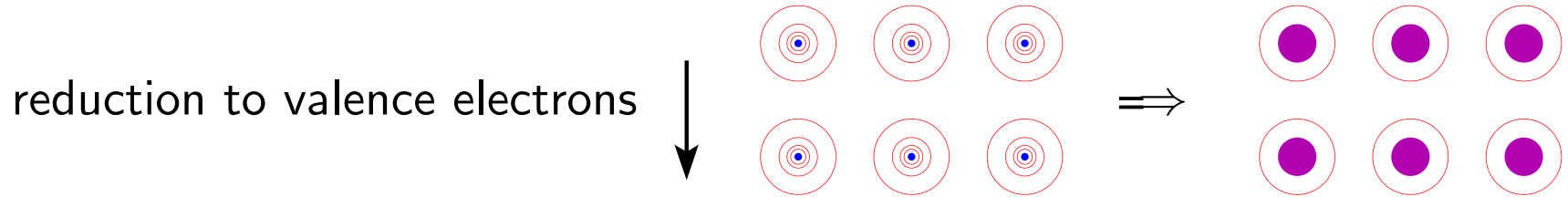
$$H = \sum_{i=1}^{N_v} \frac{\mathbf{p}_i^2}{2m} + \sum_{i=1}^{N_v} V^{\text{ion}}(\mathbf{r}_i) + \sum_{i=1}^{N_v-1} \sum_{j=i+1}^{N_v} V^{ee}(\mathbf{r}_i, \mathbf{r}_j)$$



$$\hat{H} = \sum_{i\nu j\sigma} t_{ij}^{\nu} \hat{c}_{i\nu\sigma}^{\dagger} \hat{c}_{j\nu\sigma} + \frac{1}{2} \sum_{\nu\nu'\mu\mu'} \sum_{ijmn} \sum_{\sigma\sigma'} v_{ijmn}^{\nu\nu'\mu\mu'} \hat{c}_{i\nu\sigma}^{\dagger} \hat{c}_{j\nu'\sigma'}^{\dagger} \hat{c}_{n\mu'\sigma'} \hat{c}_{m\mu\sigma}$$

Approaches for correlated lattice Fermi systems

$$H = \sum_{i=1}^{N_e} \frac{\mathbf{p}_i^2}{2m} + \sum_i V(\mathbf{r}_i) + \sum_{i < j} \frac{e^2}{|\mathbf{r}_i - \mathbf{r}_j|}$$



$$H = \sum_{i=1}^{N_v} \frac{\mathbf{p}_i^2}{2m} + \sum_{i=1}^{N_v} V^{\text{ion}}(\mathbf{r}_i) + \sum_{i=1}^{N_v-1} \sum_{j=i+1}^{N_v} V^{ee}(\mathbf{r}_i, \mathbf{r}_j)$$

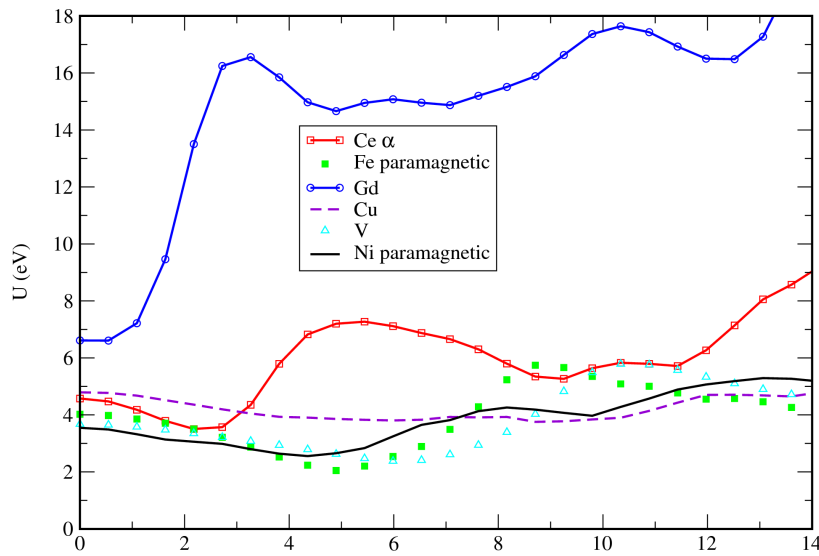


$$\hat{H} = \sum_{i\nu j\sigma} t_{ij}^{\nu} \hat{c}_{i\nu\sigma}^{\dagger} \hat{c}_{j\nu\sigma} + \frac{1}{2} \sum_{\nu\nu'\mu\mu'} \sum_{ijmn} \sum_{\sigma\sigma'} \mathcal{V}_{ijmn}^{\nu\nu'\mu\mu'} \hat{c}_{i\nu\sigma}^{\dagger} \hat{c}_{j\nu'\sigma'}^{\dagger} \hat{c}_{n\mu'\sigma'} \hat{c}_{m\mu\sigma}$$

Hubbard model

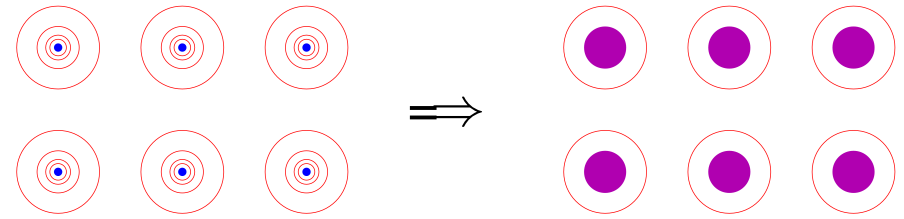
$$\hat{H} = \sum_{(i,j),\sigma} t_{ij} (\hat{c}_{i\sigma}^{\dagger} \hat{c}_{j\sigma} + \text{h.c.}) + U \sum_i \hat{n}_{i\uparrow} \hat{n}_{i\downarrow}$$

related lattice Fermi systems



$$+ \sum_i V(\mathbf{r}_i) + \sum_{i < j} \frac{e^2}{|\mathbf{r}_i - \mathbf{r}_j|}$$

ions



[Aryasetiawan et al., PRB 2006]

$$H = \sum_{i=1}^{N_V} \frac{\mathbf{p}_i^2}{2m} + \sum_{i=1}^{N_V} V^{\text{ion}}(\mathbf{r}_i) + \sum_{i=1}^{N_V-1} \sum_{j=i+1}^{N_V} V^{ee}(\mathbf{r}_i, \mathbf{r}_j) [\omega]$$

occupation number formalism

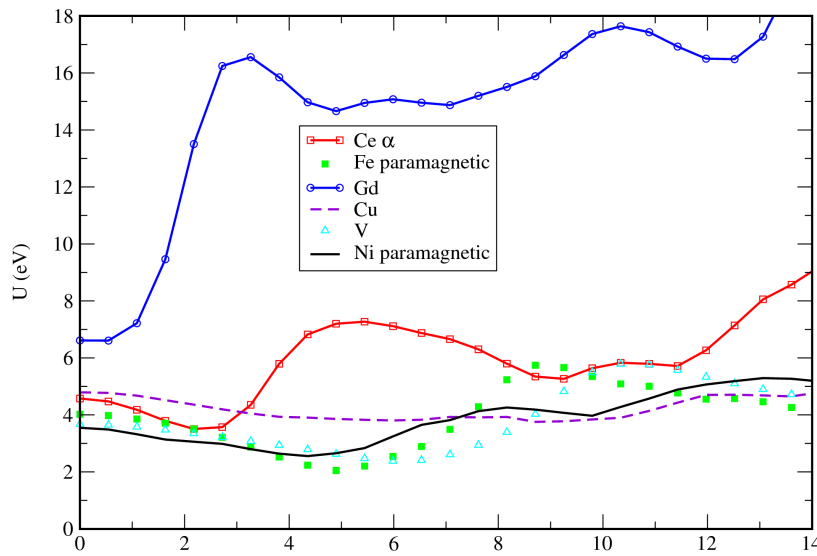
Wannier orbitals

$$\hat{H} = \sum_{i\nu j\sigma} t_{ij}^\nu \hat{c}_{i\nu\sigma}^\dagger \hat{c}_{j\nu\sigma} + \frac{1}{2} \sum_{\nu\nu'\mu\mu'} \sum_{ijmn} v_{ijmn}^{\nu\nu'\mu\mu'} \hat{c}_{i\nu\sigma}^\dagger \hat{c}_{j\nu'\sigma'}^\dagger \hat{c}_{n\mu'\sigma'} \hat{c}_{m\mu\sigma}$$

Hubbard model

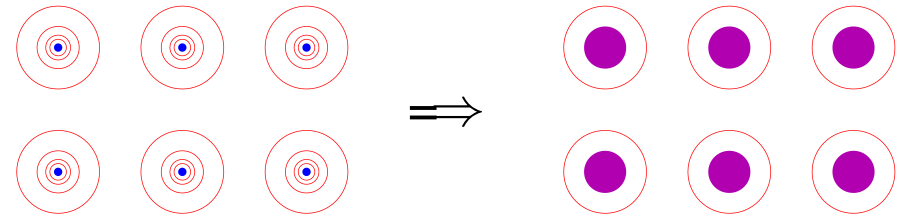
$$\hat{H} = \sum_{(i,j),\sigma} t_{ij} (\hat{c}_{i\sigma}^\dagger \hat{c}_{j\sigma} + \text{h.c.}) + U \sum_i \hat{n}_{i\uparrow} \hat{n}_{i\downarrow}$$

related lattice Fermi systems



$$+ \sum_i V(\mathbf{r}_i) + \sum_{i < j} \frac{e^2}{|\mathbf{r}_i - \mathbf{r}_j|}$$

ions



[Aryasetiawan et al., PRB 2006]

$$H = \sum_{i=1}^{N_V} \frac{\mathbf{p}_i^2}{2m} + \sum_{i=1}^{N_V} V^{\text{ion}}(\mathbf{r}_i) + \sum_{i=1}^{N_V-1} \sum_{j=i+1}^{N_V} V^{ee}(\mathbf{r}_i, \mathbf{r}_j) [\omega]$$

occupation number formalism

Wannier orbitals

$$\hat{H} = \sum_{i\nu j\sigma} t_{ij}^\nu \hat{c}_{i\nu\sigma}^\dagger \hat{c}_{j\nu\sigma} + \frac{1}{2} \sum_{\nu\nu'\mu\mu'} \sum_{ijmn} \sum_{\sigma\sigma'} v_{ijmn}^{\nu\nu'\mu\mu'} \hat{c}_{i\nu\sigma}^\dagger \hat{c}_{j\nu'\sigma'}^\dagger \hat{c}_{n\mu'\sigma'} \hat{c}_{m\mu\sigma}$$

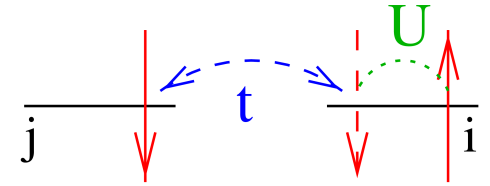
Hubbard model

$$\hat{H} = \sum_{(i,j),\sigma} t_{ij} (\hat{c}_{i\sigma}^\dagger \hat{c}_{j\sigma} + \text{h.c.}) + U \sum_i \hat{n}_{i\uparrow} \hat{n}_{i\downarrow}$$

Note: no core states in quantum gas case!

Approaches for Hubbard-type models

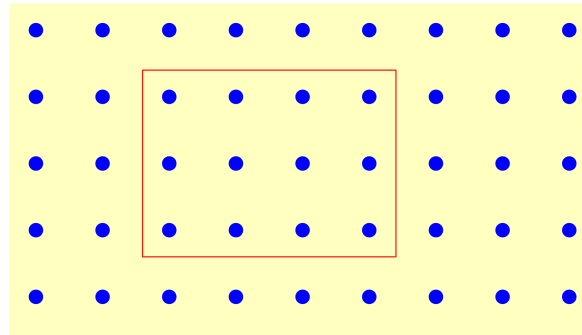
$$\hat{H} = \sum_{(i,j),\sigma} t_{ij} (\hat{c}_{i\sigma}^\dagger \hat{c}_{j\sigma} + \text{h.c.}) + U \sum_i \hat{n}_{i\uparrow} \hat{n}_{i\downarrow}$$



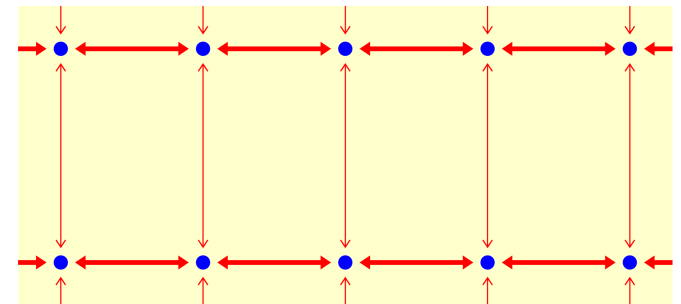
Perturbation theory

- $U \rightarrow 0$: Hartree-Fock
2nd order PT,
- $t/U \rightarrow 0$ (for $n = 1$)
 \rightsquigarrow Heisenberg model

finite clusters: ED, QMC

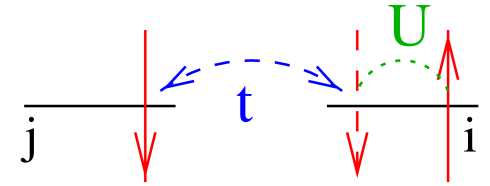


$d \rightarrow 1$: Bethe ansatz, DMRG



Approaches for Hubbard-type models

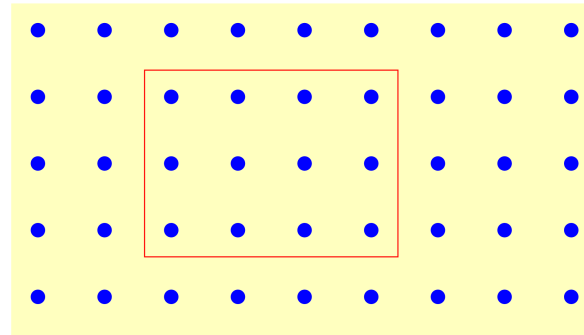
$$\hat{H} = \sum_{(i,j),\sigma} t_{ij} (\hat{c}_{i\sigma}^\dagger \hat{c}_{j\sigma} + \text{h.c.}) + U \sum_i \hat{n}_{i\uparrow} \hat{n}_{i\downarrow}$$



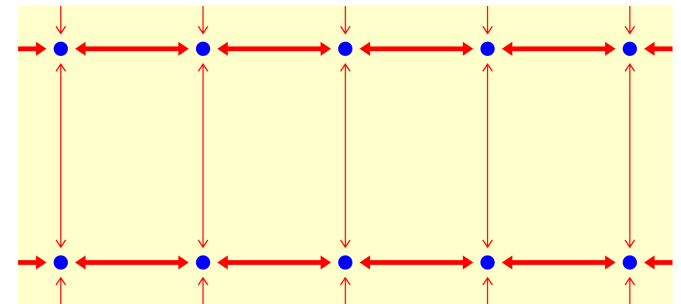
Perturbation theory

- $U \rightarrow 0$: Hartree-Fock
2nd order PT, . . .
- $t/U \rightarrow 0$ (for $n = 1$)
 \rightsquigarrow Heisenberg model

finite clusters: ED, QMC



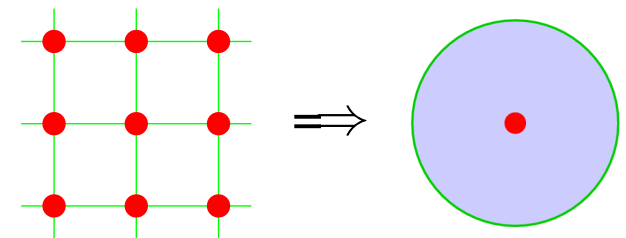
$d \rightarrow 1$: Bethe ansatz, DMRG



Dynamical mean-field theory (DMFT): local self-energy $\Sigma(\mathbf{k}, \omega) \equiv \Sigma(\omega)$

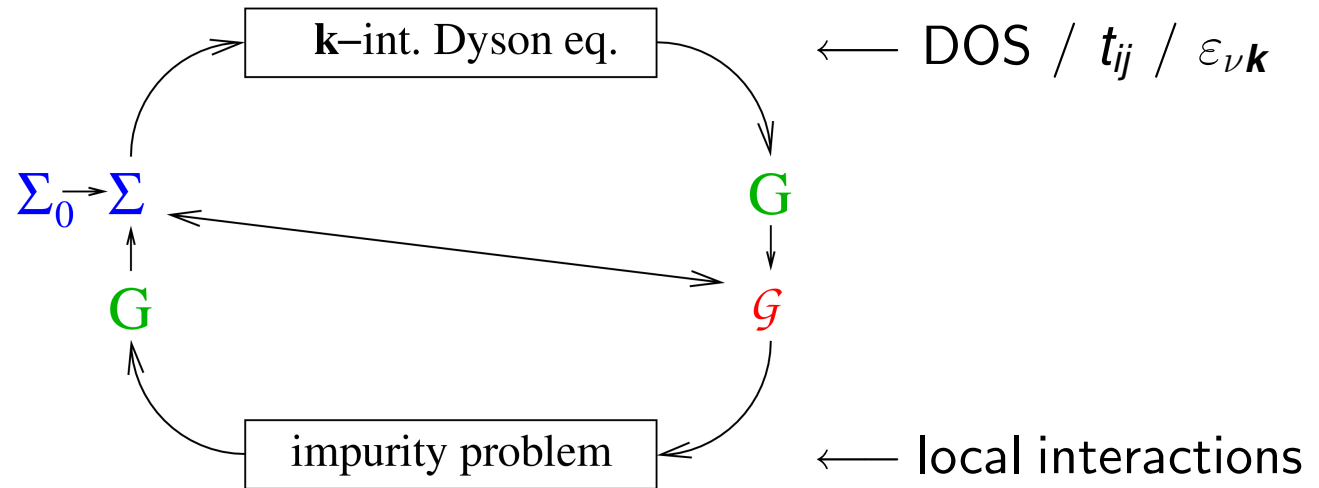
[Metzner, Vollhardt, PRL (1989), Georges, Kotliar, PRL (1992), Jarrell, PRL (1992)]

- + non-perturbative \rightsquigarrow valid at MIT
- + dynamical on-site correlations preserved
- + in thermodynamic limit
- +/- exact for coordination $Z \rightarrow \infty$



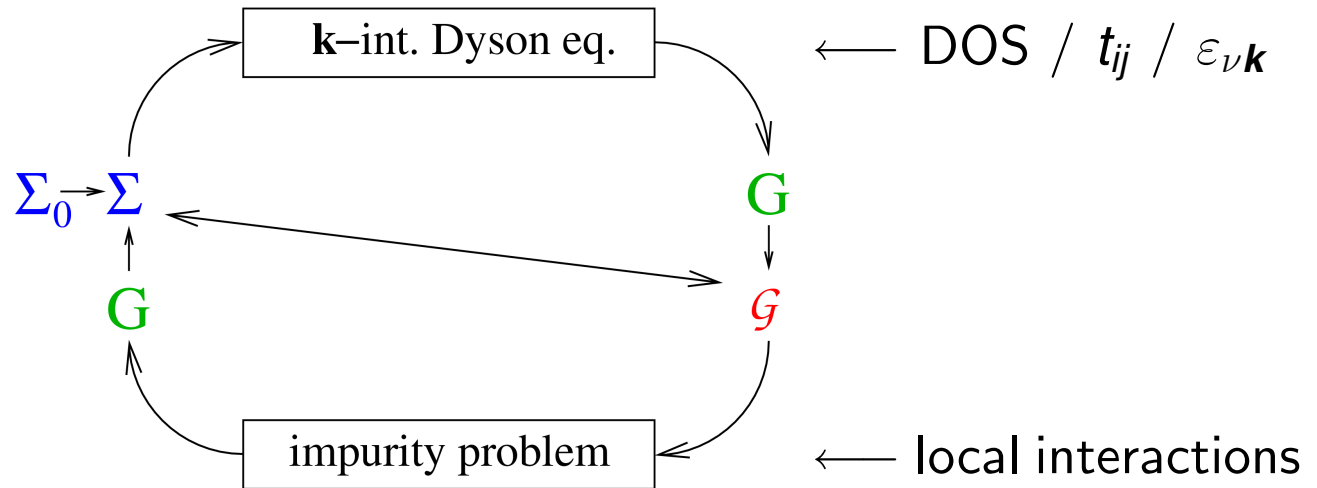
Iterative solution of DMFT equations

0. Initialize self-energy
1. Solve Dyson equation
2. Solve **single impurity**
Anderson model (SIAM)



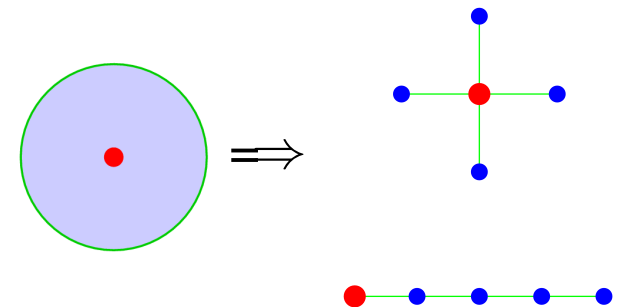
Iterative solution of DMFT equations

0. Initialize self-energy
1. Solve Dyson equation
2. Solve **single impurity Anderson model (SIAM)**



Impurity solver:

- Iterative perturbation theory (IPT; not controlled)
- Quantum Monte Carlo (QMC)
- Exact diagonalization (ED; large finite-size errors)
- Numerical renormalization group (NRG; 1-2 bands)
- Density matrix renormalization group (DMRG)
- Self-energy functional theory (SFT) + ED



Auxiliary-field QMC algorithm [Hirsch, Fye (1986)]

Green function G in imaginary time (fermionic Grassmann variables ψ, ψ^*):

$$G_{\sigma}(\tau_2 - \tau_1) = \frac{1}{Z} \int \mathcal{D}[\psi] \mathcal{D}[\psi^*] \psi_{\sigma}(\tau_1) \psi_{\sigma}^*(\tau_2) \exp \left[\mathcal{A}_0 - U \sum_{\sigma\sigma'} \int_0^{\beta} d\tau \psi_{\sigma}^* \psi_{\sigma} \psi_{\sigma'}^* \psi_{\sigma'} \right]$$

Auxiliary-field QMC algorithm [Hirsch, Fye (1986)]

Green function G in imaginary time (fermionic Grassmann variables ψ, ψ^*):

$$G_{\sigma}(\tau_2 - \tau_1) = \frac{1}{Z} \int \mathcal{D}[\psi] \mathcal{D}[\psi^*] \psi_{\sigma}(\tau_1) \psi_{\sigma}^*(\tau_2) \exp \left[\mathcal{A}_0 - U \sum_{\sigma\sigma'} \int_0^{\beta} d\tau \psi_{\sigma}^* \psi_{\sigma} \psi_{\sigma'}^* \psi_{\sigma'} \right]$$

(i) Imaginary-time discretization $\beta = \Lambda \Delta\tau$

(ii) Trotter decoupling $e^{-\beta(\hat{T}+\hat{V})} \approx [e^{-\Delta\tau\hat{T}} e^{-\Delta\tau\hat{V}}]^{\Lambda}$

Auxiliary-field QMC algorithm [Hirsch, Fye (1986)]

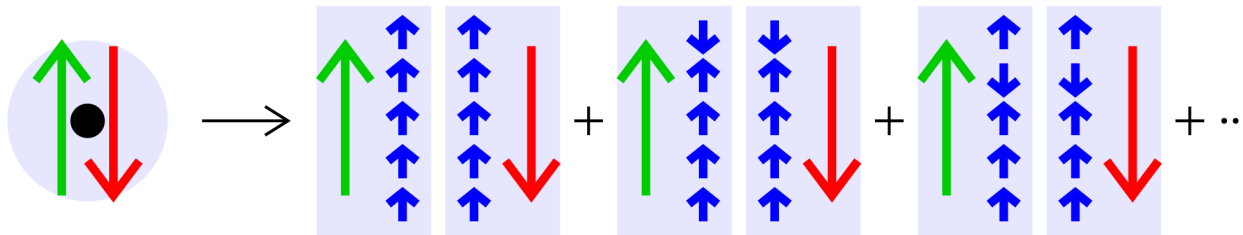
Green function G in imaginary time (fermionic Grassmann variables ψ, ψ^*):

$$G_{\sigma}(\tau_2 - \tau_1) = \frac{1}{Z} \int \mathcal{D}[\psi] \mathcal{D}[\psi^*] \psi_{\sigma}(\tau_1) \psi_{\sigma}^*(\tau_2) \exp \left[\mathcal{A}_0 - U \sum_{\sigma\sigma'} \int_0^{\beta} d\tau \psi_{\sigma}^* \psi_{\sigma} \psi_{\sigma'}^* \psi_{\sigma'} \right]$$

(i) Imaginary-time discretization $\beta = \Lambda \Delta\tau$

(ii) Trotter decoupling $e^{-\beta(\hat{T}+\hat{V})} \approx [e^{-\Delta\tau\hat{T}} e^{-\Delta\tau\hat{V}}]^{\Lambda}$

(iii) Hubbard-Stratonovich transformation



Wick theorem:

$$G = \frac{\sum M \det\{M\}}{\sum \det\{M\}}$$

Auxiliary-field QMC algorithm [Hirsch, Fye (1986)]

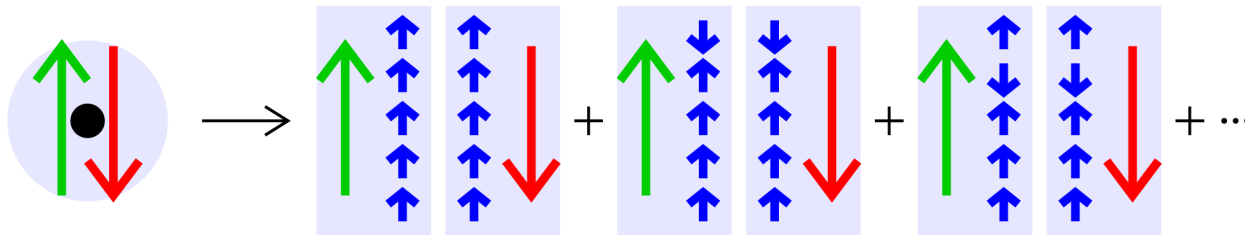
Green function G in imaginary time (fermionic Grassmann variables ψ, ψ^*):

$$G_{\sigma}(\tau_2 - \tau_1) = \frac{1}{Z} \int \mathcal{D}[\psi] \mathcal{D}[\psi^*] \psi_{\sigma}(\tau_1) \psi_{\sigma}^*(\tau_2) \exp \left[\mathcal{A}_0 - U \sum_{\sigma\sigma'} \int_0^{\beta} d\tau \psi_{\sigma}^* \psi_{\sigma} \psi_{\sigma'}^* \psi_{\sigma'} \right]$$

(i) Imaginary-time discretization $\beta = \Lambda \Delta\tau$

(ii) Trotter decoupling $e^{-\beta(\hat{T}+\hat{V})} \approx [e^{-\Delta\tau\hat{T}} e^{-\Delta\tau\hat{V}}]^{\Lambda}$

(iii) Hubbard-Stratonovich transformation



Wick theorem:

$$G = \frac{\sum M \det\{M\}}{\sum \det\{M\}}$$

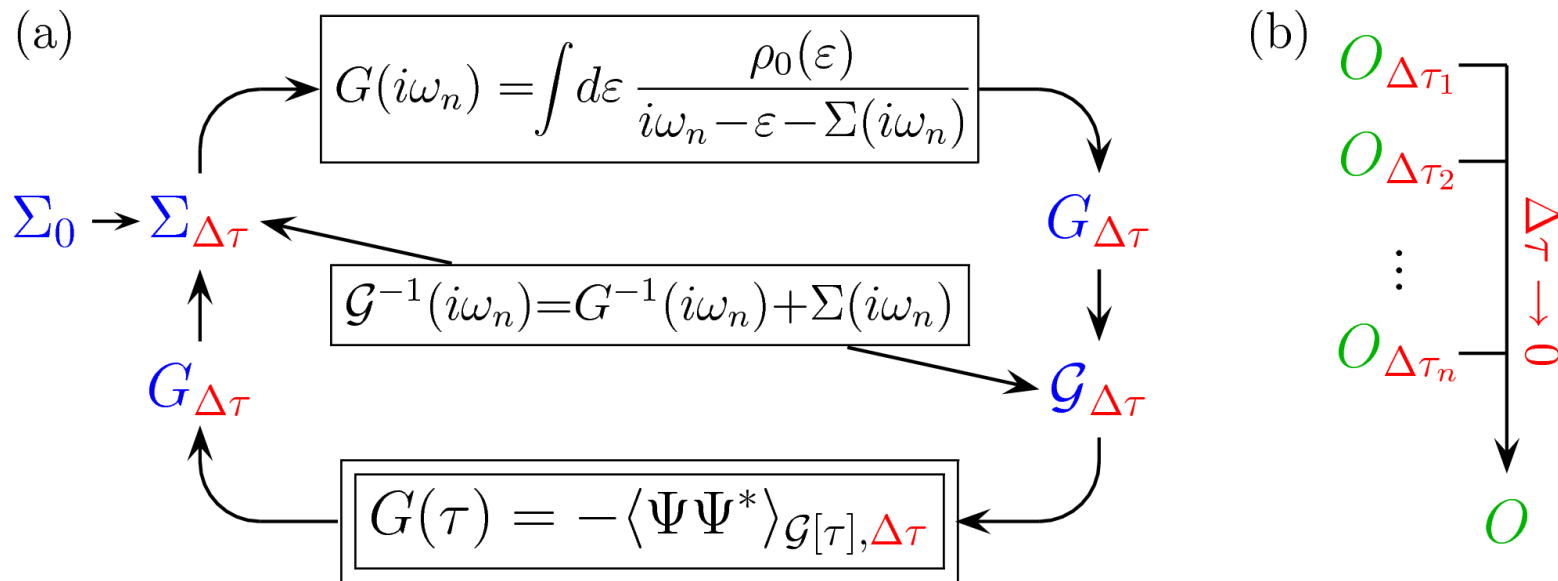
(iv) MC importance sampling over auxiliary Ising field $\{s\}$: 2^{Λ} configurations

+ numerically exact, + no sign problem, – effort scales as T^{-3}
(density-type interactions)

Multigrid Hirsch-Fye quantum Monte Carlo algorithm

State of the art: (a) conventional HF-QMC

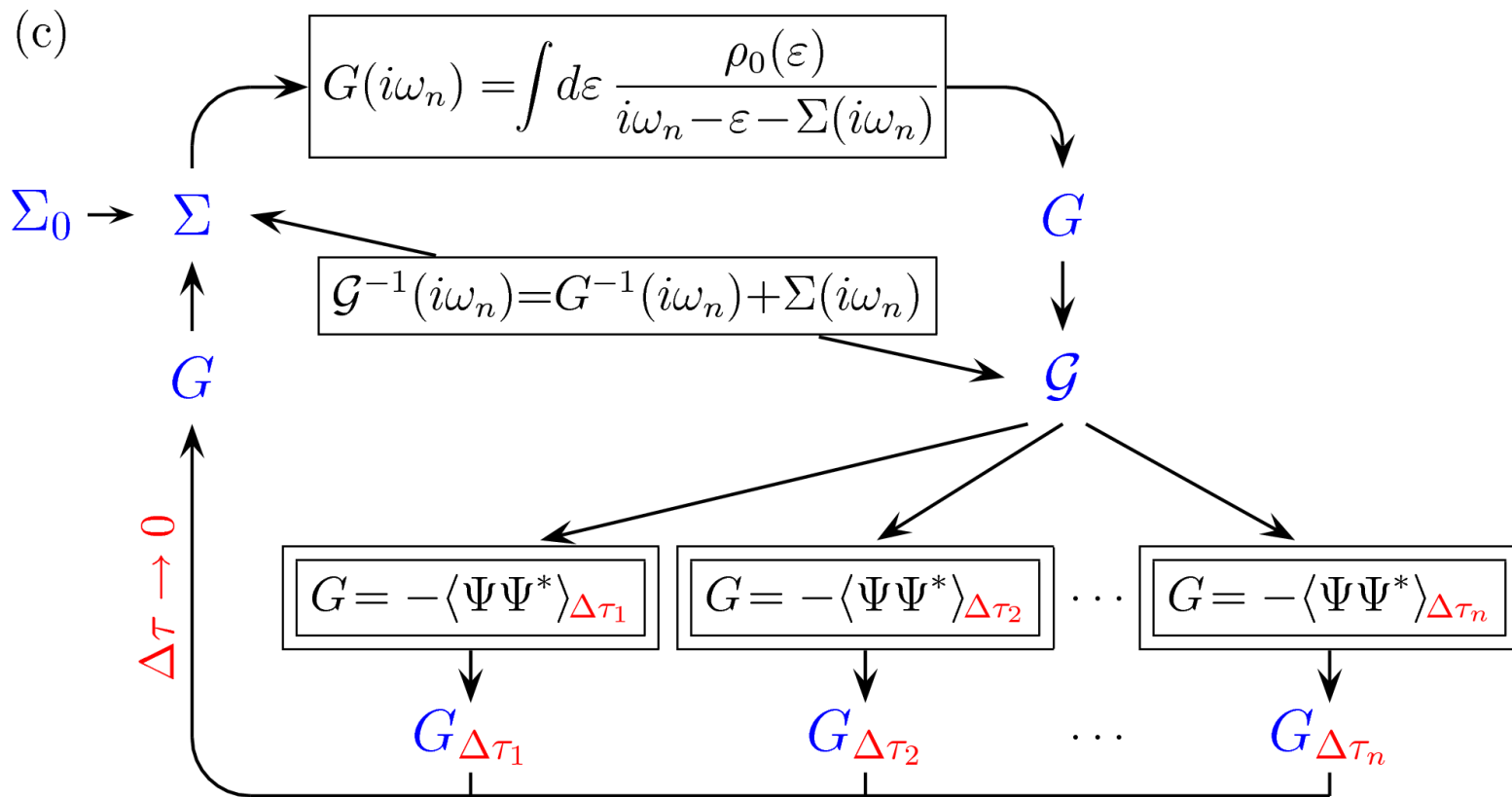
(b) *a posteriori* extrapolation of selected observables



Multigrid Hirsch-Fye quantum Monte Carlo algorithm

State of the art: (a) conventional HF-QMC

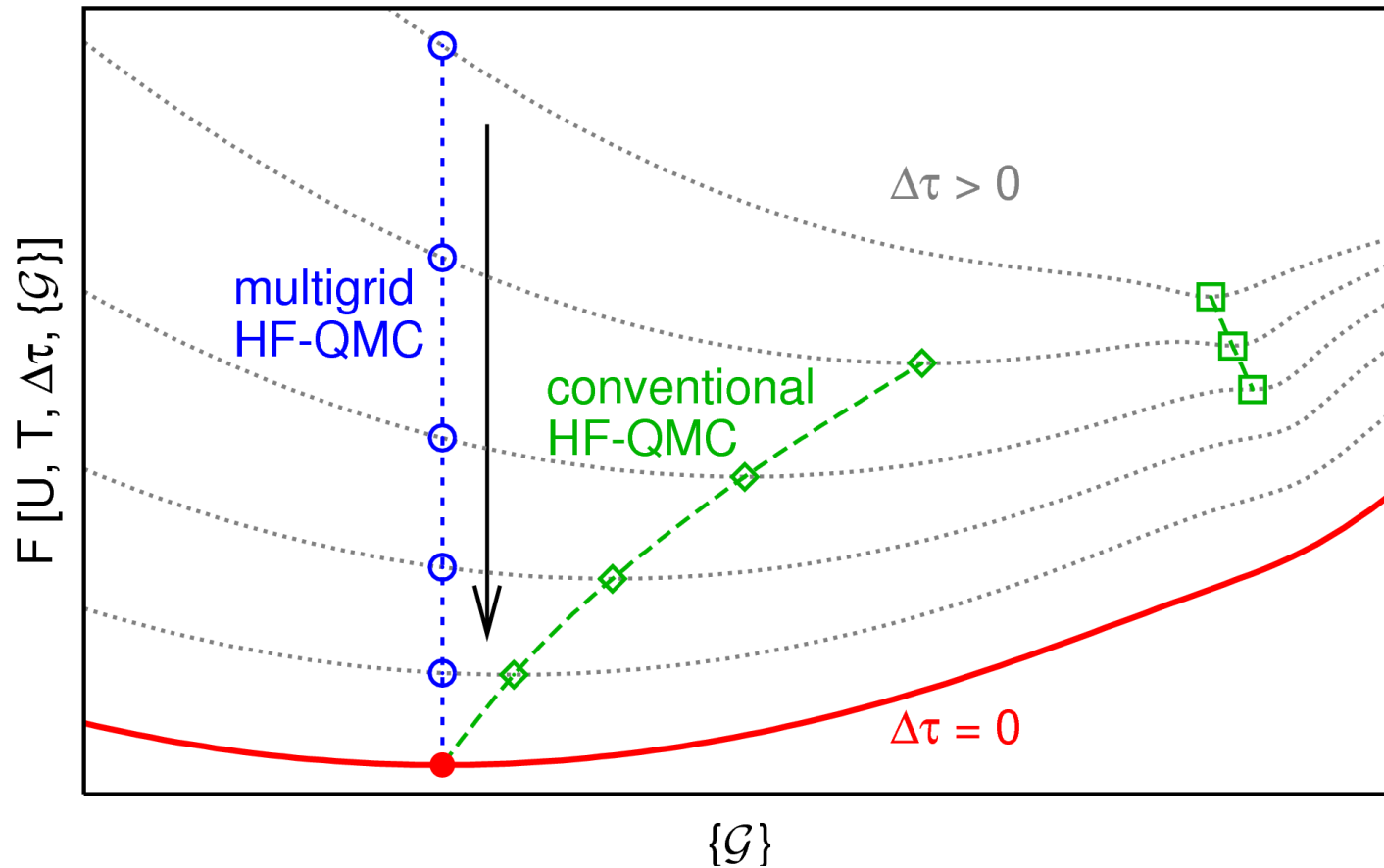
(b) *a posteriori* extrapolation of selected observables



(c) Multigrid HF-QMC: internal elimination of Trotter error

\rightsquigarrow quasi CT-QMC algorithm [NB, arXiv:0801.1222, PRA(2009)]

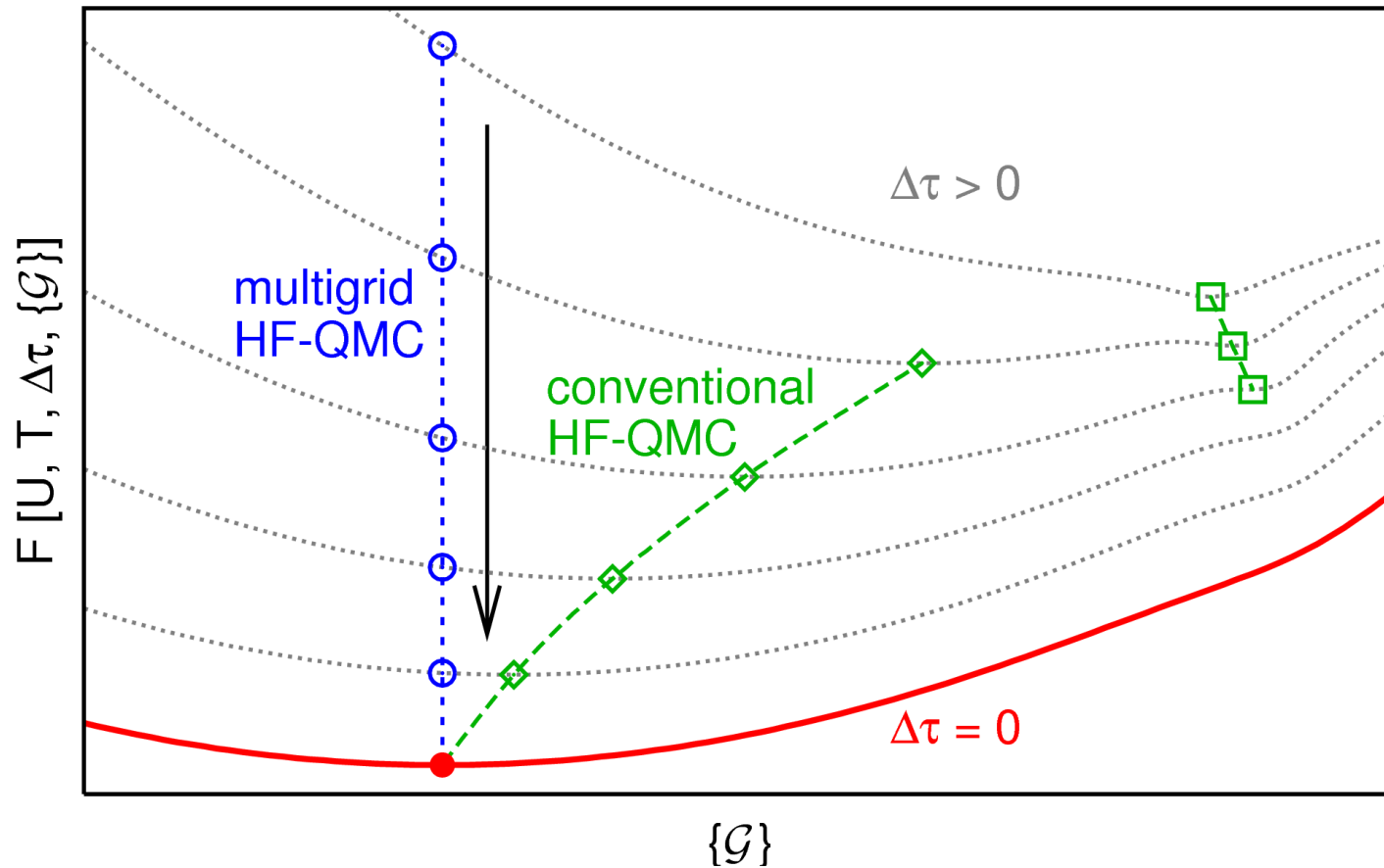
Schematic comparison via generalized Ginzburg-Landau functionals



Conventional Hirsch-Fye QMC: DMFT fixed point shifts with $\Delta\tau$

Multigrid Hirsch-Fye QMC: DMFT iteration towards exact fixed point

Schematic comparison via generalized Ginzburg-Landau functionals

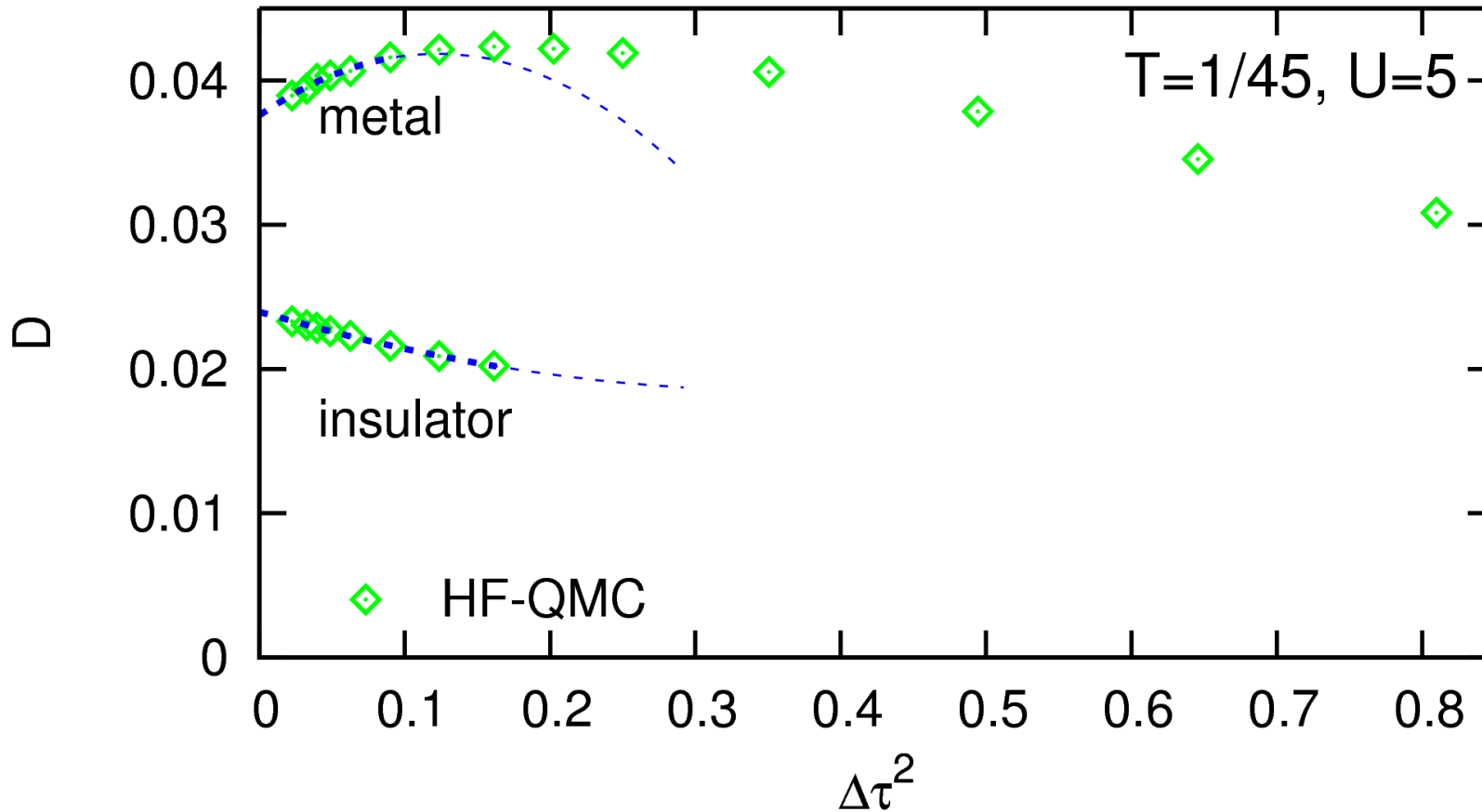


Conventional Hirsch-Fye QMC: DMFT fixed point shifts with $\Delta\tau$

Multigrid Hirsch-Fye QMC: DMFT iteration towards exact fixed point

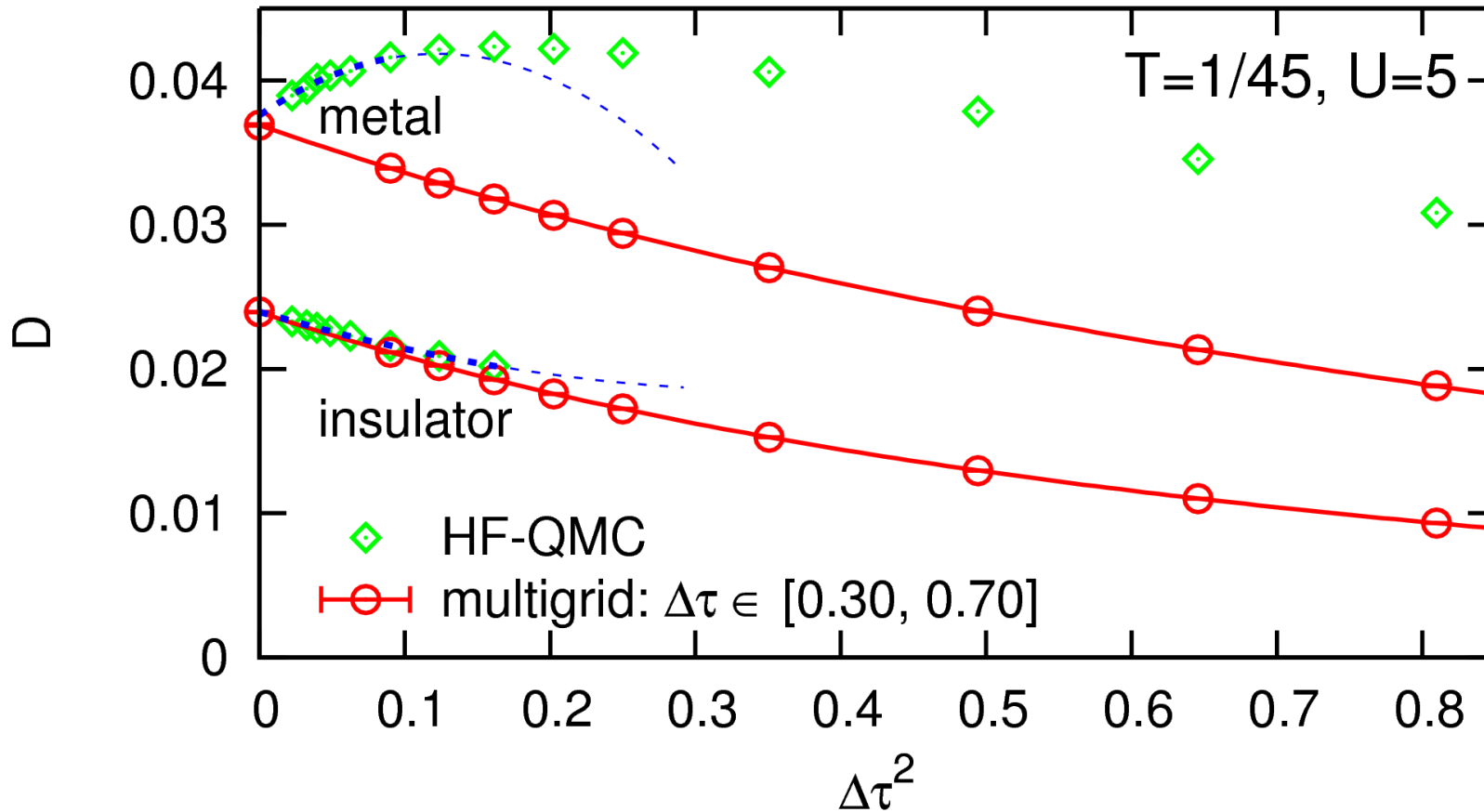
Implementation: Green function extrapolation, hierarchy of frequency scales

Comparison: double occupancy $D = \langle n_{i\uparrow} n_{i\downarrow} \rangle$ near Mott transition



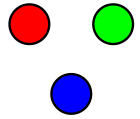
Conventional HF-QMC: no insulating solution for $\Delta\tau \gtrsim 0.4$
very irregular $\Delta\tau$ dependence beyond $\Delta\tau \approx 0.3$

Comparison: double occupancy $D = \langle n_{i\uparrow} n_{i\downarrow} \rangle$ near Mott transition



- Conventional HF-QMC: no insulating solution for $\Delta\tau \gtrsim 0.4$
very irregular $\Delta\tau$ dependence beyond $\Delta\tau \approx 0.3$
- Multigrid HF-QMC: vastly larger useful range of $\Delta\tau$

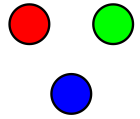
Paramagnetic Mott transitions in 3-flavor mixtures



3 flavors: simplest case beyond electronic systems

1st approximation: all flavors equivalent, bulk system

Paramagnetic Mott transitions in 3-flavor mixtures



3 flavors: simplest case beyond electronic systems

1st approximation: all flavors equivalent, bulk system

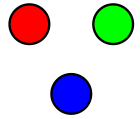
- Qualitatively new physics: $U < 0$, $n = 1.5$ [Hofstetter, PRB (2004), PRL (2007)]

Color superconductivity

Trionic phase

...

Paramagnetic Mott transitions in 3-flavor mixtures



3 flavors: simplest case beyond electronic systems

1st approximation: all flavors equivalent, bulk system

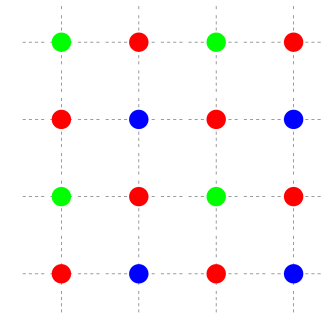
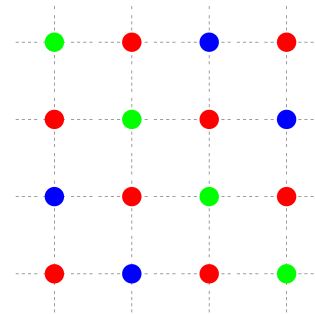
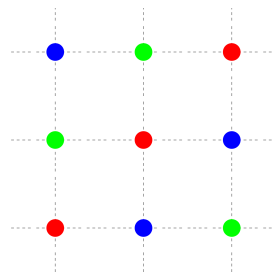
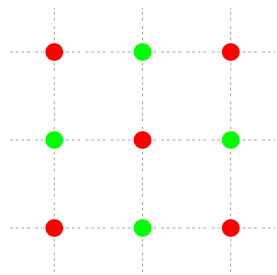
- Qualitatively new physics: $U < 0$, $n = 1.5$ [Hofstetter, PRB (2004), PRL (2007)]

Color superconductivity

Trionic phase

...

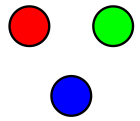
- Ordered phases: $U > 0$, $n = 1$



2 spins/flavors

3 spins/flavors

Paramagnetic Mott transitions in 3-flavor mixtures



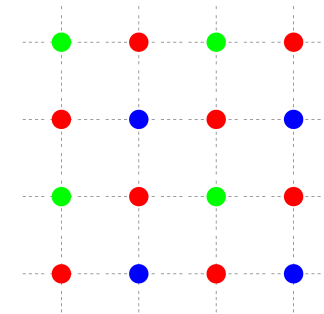
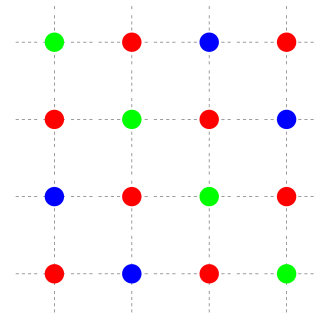
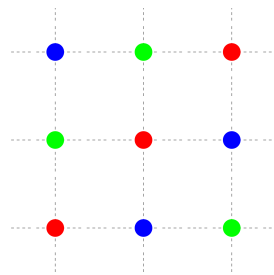
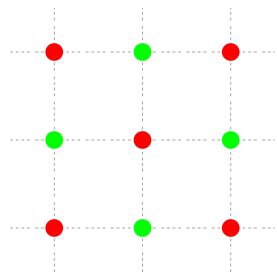
3 flavors: simplest case beyond electronic systems
 1st approximation: all flavors equivalent, bulk system

- Qualitatively new physics: $U < 0$, $n = 1.5$ [Hofstetter, PRB (2004), PRL (2007)]

Color superconductivity
 Trionic phase

...

- Ordered phases: $U > 0$, $n = 1$



2 spins/flavors

3 spins/flavors

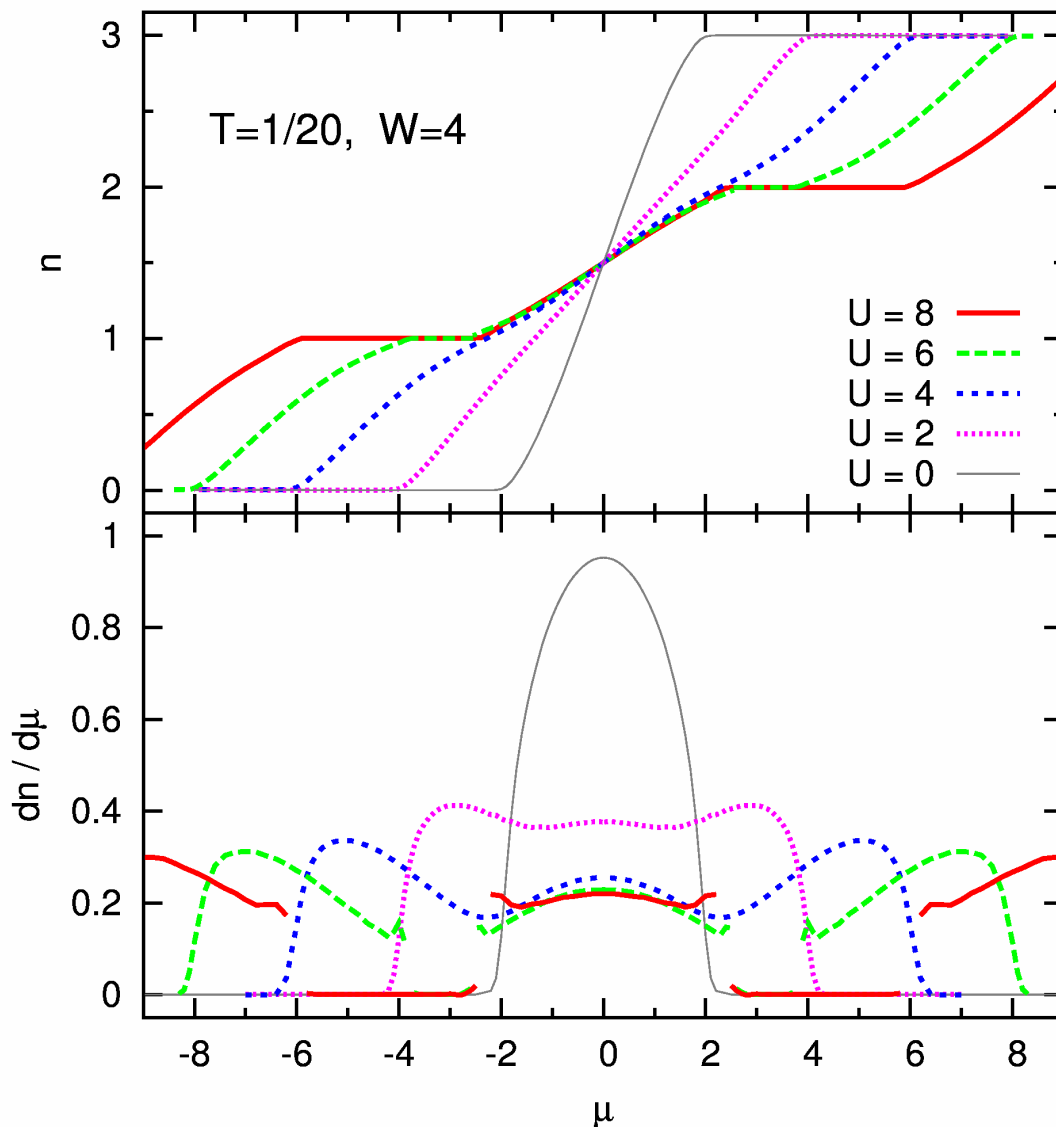
Most “electron-like”: $U > 0$, paramagnetic phase

Results at low T : particle density n and compressibility $\kappa = \frac{dn}{d\mu}$ (vs. μ)

HF-QMC, Bethe DOS ($W = 4$)

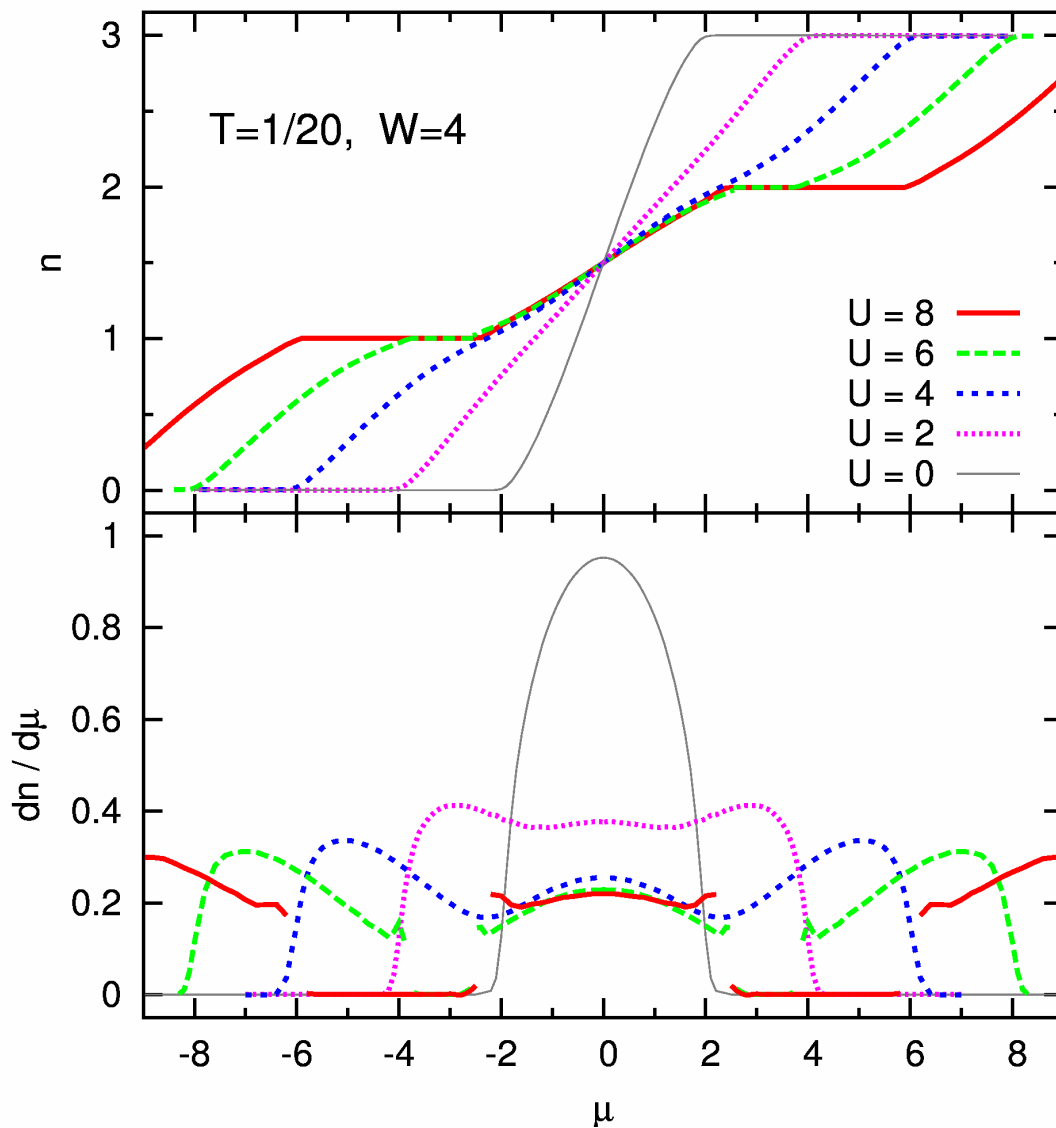
Plateaus at integer filling ($U \gtrsim 5.5$)

\rightsquigarrow incompressible Mott phases



[E. Gorelik, N. Blümer, PRA(2009)]

Results at low T : particle density n and compressibility $\kappa = \frac{dn}{d\mu}$ (vs. μ)



HF-QMC, Bethe DOS ($W = 4$)

Plateaus at integer filling ($U \gtrsim 5.5$)

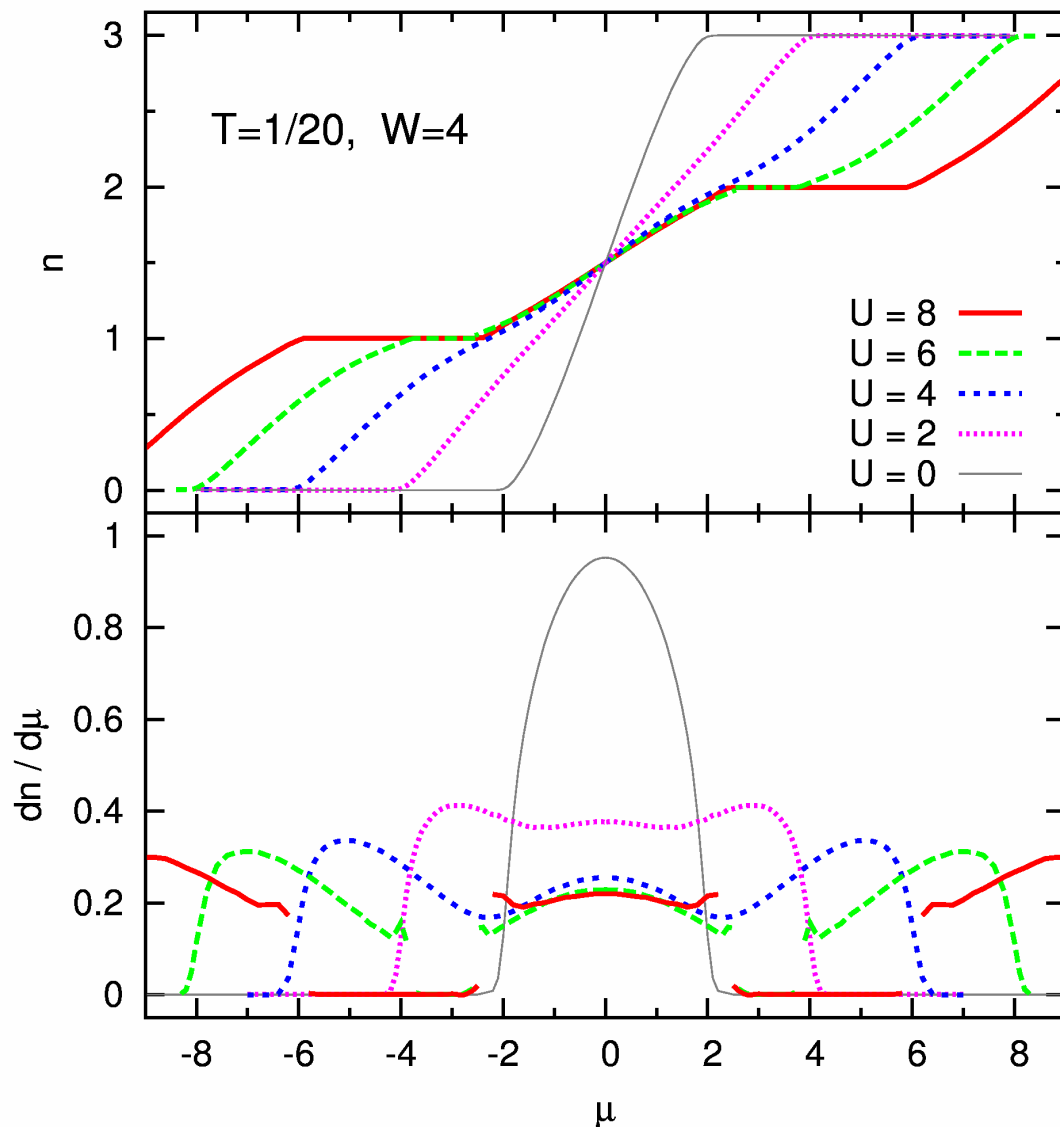
\rightsquigarrow incompressible Mott phases

$1 < n < 2$: semi-compressible phase

κ independent of μ , U , T

[E. Gorelik, N. Blümer, PRA(2009)]

Results at low T : particle density n and compressibility $\kappa = \frac{dn}{d\mu}$ (vs. μ)



HF-QMC, Bethe DOS ($W = 4$)

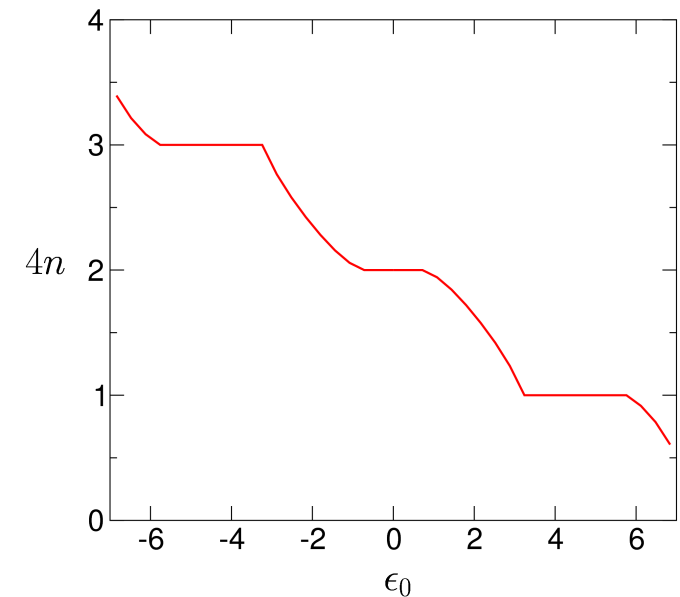
Plateaus at integer filling ($U \gtrsim 5.5$)

\rightsquigarrow incompressible Mott phases

$1 < n < 2$: semi-compressible phase

κ independent of μ , U , T

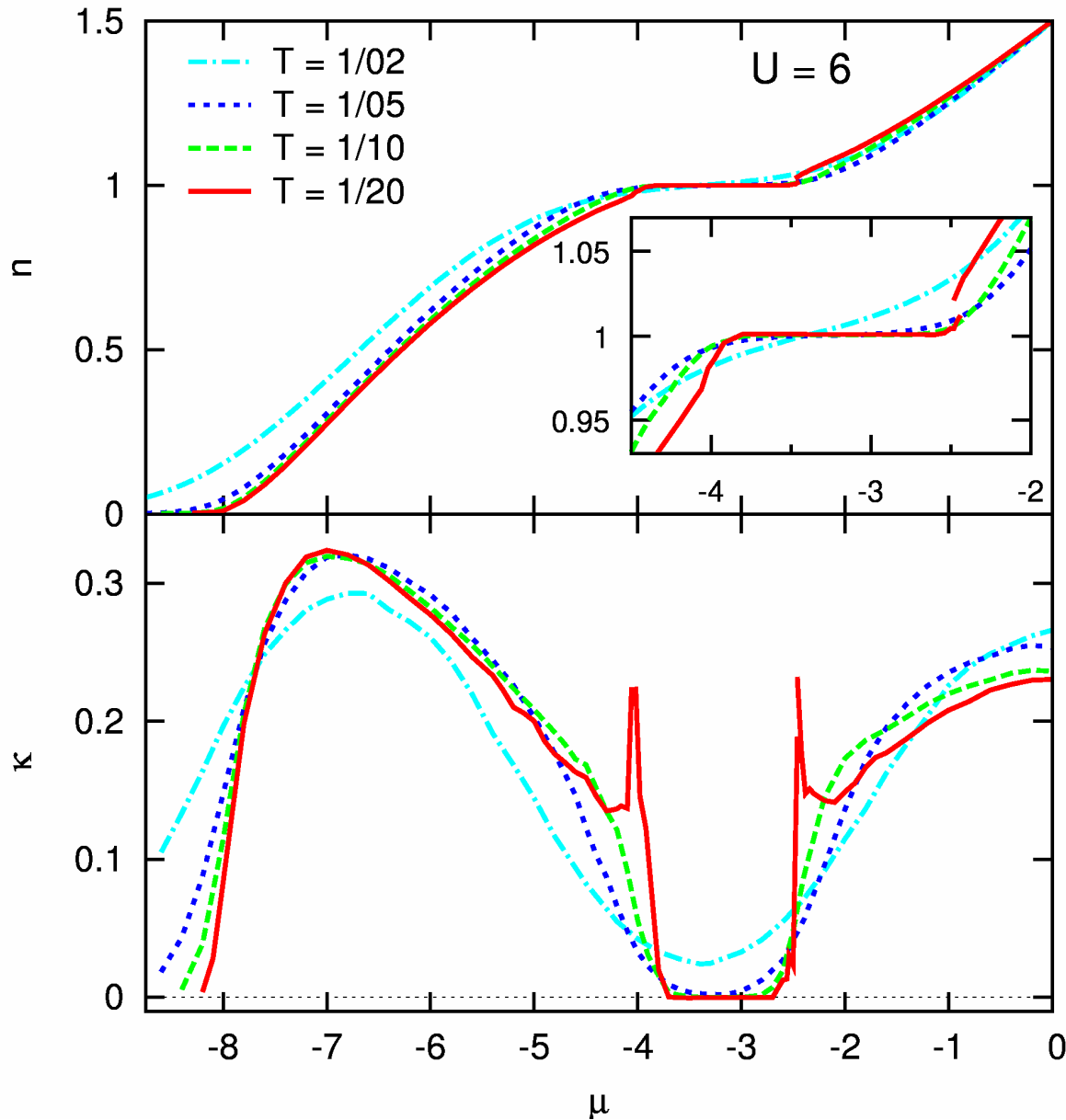
Contrast with SU(4) system:



[E. Gorelik, N. Blümer, PRA(2009)]

[Florens, Georges, PRB **70**, 035114 (2004)]

T dependence of density n and compressibility κ

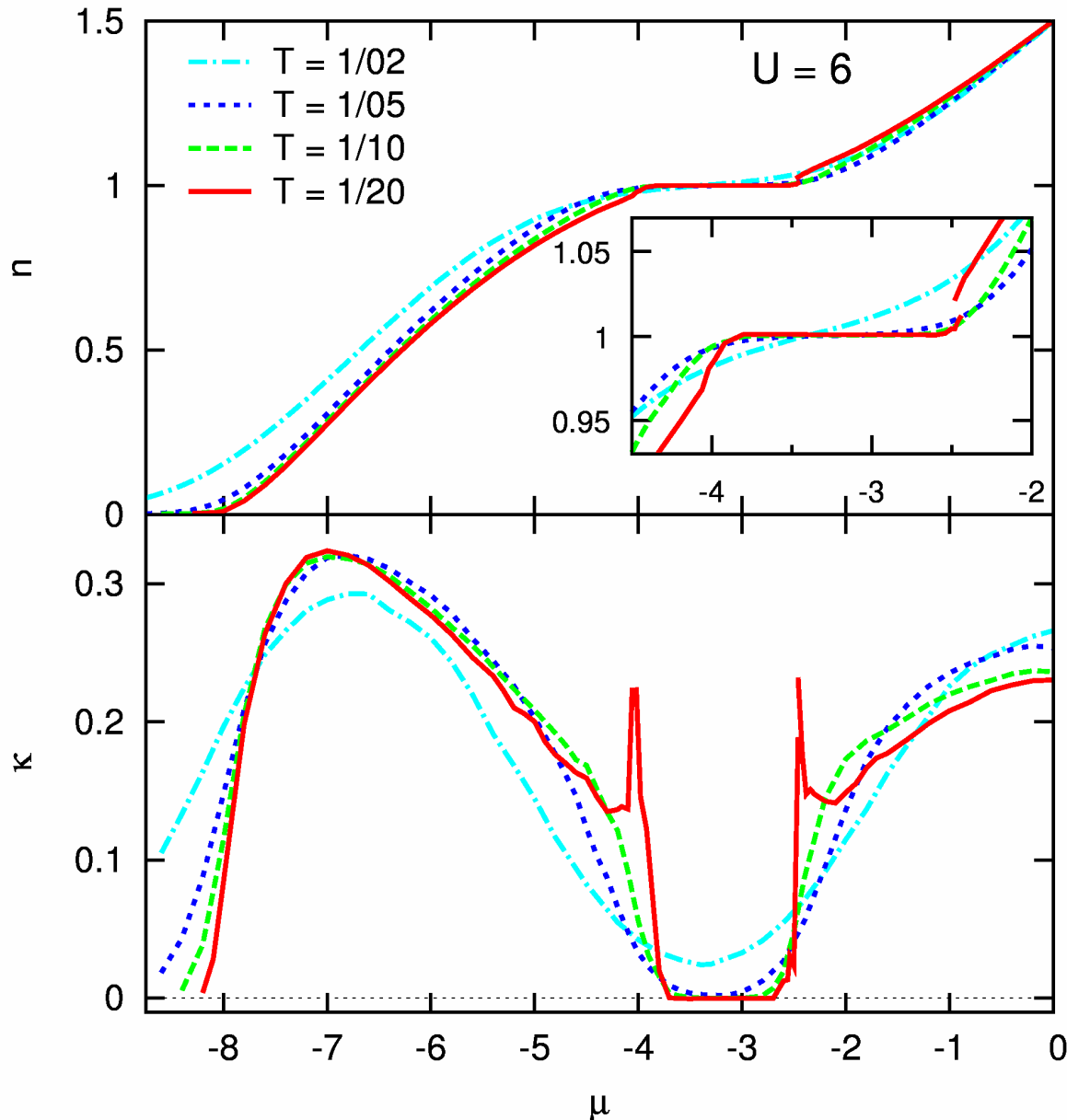


Multigrid HF-QMC results

Critical temperature $T^* \approx 1/20$

not shown: hysteresis at $T = 1/30$

T dependence of density n and compressibility κ



Multigrid HF-QMC results

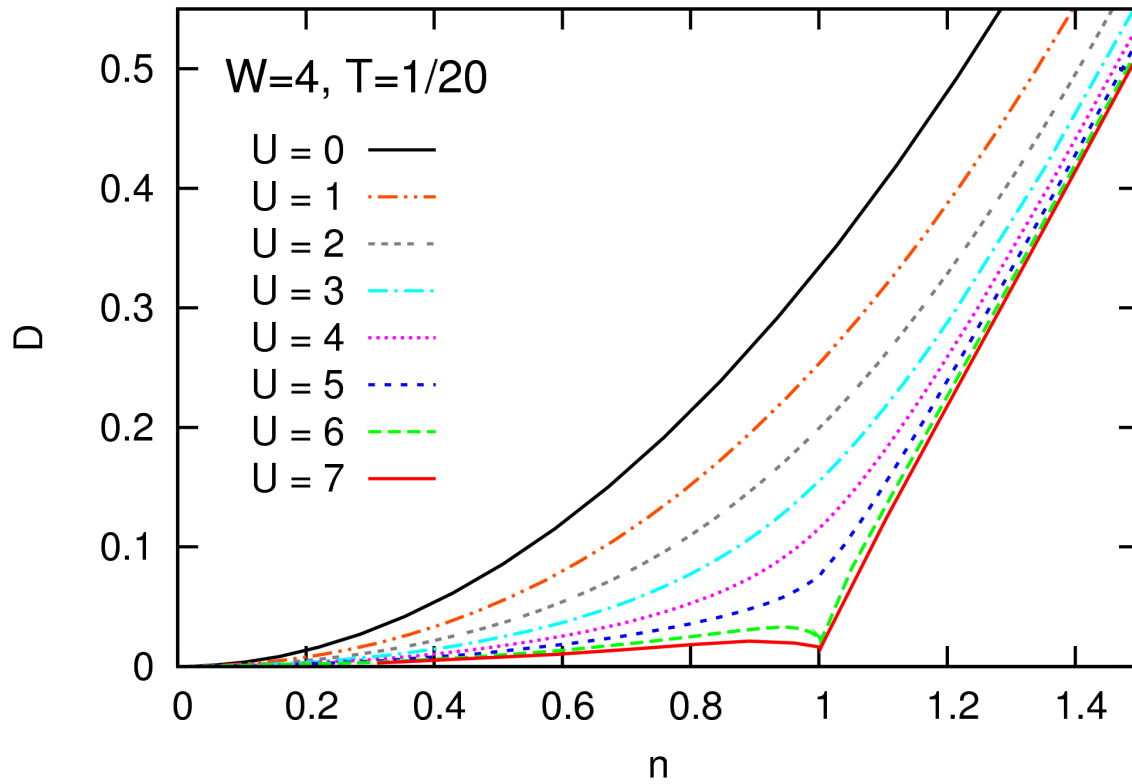
Critical temperature $T^* \approx 1/20$

not shown: hysteresis at $T = 1/30$

Important for experiments:

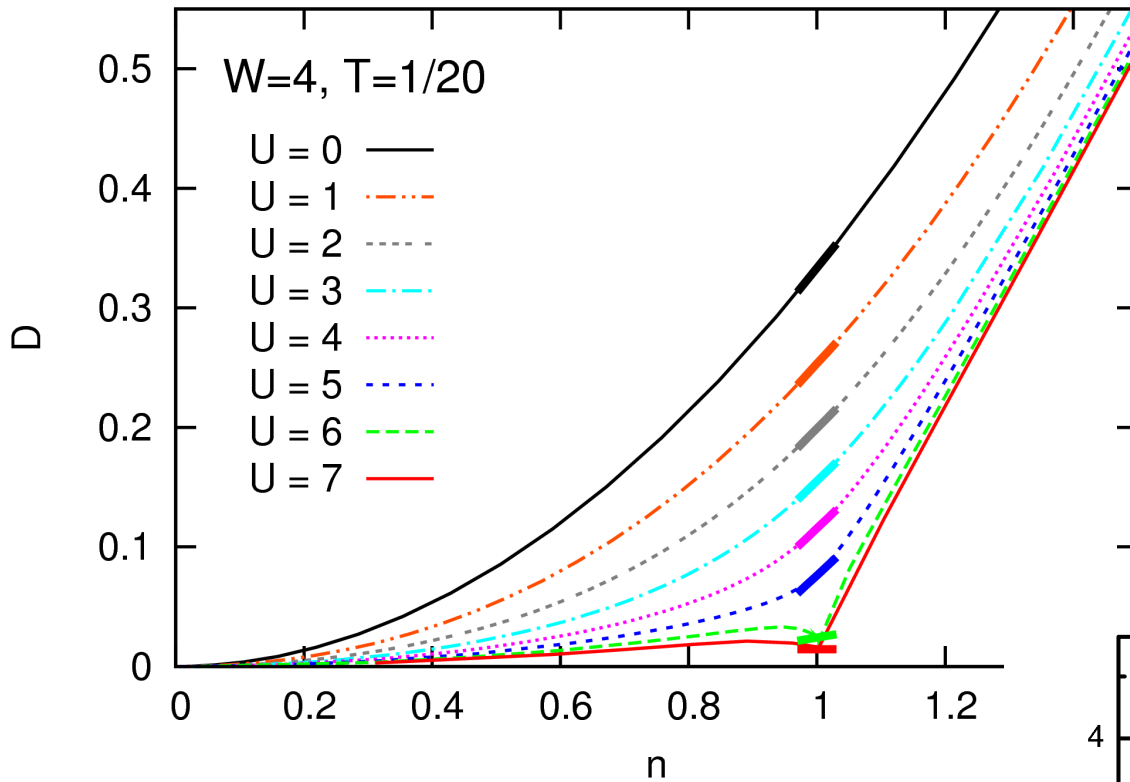
Signatures of Mott transition
persist to high temperatures:

nearly complete suppression of κ
(at $n \approx 1$) up to $T \approx 1/5$.



3-spin/ flavor system:

Pair occupancy vs. density



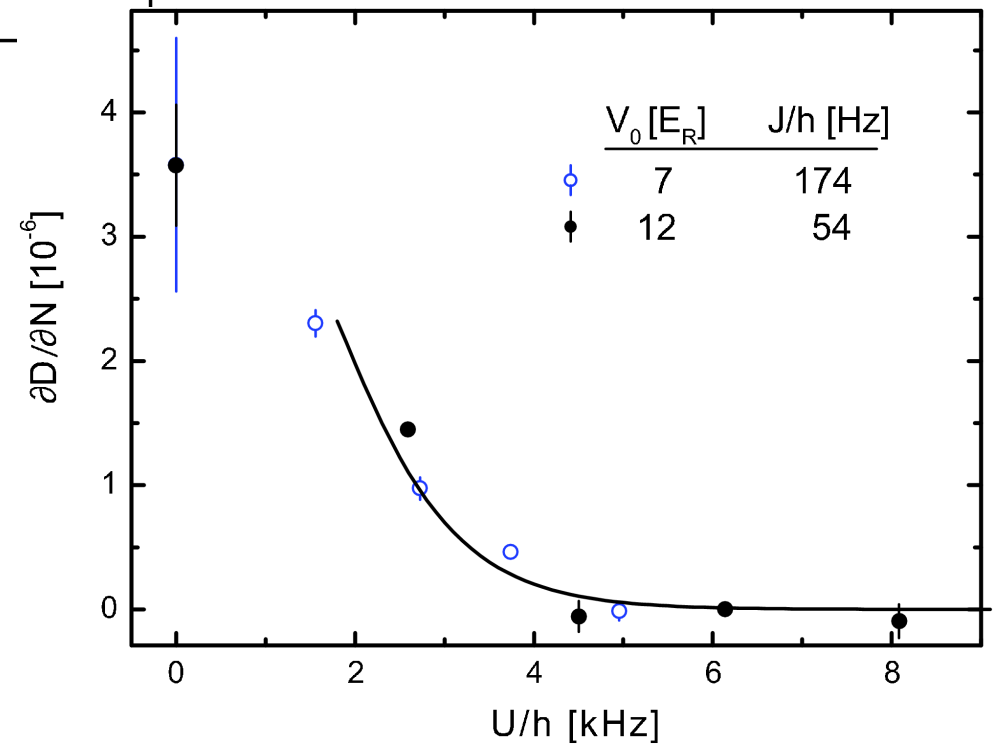
3-spin/3-flavor system:

Pair occupancy vs. density

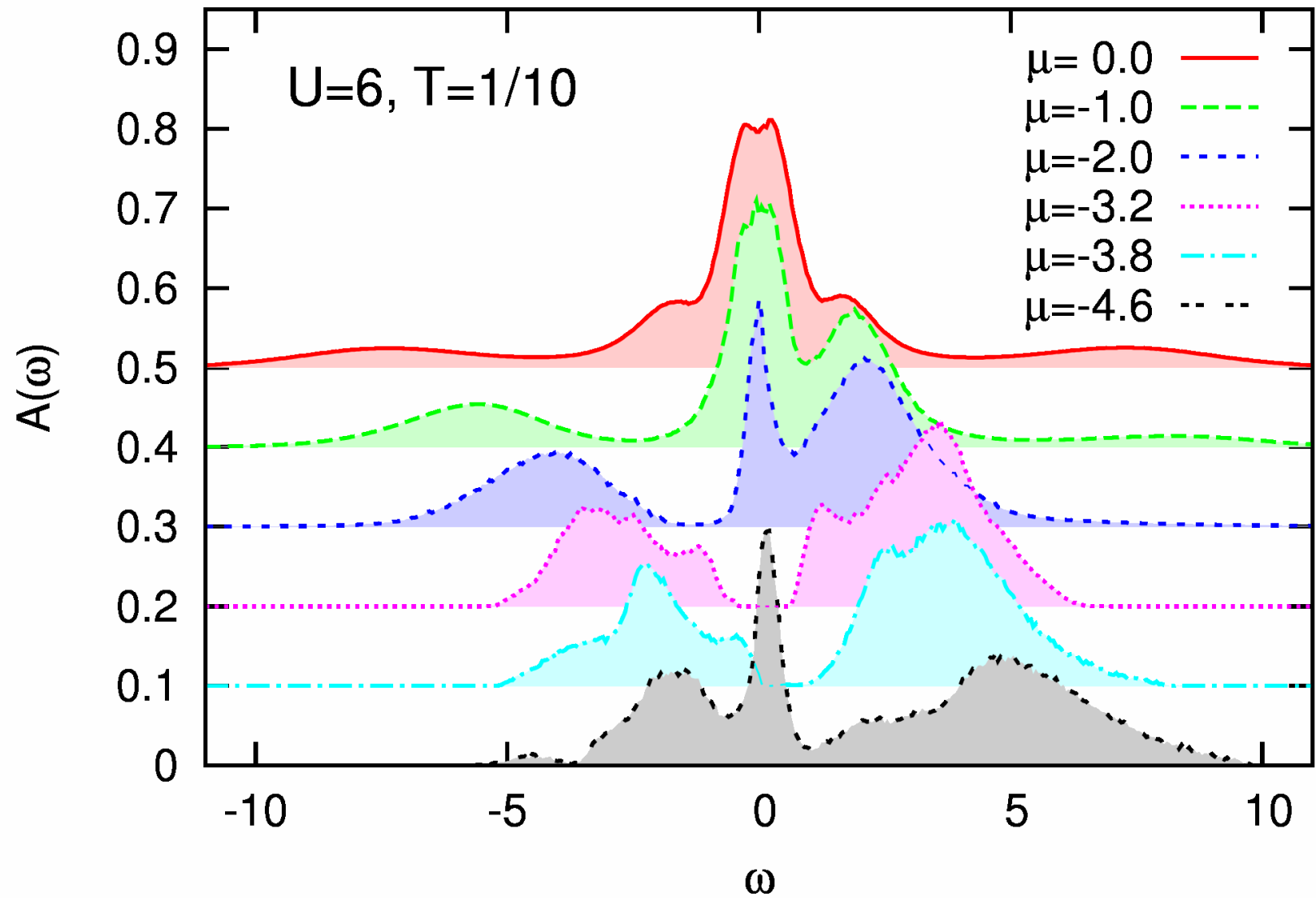
Experiment: 2-spin system

Transition to an incompressible phase

[Jördens et al., Nature (2008)]



Local spectral function



PHYSICAL REVIEW A **80**, 051602(R) (2009)**Mott transitions in ternary flavor mixtures of ultracold fermions on optical lattices**

E. V. Gorelik and N. Blümer

Institute of Physics, Johannes Gutenberg University, 55099 Mainz, Germany

(Received 7 May 2009; revised manuscript received 9 July 2009; published 11 November 2009)

PHYSICAL REVIEW A **81**, 021603(R) (2010)**Three-component fermionic atoms with repulsive interaction in optical lattices**Shin-ya Miyatake,¹ Kensuke Inaba,² and Sei-ichiro Suga^{1,3}¹*Department of Applied Physics, Osaka University, Suita, Osaka 565-0871, Japan*²*NTT Basic Research Laboratories, NTT Corporation, Atsugi 243-0198, Japan, and CREST, JST, Chiyoda-ku, Tokyo 102-0075, Japan*³*Department of Materials Science and Chemistry, University of Hyogo, Himeji 671-2280, Japan*

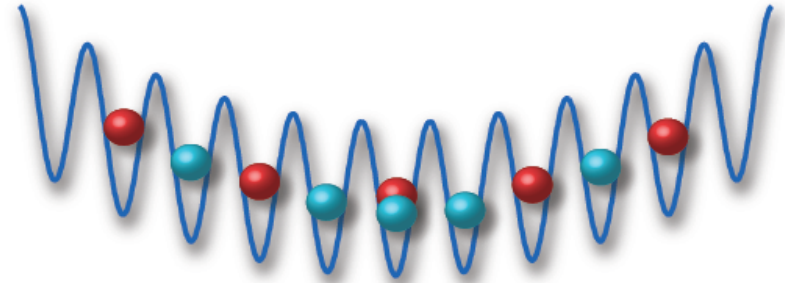
(Received 4 December 2009; published 17 February 2010)

- MIT at integer filling (same authors, Physica C)
- inequivalent flavors
- ordering at half filling

Antiferromagnetic order at finite T in an optical trap

Now include trapping potential, e.g.: $V_i = Vr_i^2$

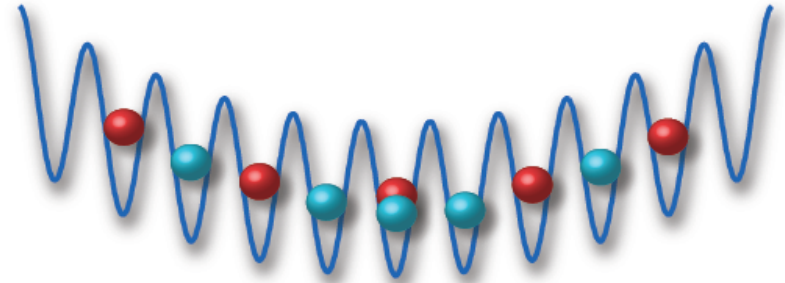
$$H = - \sum_{(ij),\sigma} t_{ij} c_{i\sigma}^\dagger c_{j\sigma} + U \sum_{i=1}^N n_{i\uparrow} n_{i\downarrow} + \sum_{i,\sigma} V_i n_{i\sigma}$$



Antiferromagnetic order at finite T in an optical trap

Now include **trapping potential**, e.g.: $V_i = V r_i^2$

$$H = - \sum_{(ij),\sigma} t_{ij} c_{i\sigma}^\dagger c_{j\sigma} + U \sum_{i=1}^N n_{i\uparrow} n_{i\downarrow} + \sum_{i,\sigma} V_i n_{i\sigma}$$



Real-space DMFT: use local self-energy in inhomogeneous system

\rightsquigarrow N single-site impurities, coupled by modified lattice Dyson equation:

$$\left[G_\sigma(i\omega_n) \right]_{ij}^{-1} = (\mu_\sigma + i\omega_n) \delta_{ij} - t_{ij} - (V_i + \Sigma_{i\sigma}(i\omega_n)) \delta_{ij} \equiv z_i(i\omega_n) \delta_{ij} - t_{ij}$$

[M. Snoek, I. Titvinidze, C. Toke, K. Byczuk, and W. Hofstetter, *New Journal of Physics* (2008);
R. Helmes, T. A. Costi, and A. Rosch, *PRL* (2008)]

Also: **inhomogeneous DMFT** (for Falicov-Kimball model) [Freericks]

RDMFT algorithm

0) Choose $\Sigma_i(i\omega_n) \rightsquigarrow z_i(i\omega_n)$

1) For each ω_n evaluate lattice Dyson equation ($z_i \equiv z_i(i\omega_n)$):

Example: 1d chain with open bc

$$\begin{pmatrix} G_{-2,-2} & G_{-2,-1} & G_{-2,0} & G_{-2,1} & G_{-2,2} \\ G_{-1,-2} & G_{-1,-1} & G_{-1,0} & G_{-1,1} & G_{-1,2} \\ G_{0,-2} & G_{0,-1} & G_{0,0} & G_{0,1} & G_{0,2} \\ G_{1,-2} & G_{1,-1} & G_{1,0} & G_{1,1} & G_{1,2} \\ G_{2,-2} & G_{2,-1} & G_{2,0} & G_{2,1} & G_{2,2} \end{pmatrix} = \begin{pmatrix} z_{-2} & -t & 0 & 0 & 0 \\ -t & z_{-1} & -t & 0 & 0 \\ 0 & -t & z_0 & -t & 0 \\ 0 & 0 & -t & z_1 & -t \\ 0 & 0 & 0 & -t & z_2 \end{pmatrix}^{-1}$$

RDMFT algorithm

0) Choose $\Sigma_i(i\omega_n) \rightsquigarrow \mathbf{z}_i(i\omega_n)$

1) For each ω_n evaluate lattice Dyson equation ($\mathbf{z}_i \equiv \mathbf{z}_i(i\omega_n)$):

Example: 1d chain with open bc

$$\begin{pmatrix} \mathbf{G}_{-2,-2} & \mathbf{G}_{-2,-1} & \mathbf{G}_{-2,0} & \mathbf{G}_{-2,1} & \mathbf{G}_{-2,2} \\ \mathbf{G}_{-1,-2} & \mathbf{G}_{-1,-1} & \mathbf{G}_{-1,0} & \mathbf{G}_{-1,1} & \mathbf{G}_{-1,2} \\ \mathbf{G}_{0,-2} & \mathbf{G}_{0,-1} & \mathbf{G}_{0,0} & \mathbf{G}_{0,1} & \mathbf{G}_{0,2} \\ \mathbf{G}_{1,-2} & \mathbf{G}_{1,-1} & \mathbf{G}_{1,0} & \mathbf{G}_{1,1} & \mathbf{G}_{1,2} \\ \mathbf{G}_{2,-2} & \mathbf{G}_{2,-1} & \mathbf{G}_{2,0} & \mathbf{G}_{2,1} & \mathbf{G}_{2,2} \end{pmatrix} = \begin{pmatrix} \mathbf{z}_{-2} & -t & 0 & 0 & 0 \\ -t & \mathbf{z}_{-1} & -t & 0 & 0 \\ 0 & -t & \mathbf{z}_0 & -t & 0 \\ 0 & 0 & -t & \mathbf{z}_1 & -t \\ 0 & 0 & 0 & -t & \mathbf{z}_2 \end{pmatrix}^{-1}$$

2) Compute bath Green function: $\mathcal{G}_i^{-1}(i\omega_n) = \mathbf{G}_{ii}^{-1} + \Sigma_i(i\omega_n) \quad \forall i, \omega_n$

3) Solve impurity model ($\mathcal{G}_i, U_i, V_i, \mu, T$) for each inequivalent site i

4) Compute new self-energy $\Sigma_i(i\omega_n) = \mathcal{G}_i^{-1}(i\omega_n) - \mathbf{G}_{ii}^{-1} \quad \forall i, \omega_n$

Repeat steps 1) – 4) until convergence

RDMFT algorithm

0) Choose $\Sigma_i(i\omega_n) \rightsquigarrow z_i(i\omega_n)$

1) For each ω_n evaluate lattice Dyson equation ($z_i \equiv z_i(i\omega_n)$):

Example: 1d chain with open bc

$$\begin{pmatrix} \mathbf{G}_{-2,-2} & \mathbf{G}_{-2,-1} & \mathbf{G}_{-2,0} & \mathbf{G}_{-2,1} & \mathbf{G}_{-2,2} \\ \mathbf{G}_{-1,-2} & \mathbf{G}_{-1,-1} & \mathbf{G}_{-1,0} & \mathbf{G}_{-1,1} & \mathbf{G}_{-1,2} \\ \mathbf{G}_{0,-2} & \mathbf{G}_{0,-1} & \mathbf{G}_{0,0} & \mathbf{G}_{0,1} & \mathbf{G}_{0,2} \\ \mathbf{G}_{1,-2} & \mathbf{G}_{1,-1} & \mathbf{G}_{1,0} & \mathbf{G}_{1,1} & \mathbf{G}_{1,2} \\ \mathbf{G}_{2,-2} & \mathbf{G}_{2,-1} & \mathbf{G}_{2,0} & \mathbf{G}_{2,1} & \mathbf{G}_{2,2} \end{pmatrix} = \begin{pmatrix} z_{-2} & -t & 0 & 0 & 0 \\ -t & z_{-1} & -t & 0 & 0 \\ 0 & -t & z_0 & -t & 0 \\ 0 & 0 & -t & z_1 & -t \\ 0 & 0 & 0 & -t & z_2 \end{pmatrix}^{-1}$$

2) Compute bath Green function: $\mathcal{G}_i^{-1}(i\omega_n) = \mathbf{G}_{ii}^{-1} + \Sigma_i(i\omega_n) \quad \forall i, \omega_n$

3) Solve impurity model ($\mathcal{G}_i, U_i, V_i, \mu, T$) for each inequivalent site i

4) Compute new self-energy $\Sigma_i(i\omega_n) = \mathcal{G}_i^{-1}(i\omega_n) - \mathbf{G}_{ii}^{-1} \quad \forall i, \omega_n$

Repeat steps 1) – 4) until convergence

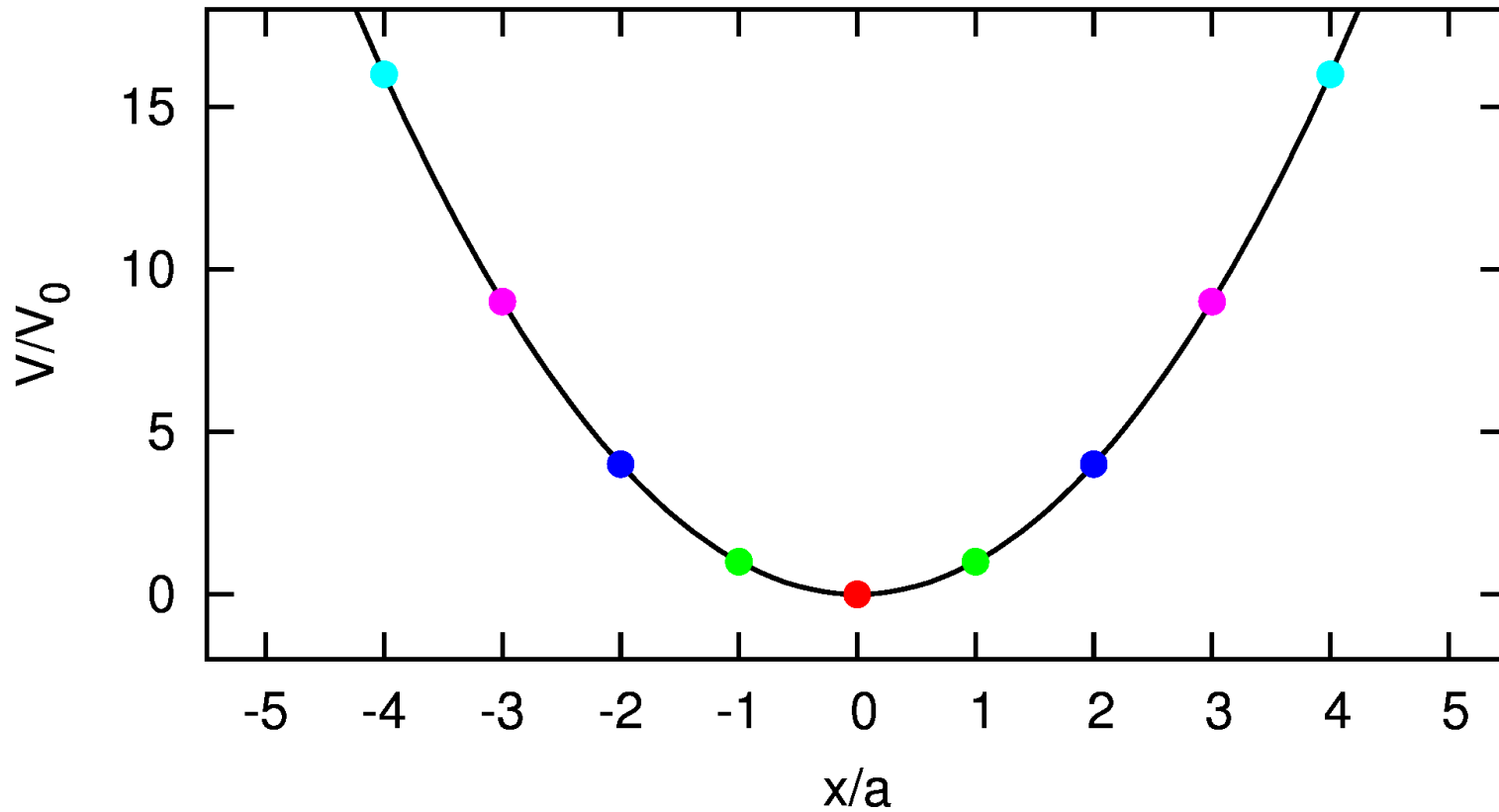
Note: impurity problem is **site-parallel**, lattice Dyson equation is **frequency-parallel**

All previous implementations: **RDMFT+NRG**

Simple approximation: “local density approximation (LDA)”

Approximate properties of each site by properties of homogeneous system with same effective chemical potential (\rightsquigarrow standard DMFT)

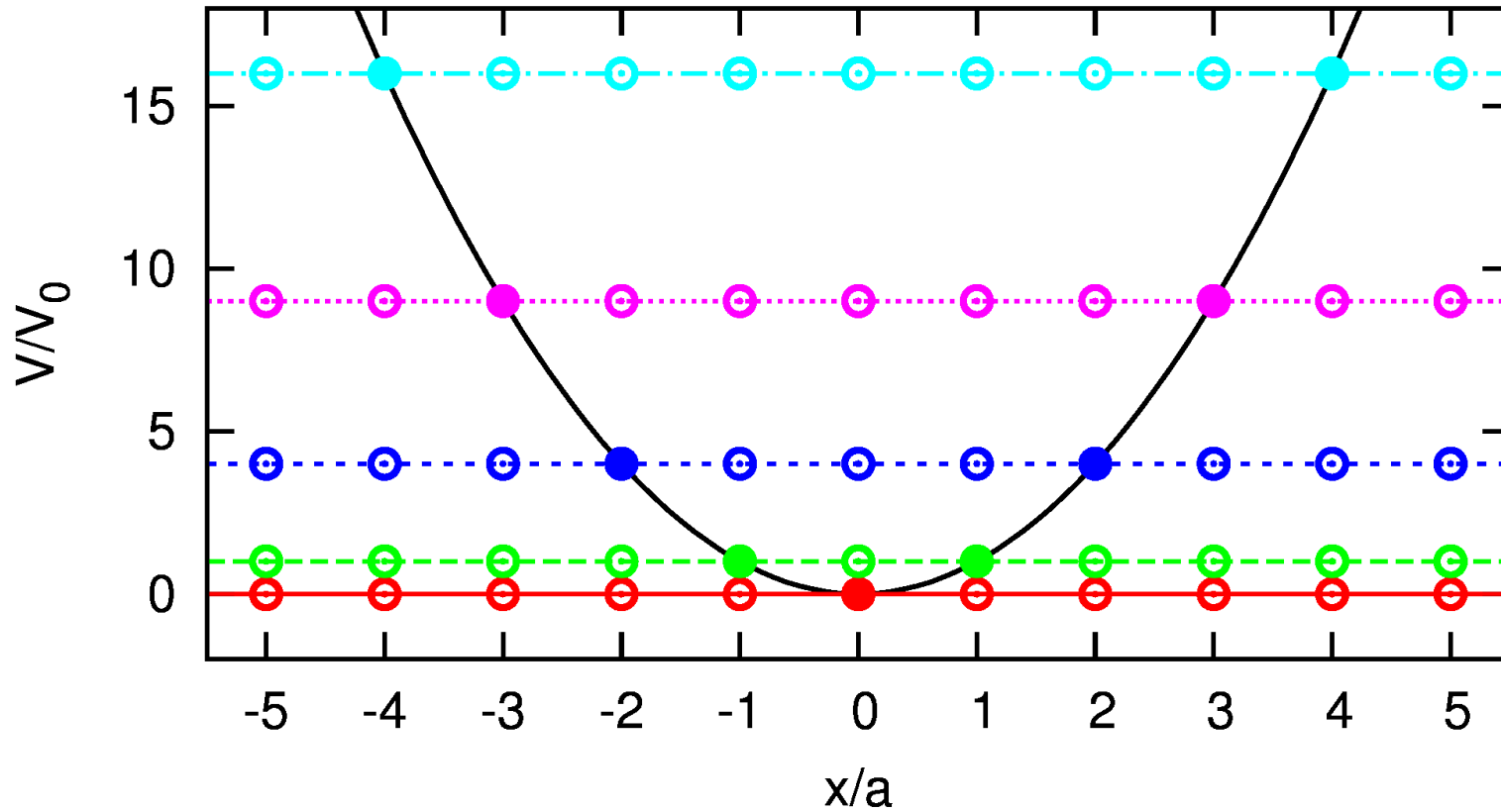
Example: 1d chain



Simple approximation: “local density approximation (LDA)”

Approximate properties of each site by properties of homogeneous system with same effective chemical potential (\rightsquigarrow standard DMFT)

Example: 1d chain



... will be used for comparison to RDMFT

RDMFT-NRG results in 2 dimensions ($T = 0$)

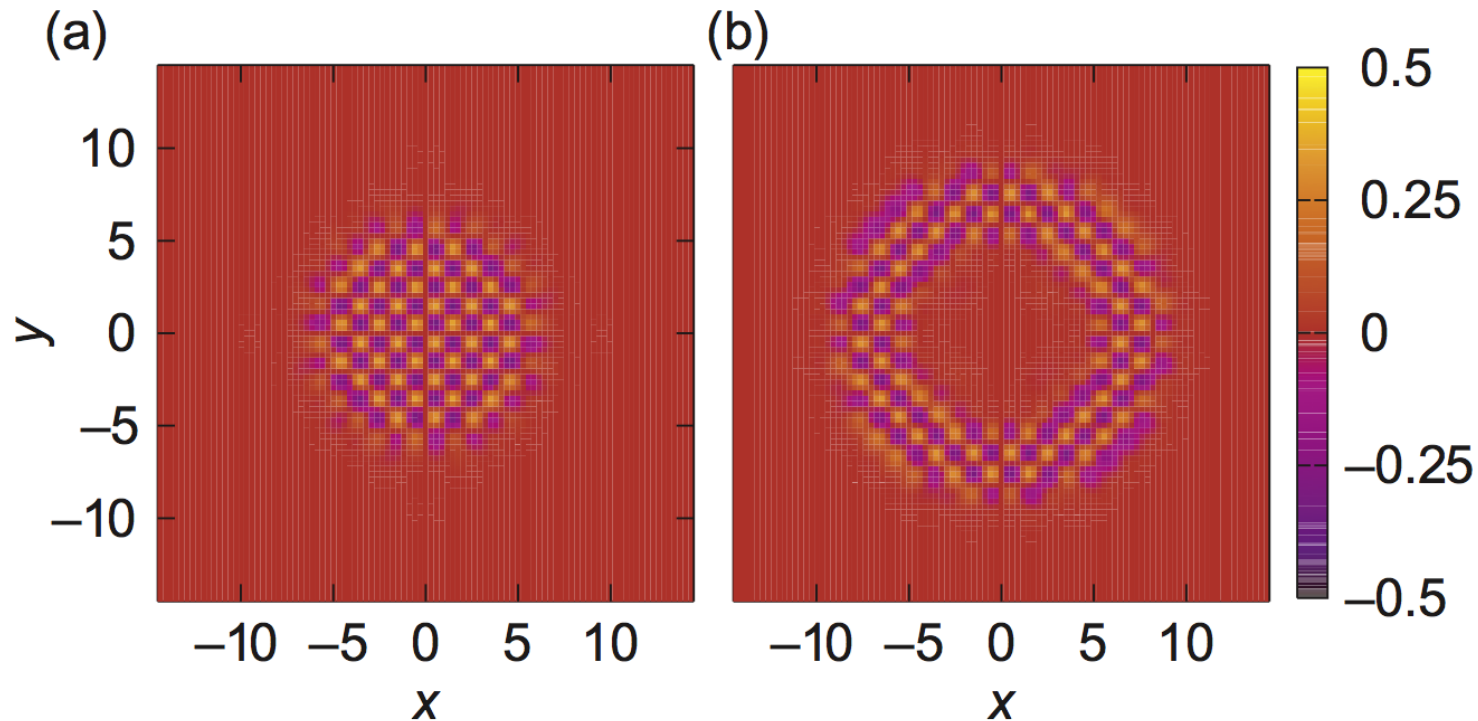
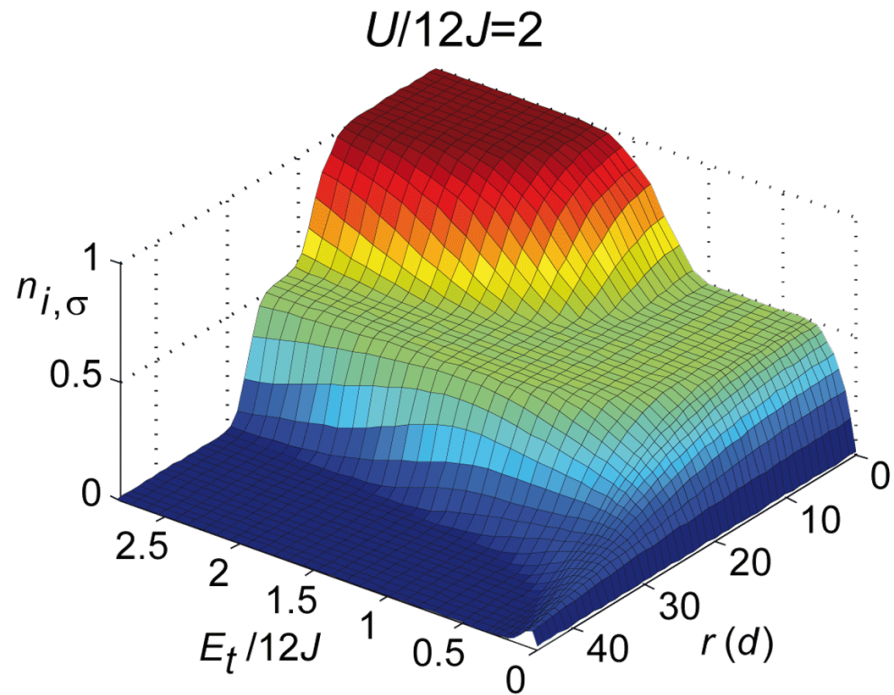


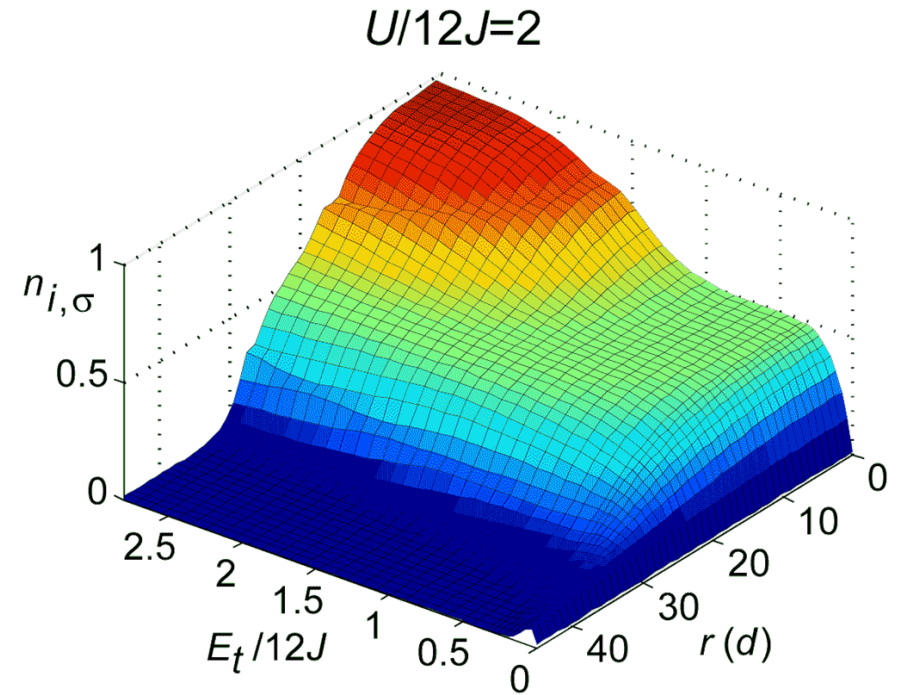
Figure 1. Real-space magnetization profiles for $U = 10$ on a square (30×30) lattice; (a) $V = 0.1$ and $\mu_{\uparrow} = \mu_{\downarrow} = 5$; (b) $V = 0.2$ and $\mu_{\uparrow} = \mu_{\downarrow} = 15$. Energies are expressed in units of the hopping parameter J .

[Snoek, Titvinidze, Töke, Byczuk, Hofstetter, *NJP* **10**, 093008 (2008)]

But: NRG problematic at elevated temperatures



$$T = 0.07t$$

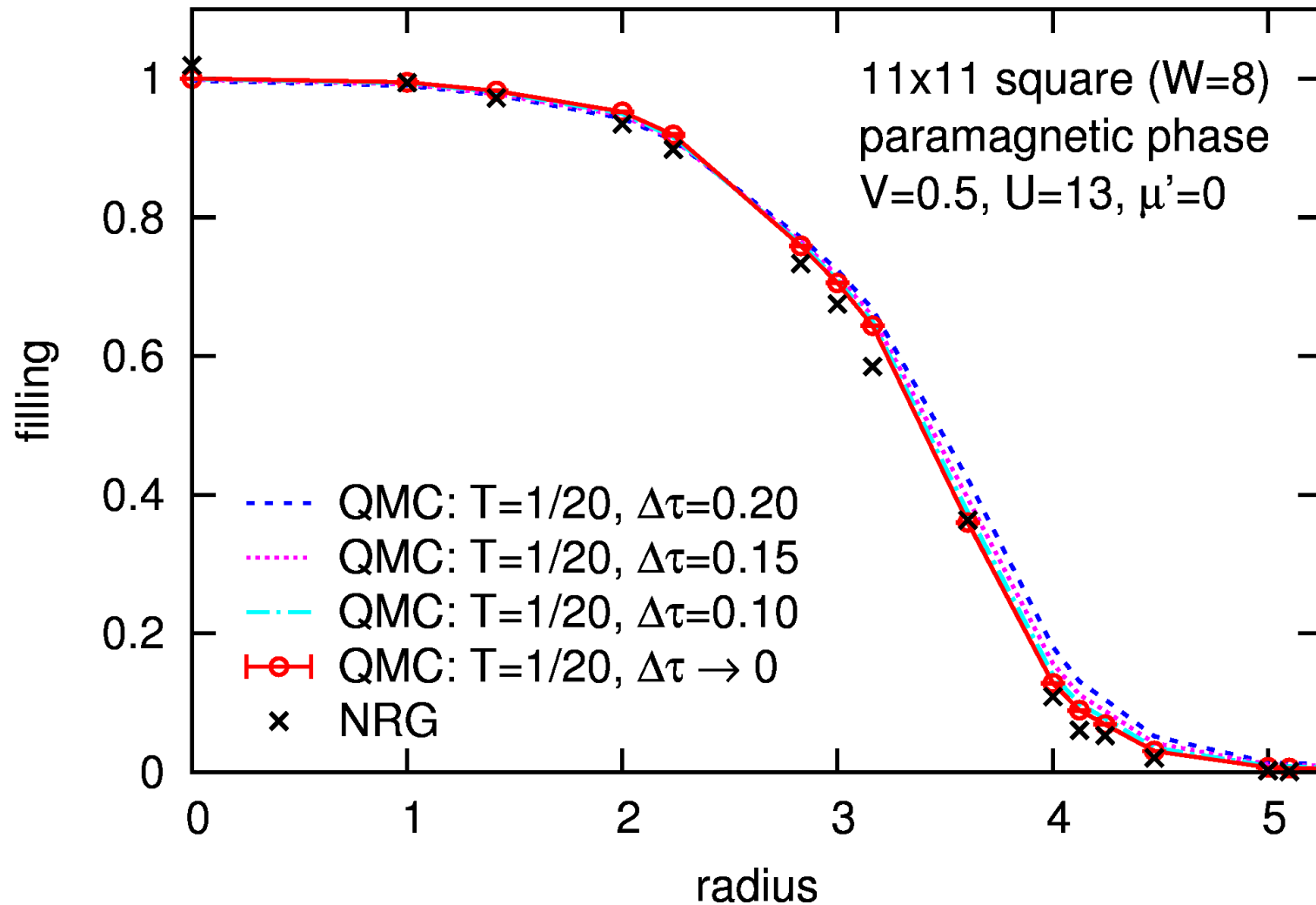


$$T = 0.15t$$

Additional plateau/kinks at $n_{\sigma} \approx 0.8$ for $T = 0.15t$ [Rosch group, courtesy of U. Schneider]

However: experimental temperatures are high \rightsquigarrow advantage for QMC!

Real-space DMFT results for paramagnetic phase: QMC vs. NRG



Good agreement QMC \leftrightarrow NRG (at low/zero T) not shown: NRG worse for AF

[NRG data by I. Titvinidze (collaboration within SFB/TR 49)]

Simulations of 3D systems with $\mathcal{O}(10^5)$ particles

Naive full RDMFT simulation of experimental situation requires $M=100^3$ lattice

Scaling: QMC CPU time $\propto M$

Green function memory $\propto M^2$

Green function inversion time $\propto M^3$

Simulations of 3D systems with $\mathcal{O}(10^5)$ particles

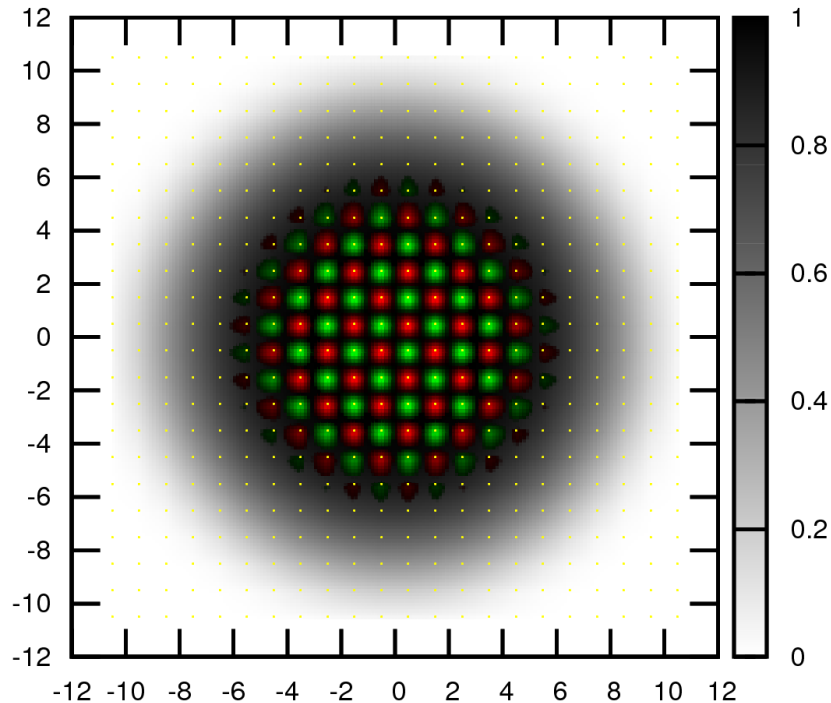
Naive full RDMFT simulation of experimental situation requires $M=100^3$ lattice

Scaling: QMC CPU time $\propto M$

Green function memory $\propto M^2$

Green function inversion time $\propto M^3$

Practical (dense inversion, fully parallel): $\lesssim 10000$ sites \rightsquigarrow need smart strategies



Simulations of 3D systems with $\mathcal{O}(10^5)$ particles

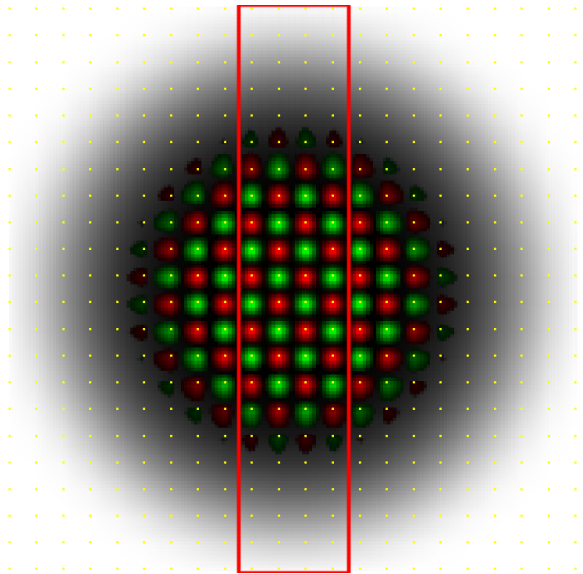
Naive full RDMFT simulation of experimental situation requires $M=100^3$ lattice

Scaling: QMC CPU time $\propto M$

Green function memory $\propto M^2$

Green function inversion time $\propto M^3$

Practical (dense inversion, fully parallel): $\lesssim 10000$ sites \rightsquigarrow need smart strategies



Simulations of 3D systems with $\mathcal{O}(10^5)$ particles

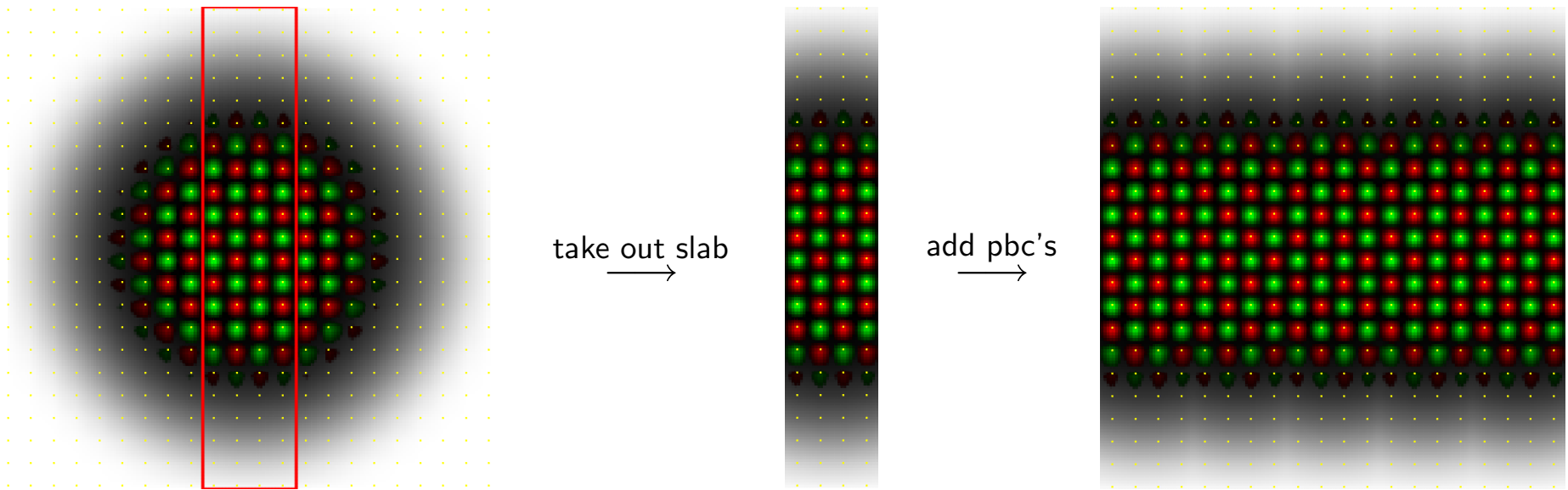
Naive full RDMFT simulation of experimental situation requires $M=100^3$ lattice

Scaling: QMC CPU time $\propto M$

Green function memory $\propto M^2$

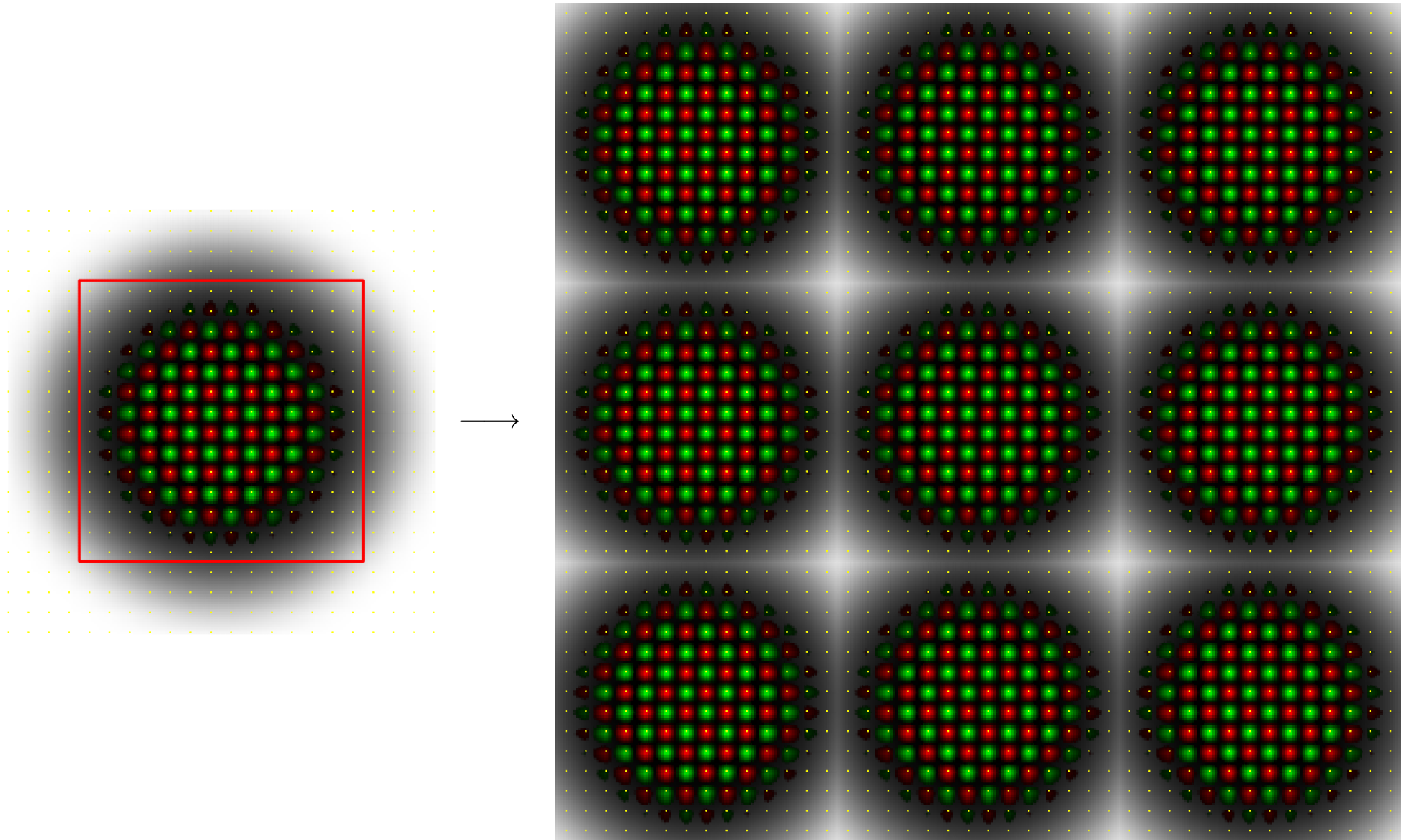
Green function inversion time $\propto M^3$

Practical (dense inversion, fully parallel): $\lesssim 10000$ sites \rightsquigarrow need smart strategies



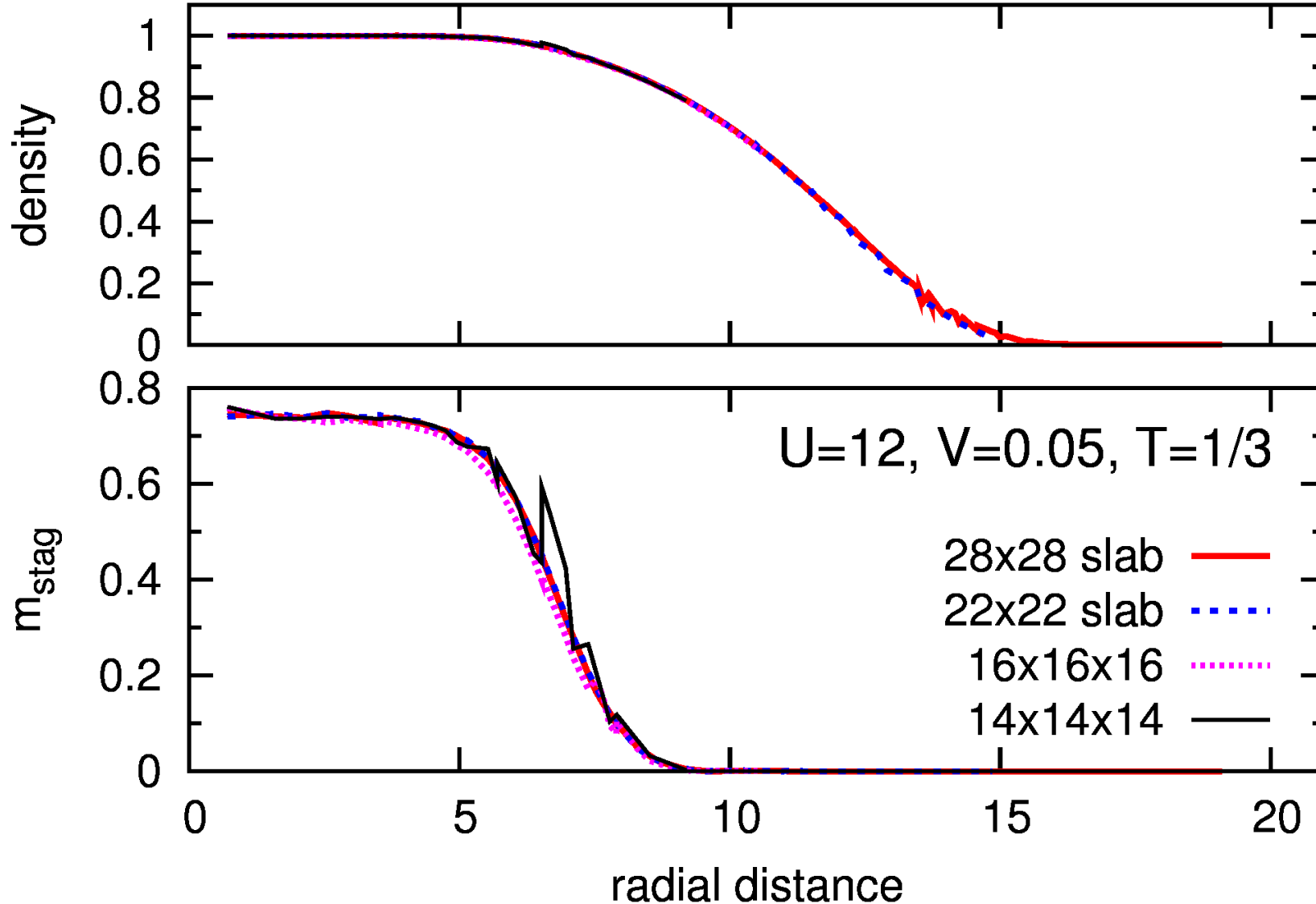
In practice: cylindrical potential (equivalent layers)

Alternative: 3D calculation, but focus on AF core (pbc's in all 3 directions):



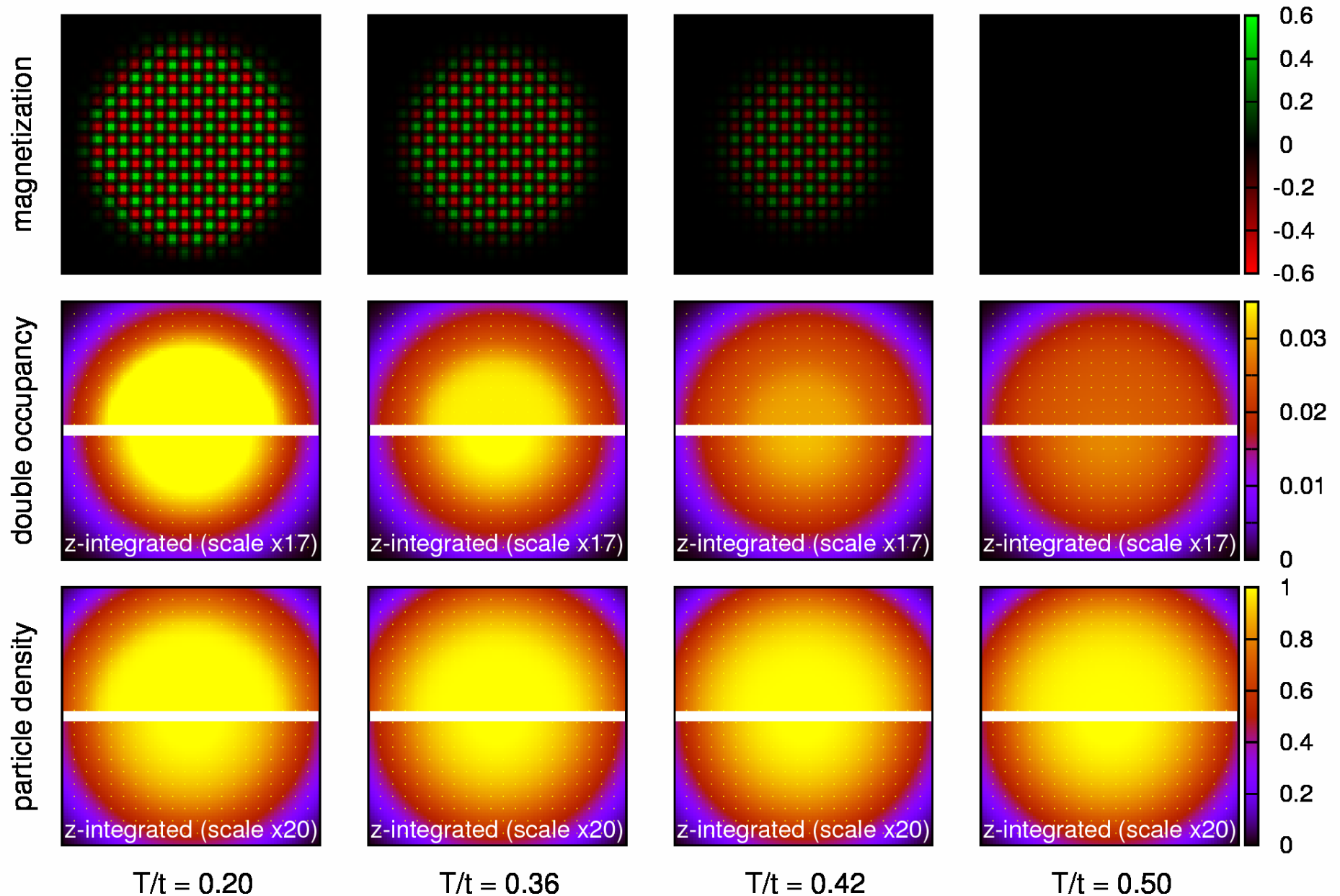
Most efficient: slab calculation focussing on AF core (with pbc)

Test: slab versus minimal core 3D calculation (all with pbc)

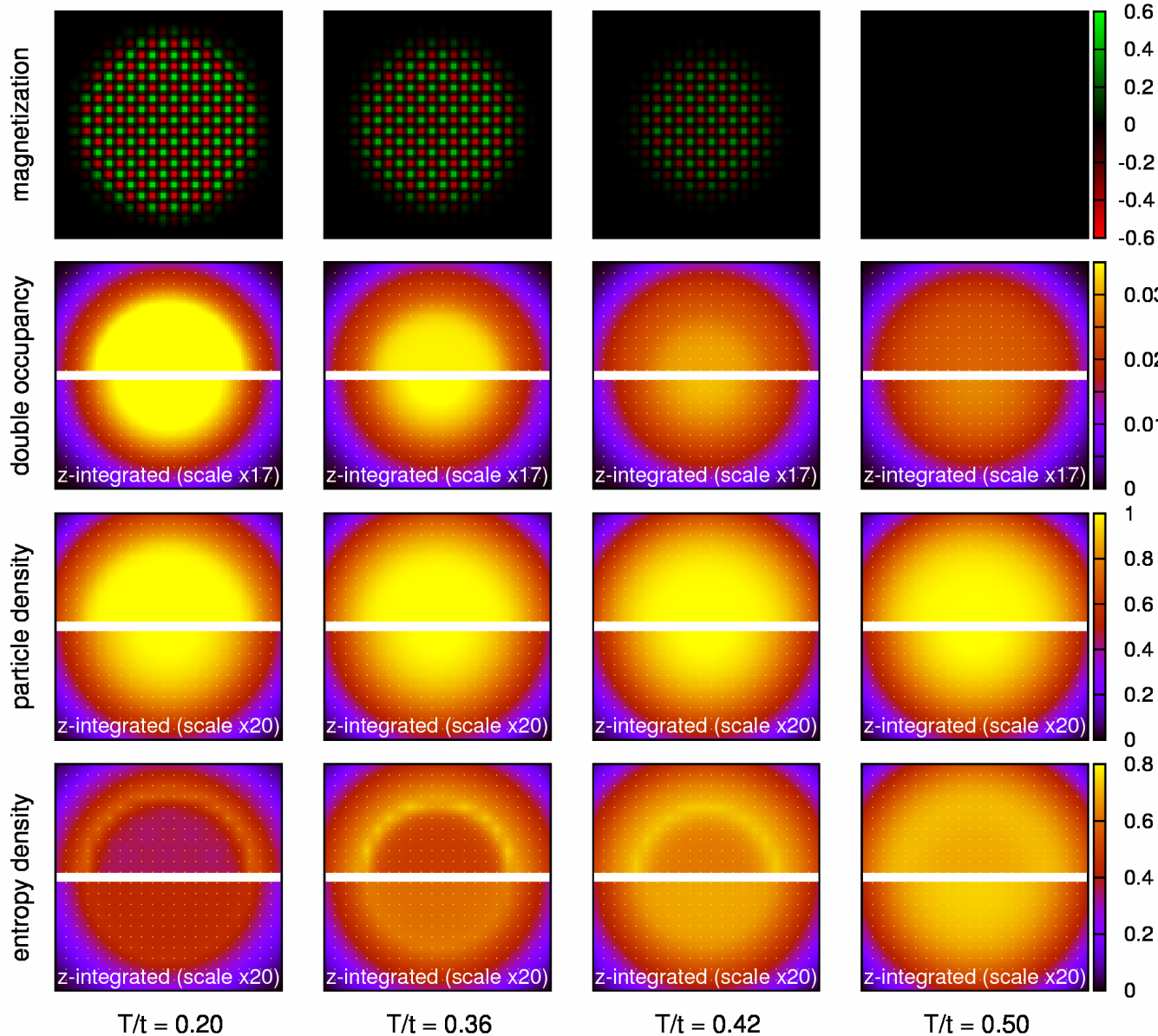


Significant deviations only if core touches boundaries!

RDMFT-QMC results (cubic lattice, $V = 0.05t$, $U = W = 12t$)



RDMFT-QMC results (cubic lattice, $V = 0.05t$, $U = W = 12t$)



AF core:

nearly fully polarized at
 $T = 0.20t$

vanishes at $T_N \approx 0.46t$

AF \leftrightarrow enhanced $D!$

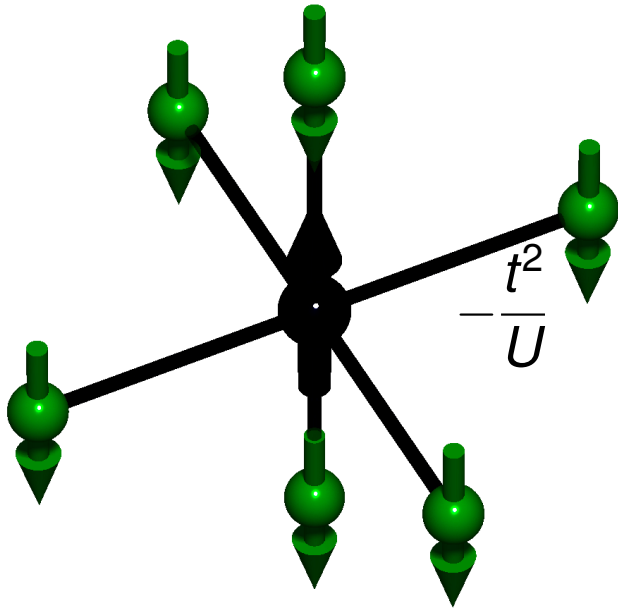
~ 6000 atoms
(naively $\sim 30^3 = 27000$
sites needed)

Entropy

$$S = \int_{-\infty}^0 d\mu' \frac{dN}{dT}$$

Enhanced double occupancy: a signature of AF order

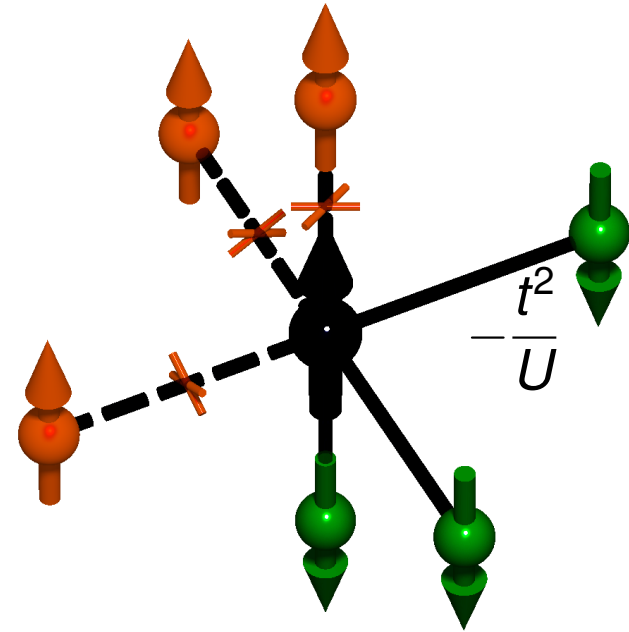
Illustration of mechanism for enhanced double occupancy (at strong coupling):



AF state:

electron can hop to all
 $Z = 6$ next neighbors

$$E_{\text{AF}} = -\frac{Z t^2}{U}$$



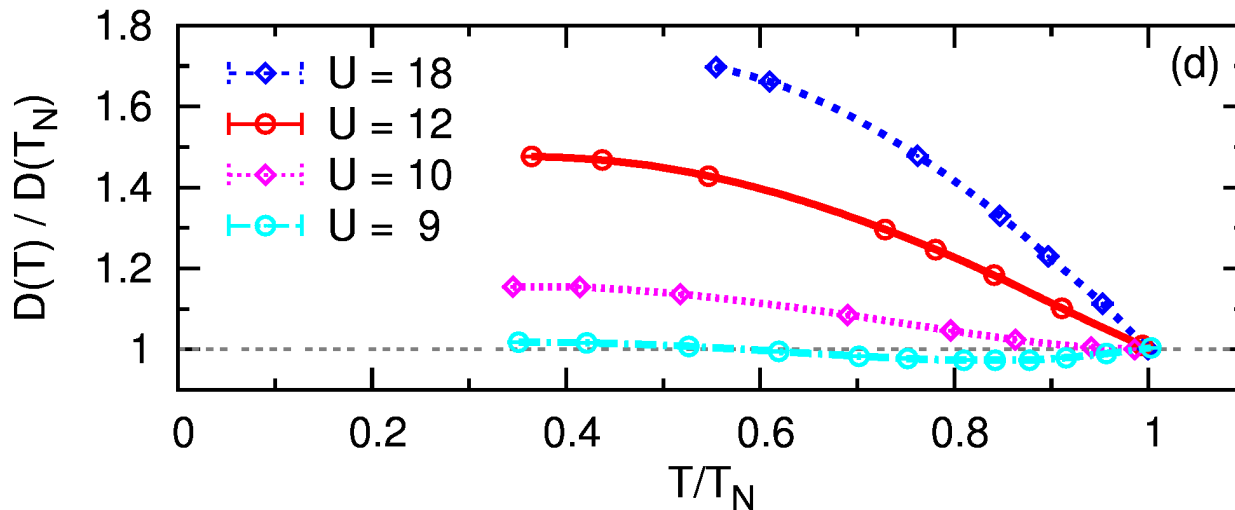
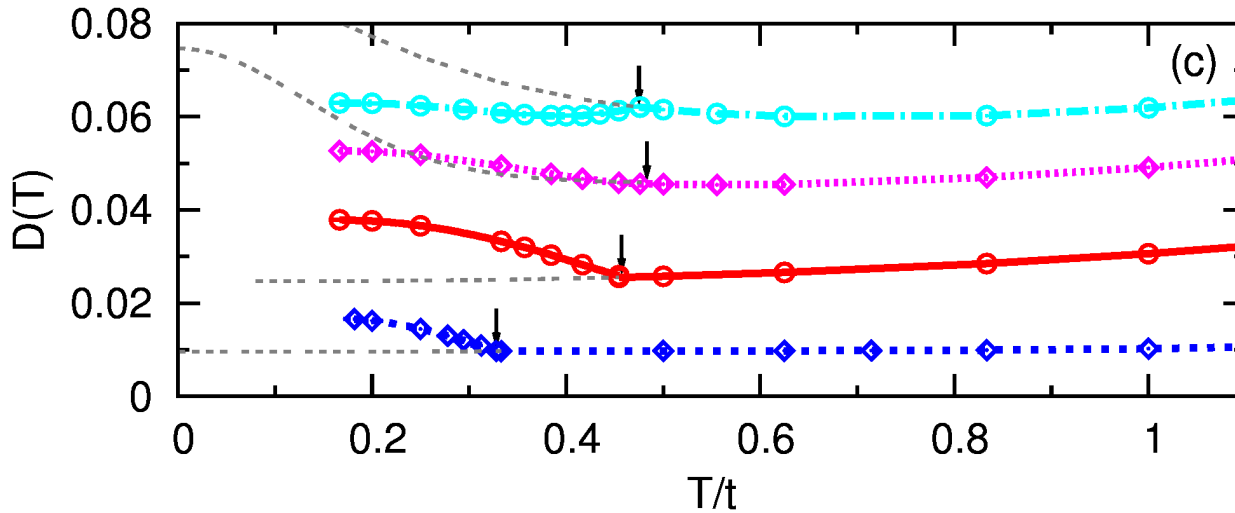
Paramagnetic state:

1/2 of the neighboring sites
are forbidden for hopping

$$E_{\text{p}} = -\frac{Z t^2}{2U}$$

By $D = dE/dU$ (at $T = 0$), the argument implies $D_{\text{AF}}/D_{\text{p}} \xrightarrow{U \rightarrow \infty} 2$.

DMFT-QMC estimates of D at half filling



AF \Rightarrow

enhanced D at $U \gtrsim 10t$

arrows: Néel temperatures

thin lines: metastable paramagnetic phase.

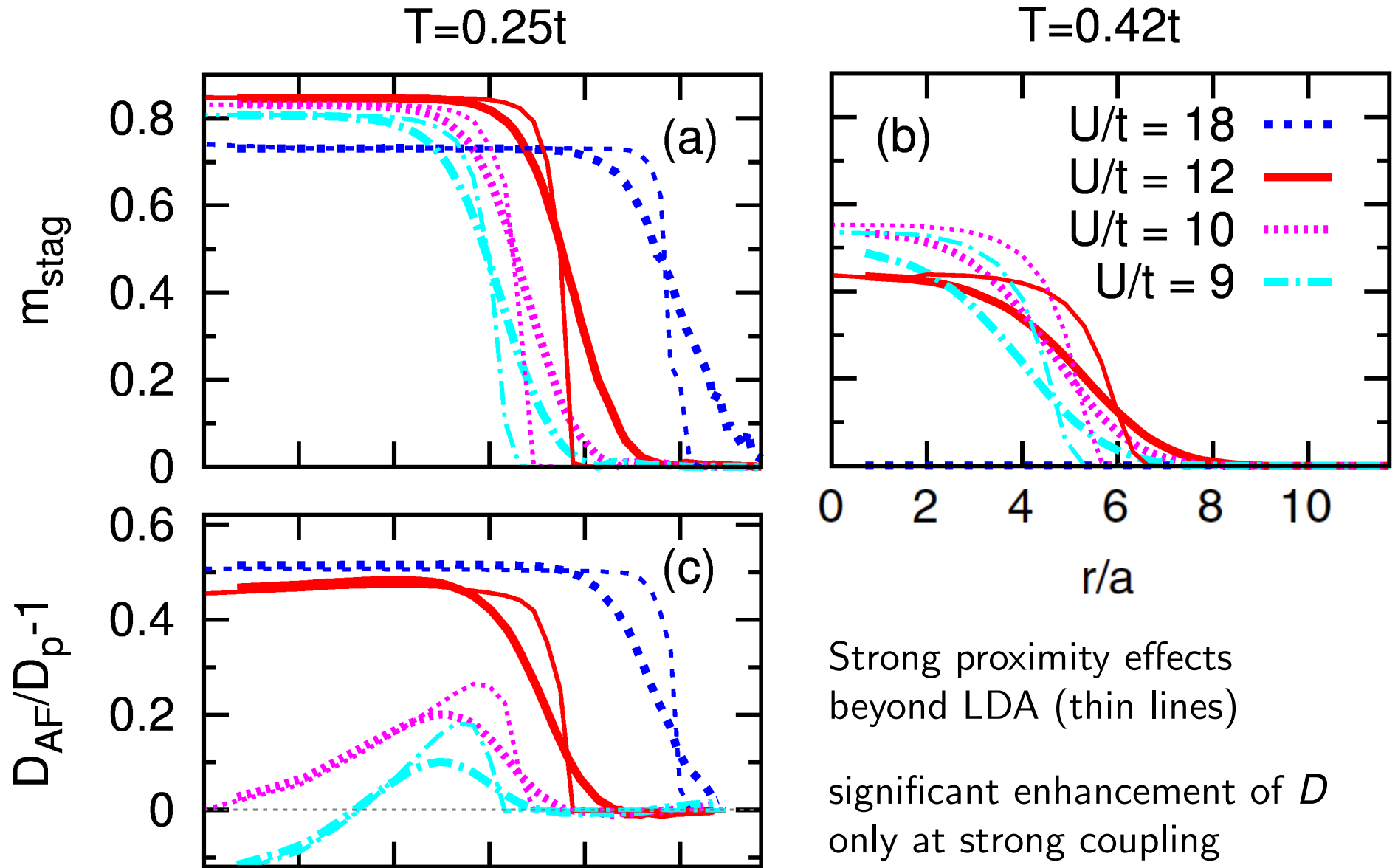
Data scaled to values of critical point:

relative enhancement

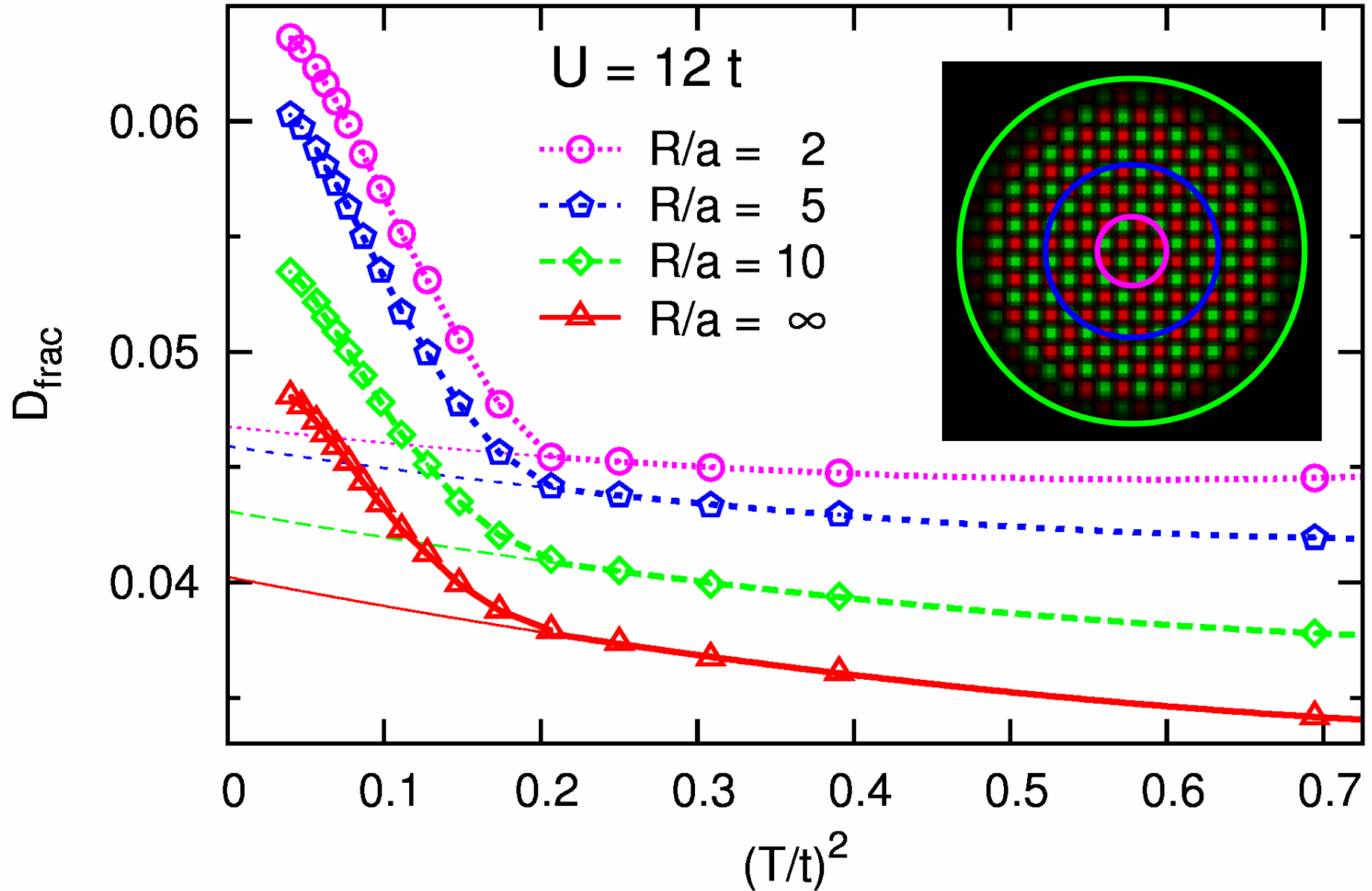
$$D/D(T_N) \xrightarrow{U \rightarrow \infty} 2$$

Note: AF kills Pomeranchuk cooling [Werner, Parcollet, Georges, Hassan, PRL (2005)]!

Radial dependence of m_{stag} and D : RDMFT calculations ($V = 0.05t$)

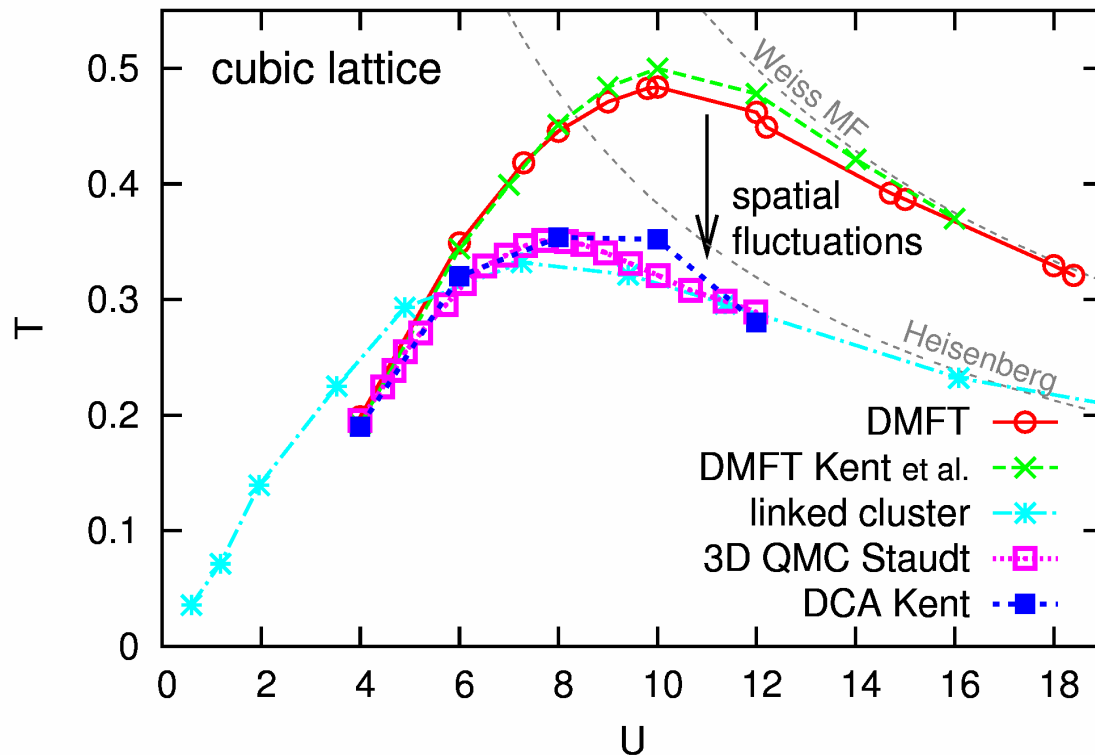
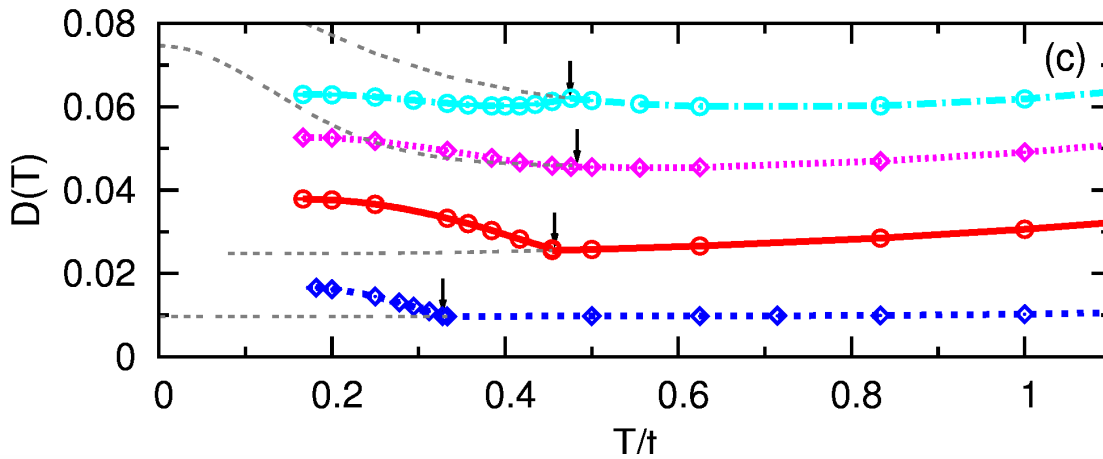


Néel transition visible in integrated quantities? Yes!

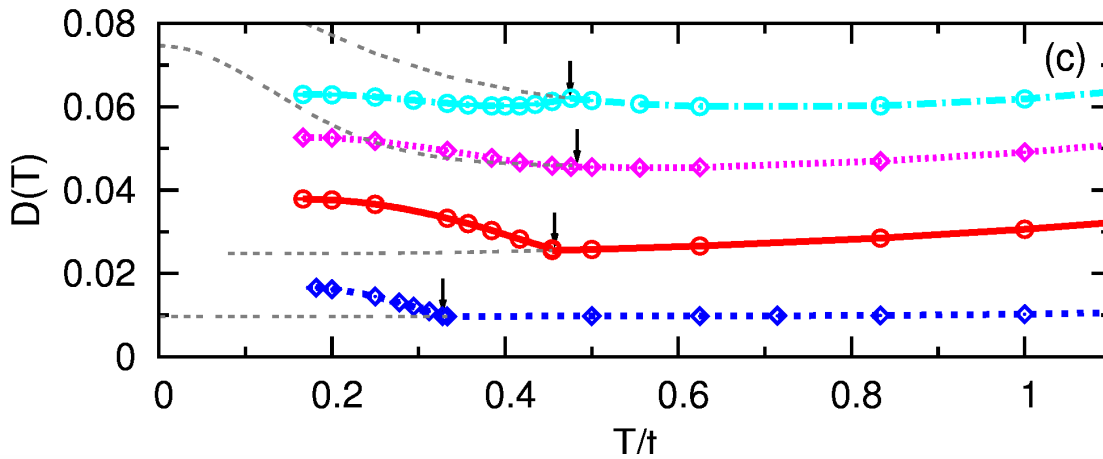


Effects of nonlocal correlations?

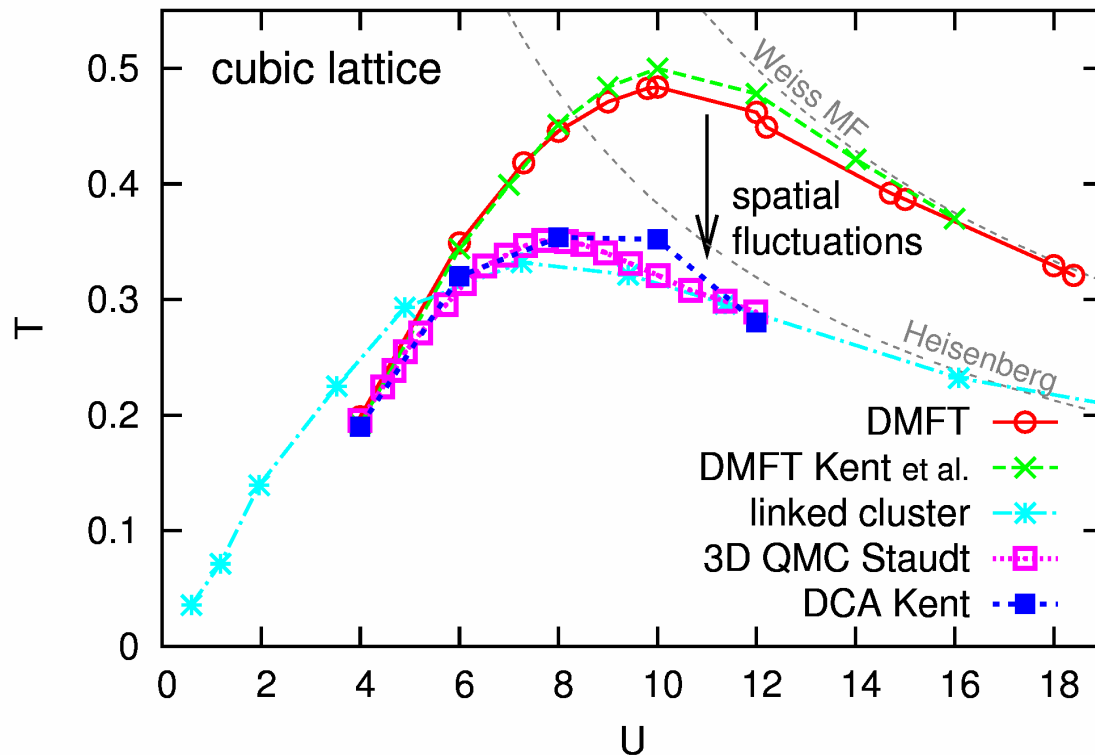
Modification of DMFT predictions by spatial fluctuations in 3d: how?



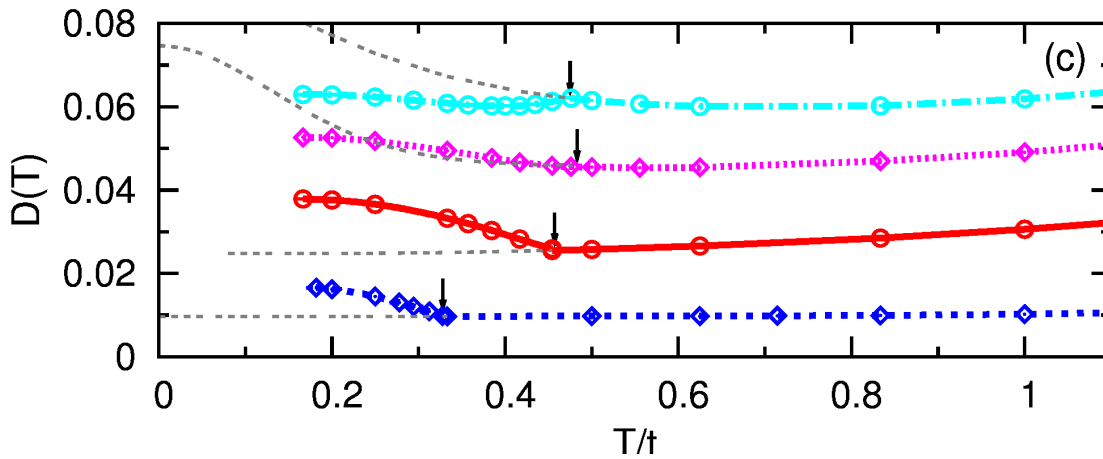
Modification of DMFT predictions by spatial fluctuations in 3d: how?



Unavoidable change: kinks cannot remain at $T = T_N^{\text{DMFT}} > T_N!$



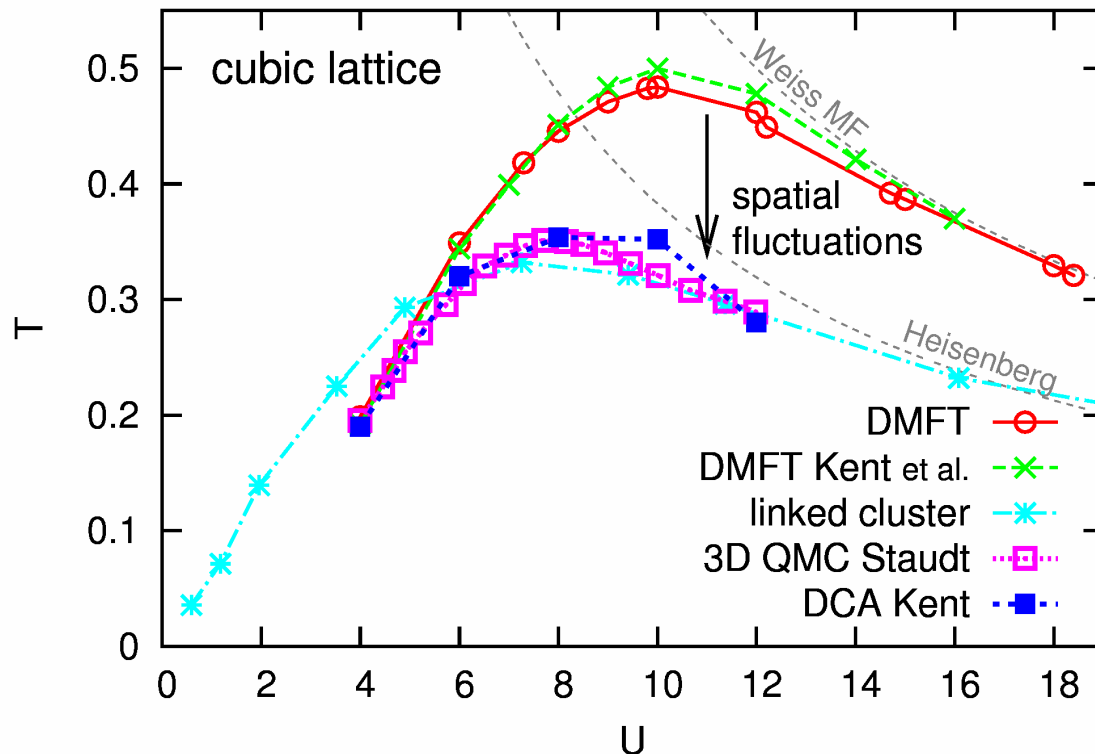
Modification of DMFT predictions by spatial fluctuations in 3d: how?



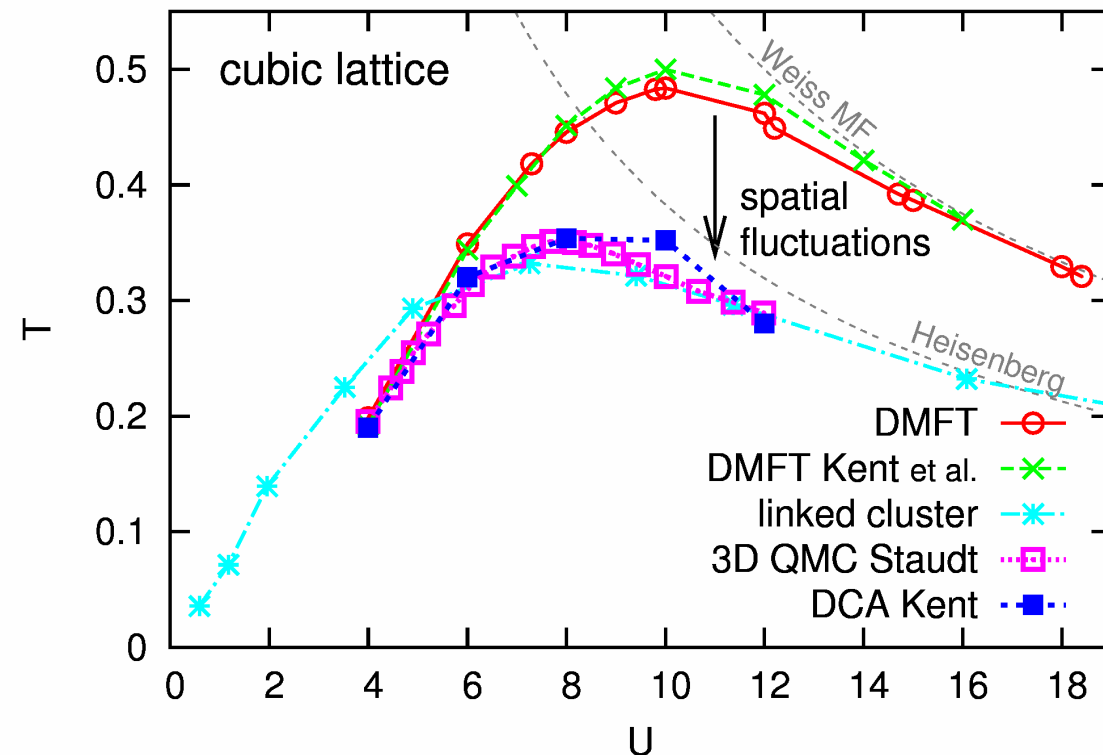
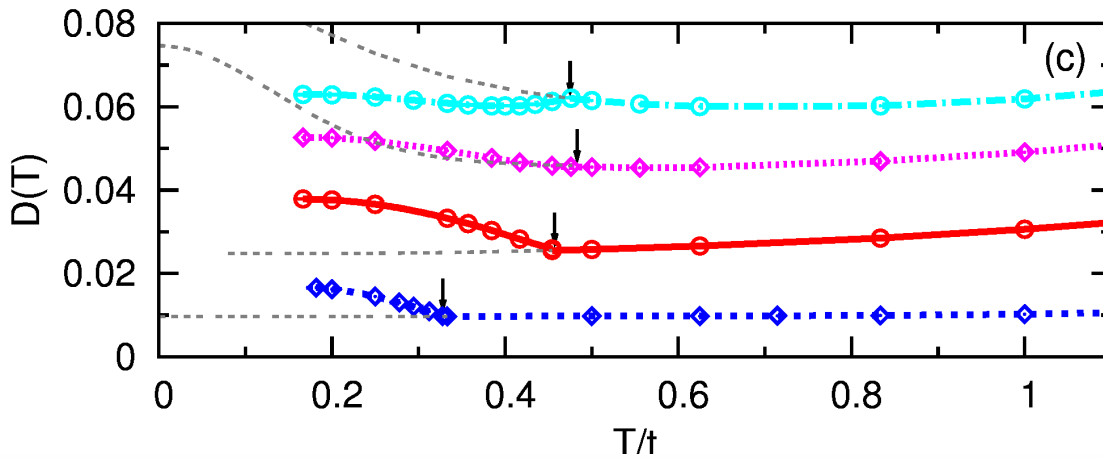
Unavoidable change: kinks cannot remain at $T = T_N^{\text{DMFT}} > T_N!$

Constraints:

- DMFT results for $D(T)$ agree with high- T expansion at $T \gg T_N$ [Jördens et al., PRL (2010)]



Modification of DMFT predictions by spatial fluctuations in 3d: how?

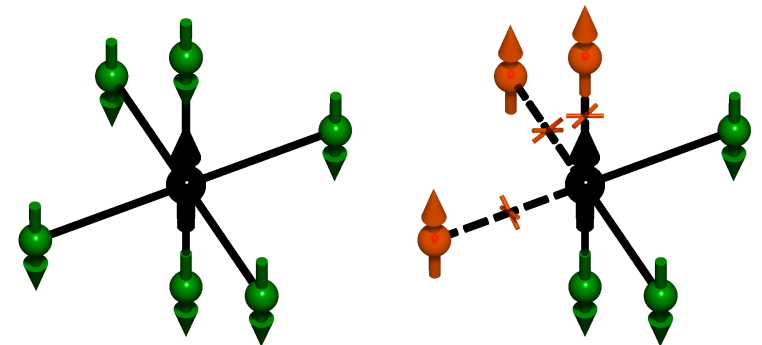


Unavoidable change: kinks cannot remain at $T = T_N^{\text{DMFT}} > T_N!$

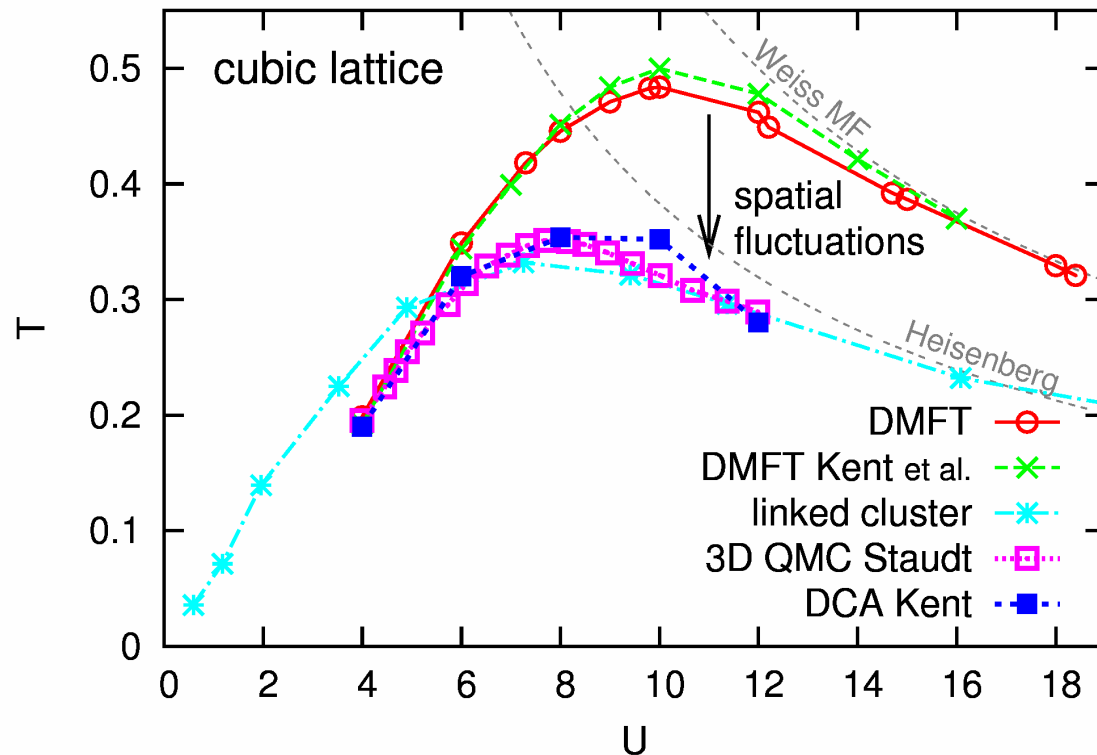
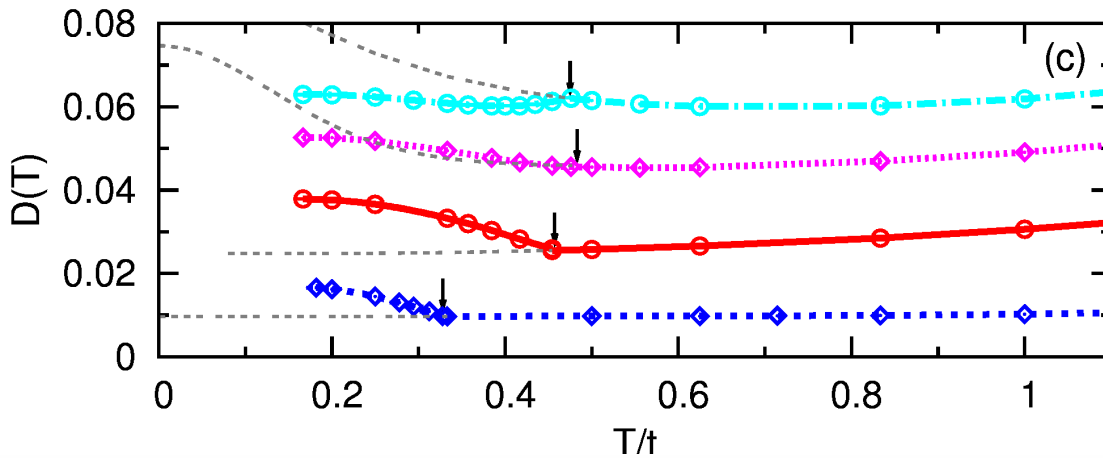
Constraints:

- DMFT results for $D(T)$ agree with high- T expansion at $T \gg T_N$ [Jördens et al., PRL (2010)]

- argument for $D_{\text{AF}}/D_{\text{para}} \xrightarrow{U \rightarrow \infty} 2$ is independent of dimension



Modification of DMFT predictions by spatial fluctuations in 3d: how?

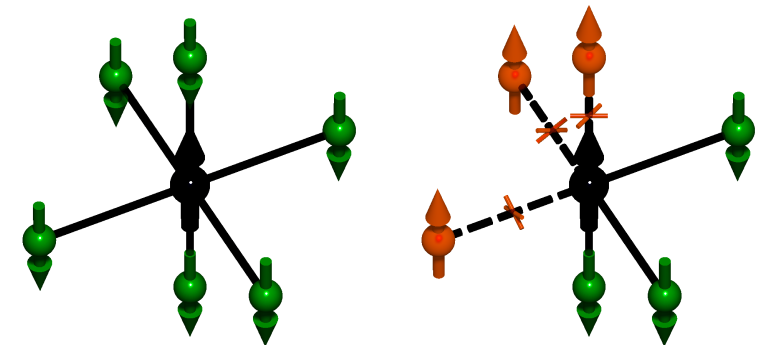


Unavoidable change: kinks cannot remain at $T = T_N^{\text{DMFT}} > T_N!$

Constraints:

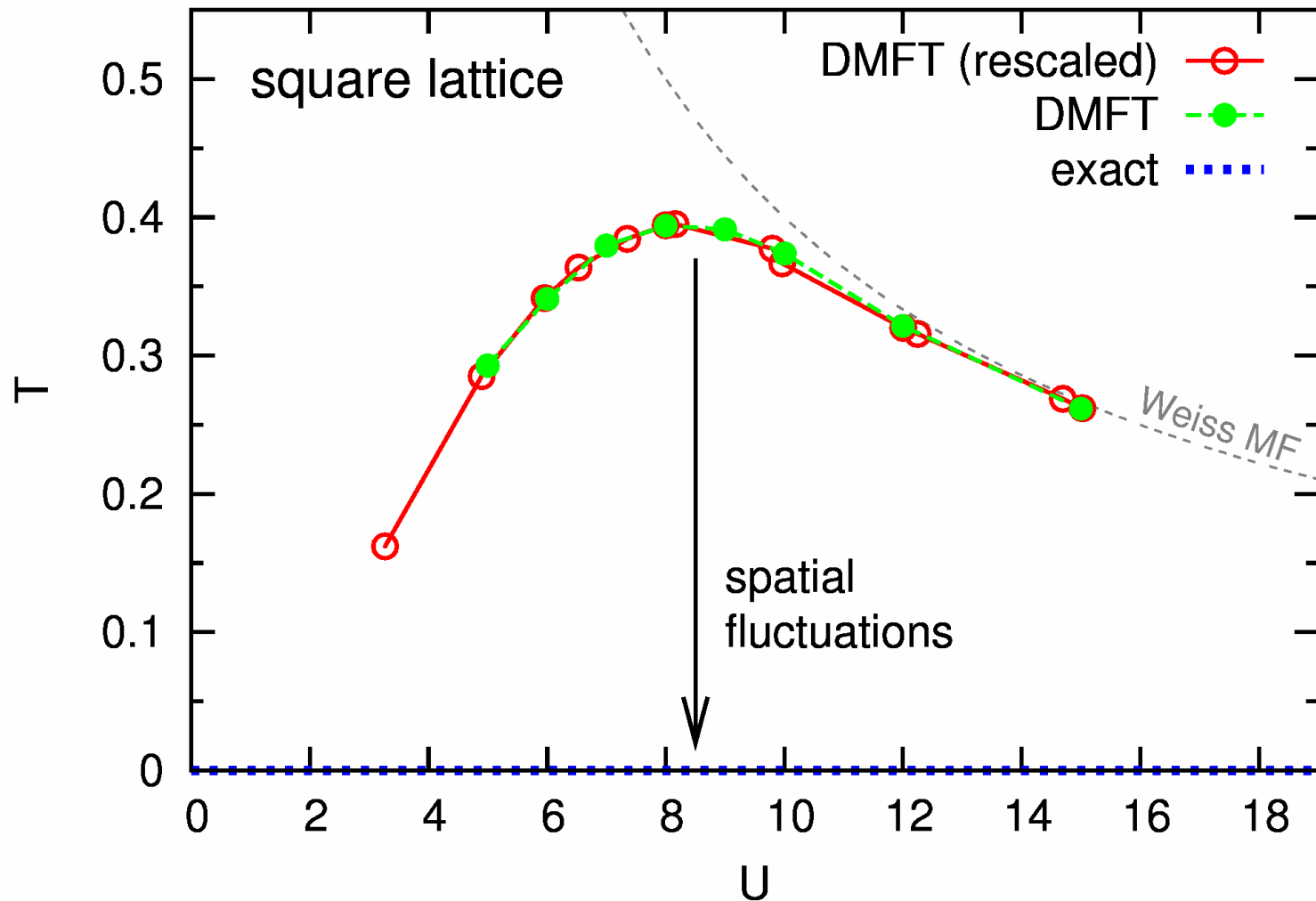
- DMFT results for $D(T)$ agree with high- T expansion at $T \gg T_N$ [Jördens et al., PRL (2010)]

- argument for $D_{\text{AF}}/D_{\text{para}} \xrightarrow{U \rightarrow \infty} 2$ is independent of dimension



and independ. of long-range order

Situation “worse” in 2d: no antiferromagnetism at finite T !



Will any enhancement of D at low T remain? At which temperature scale?

How large are the DMFT errors in $D(T)$ for $T \gtrsim T_N^{\text{DMFT}}$?

Fermions in 2D Optical Lattices: Temperature and Entropy Scales for Observing Antiferromagnetism and Superfluidity

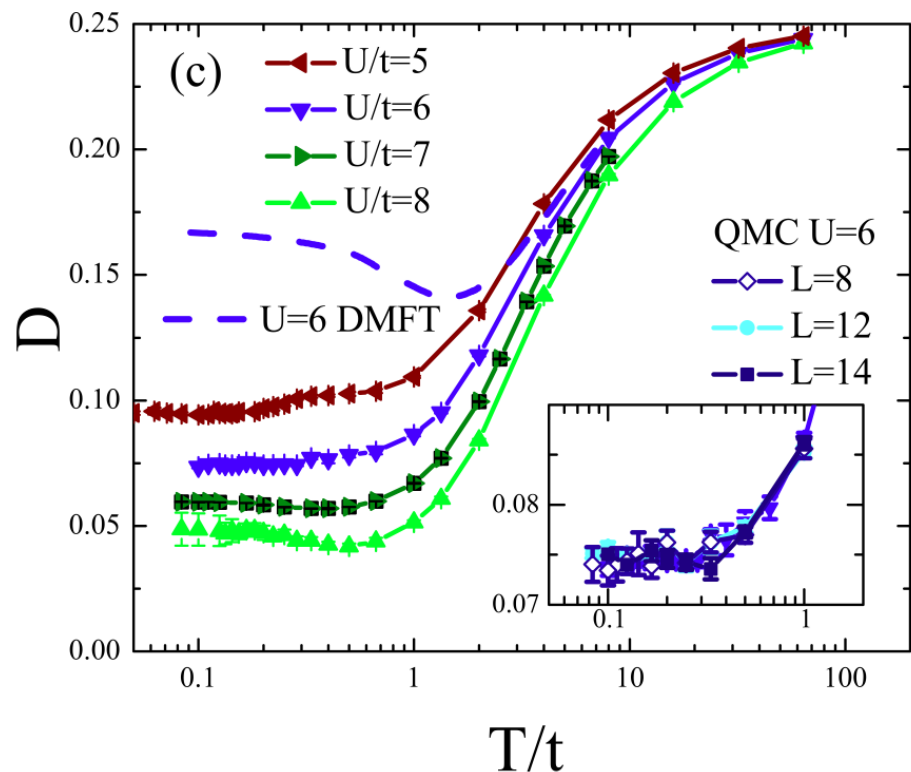
Thereza Paiva,¹ Richard Scalettar,² Mohit Randeria,³ and Nandini Trivedi³

¹*Instituto de Física, Universidade Federal do Rio de Janeiro Cx.P. 68.528, 21941-972 Rio de Janeiro RJ, Brazil*

²*Department of Physics, University of California, Davis, California 95616, USA*

³*Department of Physics, The Ohio State University, Columbus, Ohio 43210, USA*

(Received 18 June 2009; published 11 February 2010)



Fermions in 2D Optical Lattices: Temperature and Entropy Scales for Observing Antiferromagnetism and Superfluidity

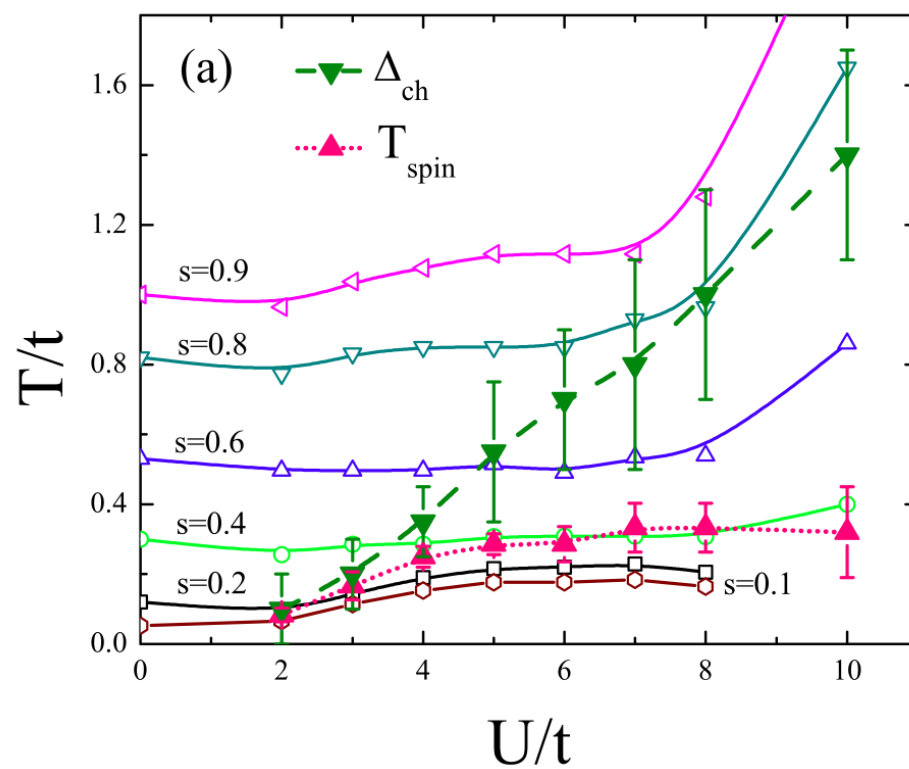
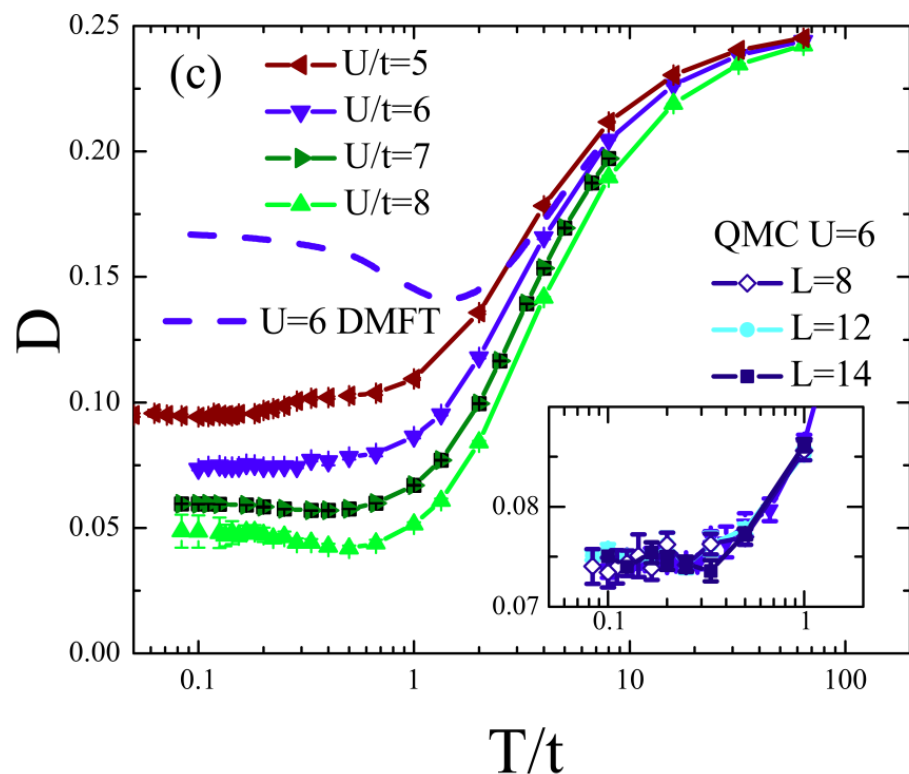
Thereza Paiva,¹ Richard Scalettar,² Mohit Randeria,³ and Nandini Trivedi³

¹*Instituto de Física, Universidade Federal do Rio de Janeiro Cx.P. 68.528, 21941-972 Rio de Janeiro RJ, Brazil*

²*Department of Physics, University of California, Davis, California 95616, USA*

³*Department of Physics, The Ohio State University, Columbus, Ohio 43210, USA*

(Received 18 June 2009; published 11 February 2010)



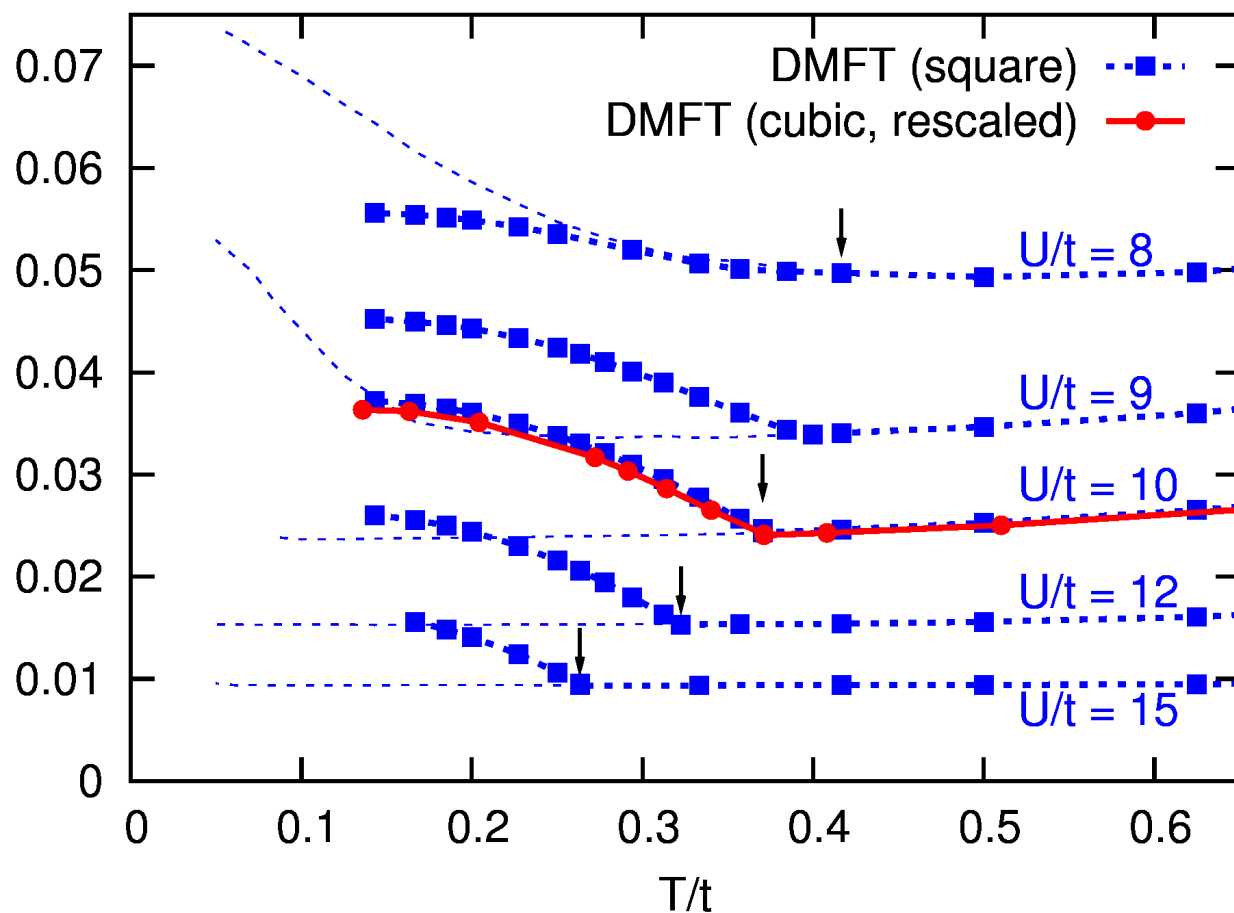
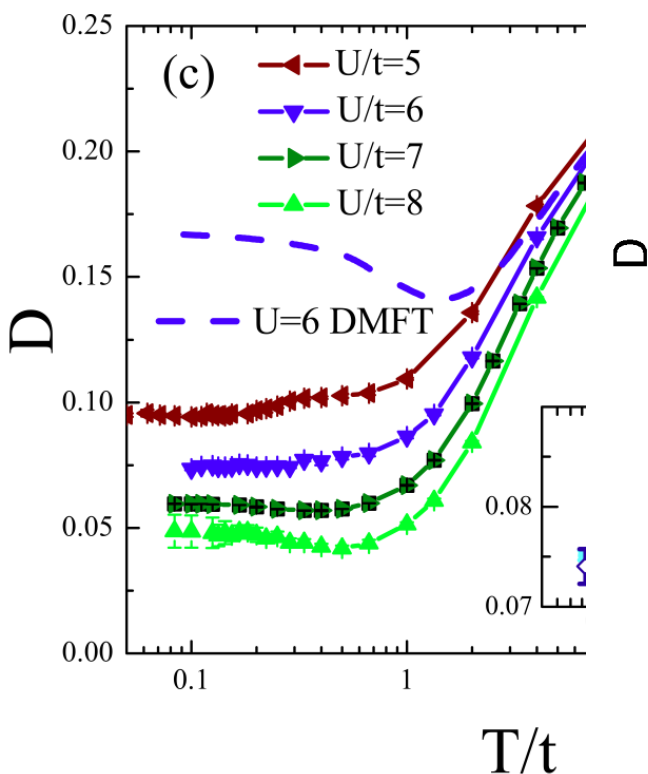
Fermions in 2D Optical Lattices: Temperature and Entropy Scales for Observing Antiferromagnetism and Superfluidity

Thereza Paiva,¹ Richard Scalettar,² Mohit Randeria,³ and Nandini Trivedi³

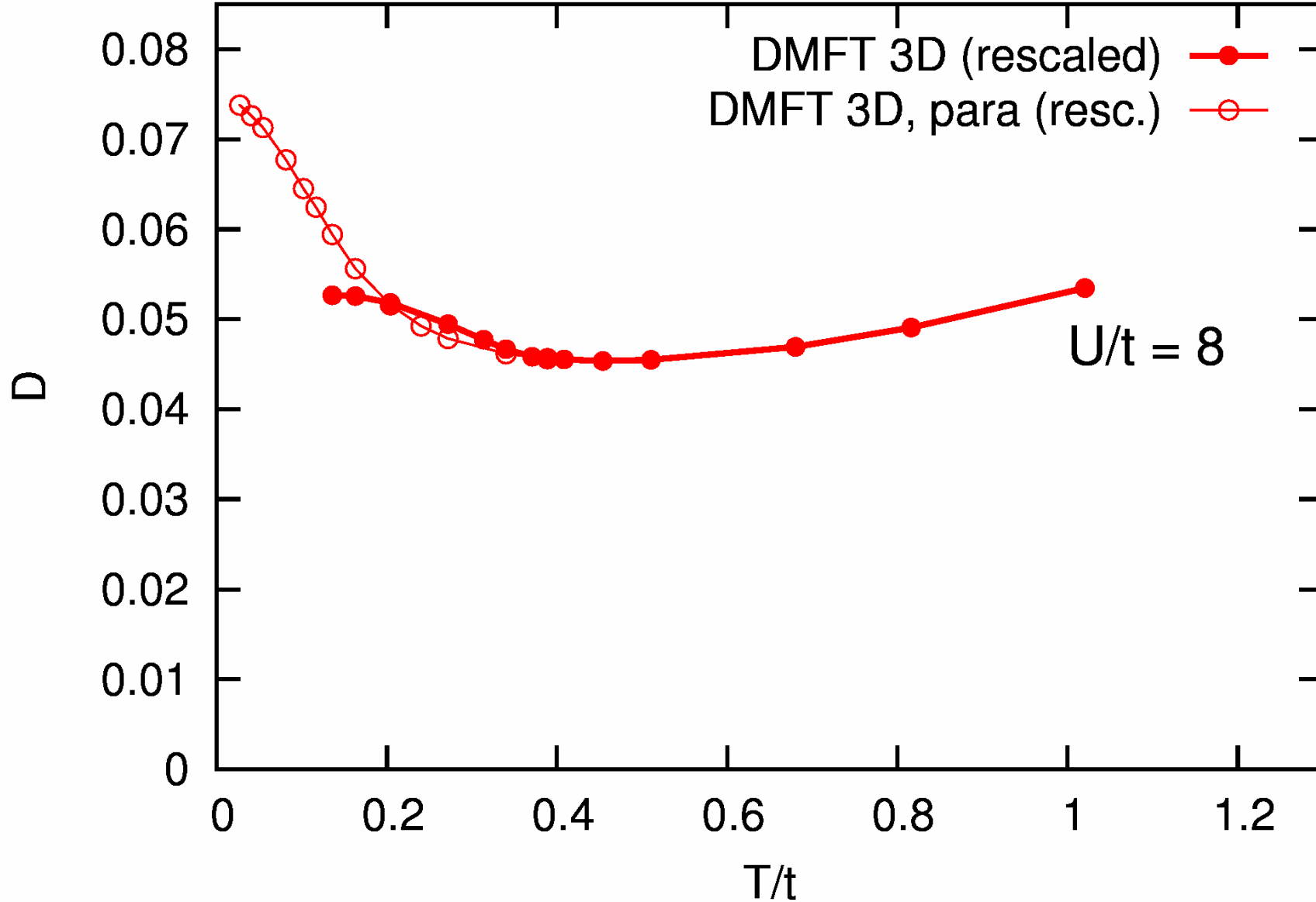
¹Instituto de Física, Universidade

²Department of Physics, University of

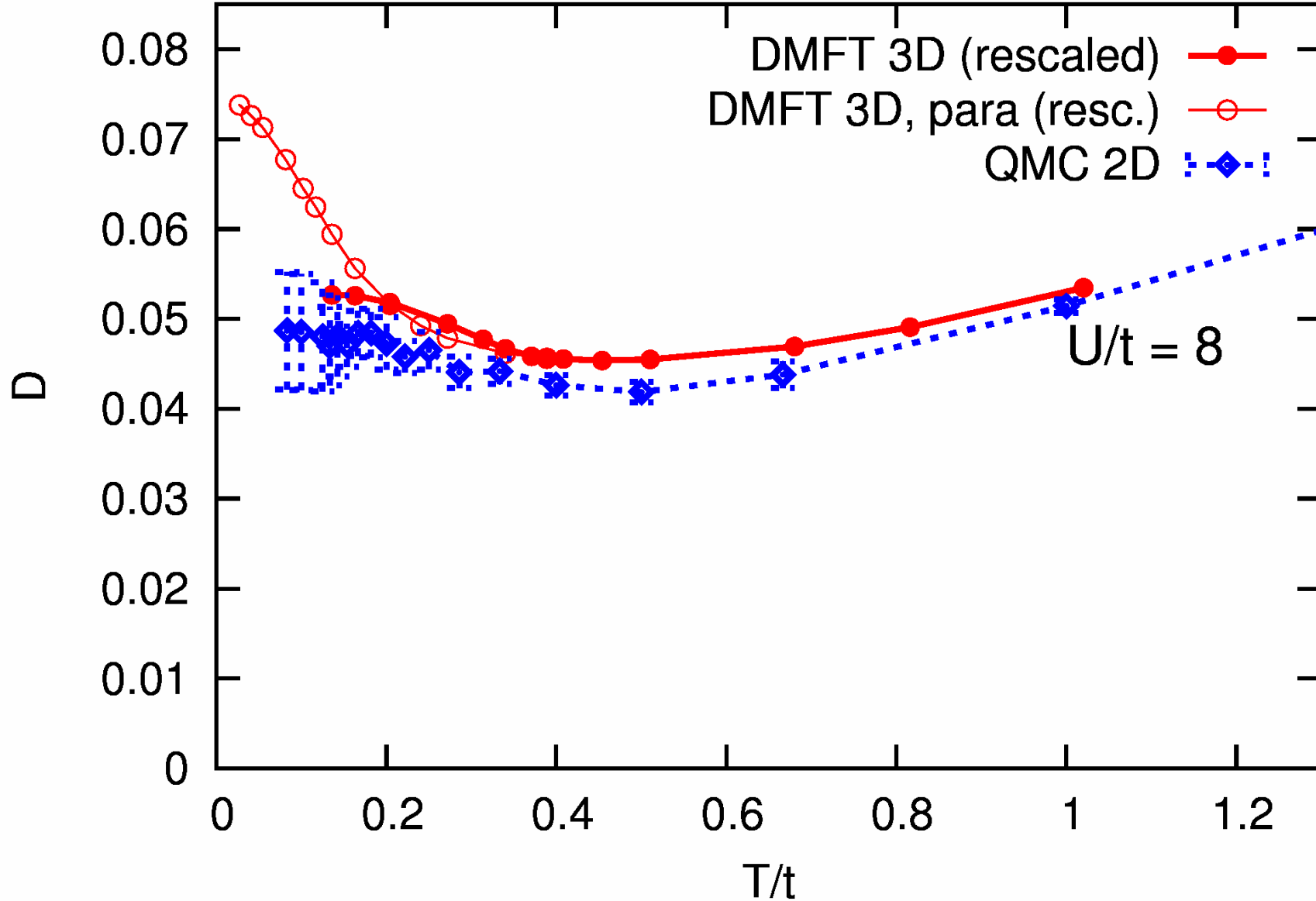
³Department of Physics, University of



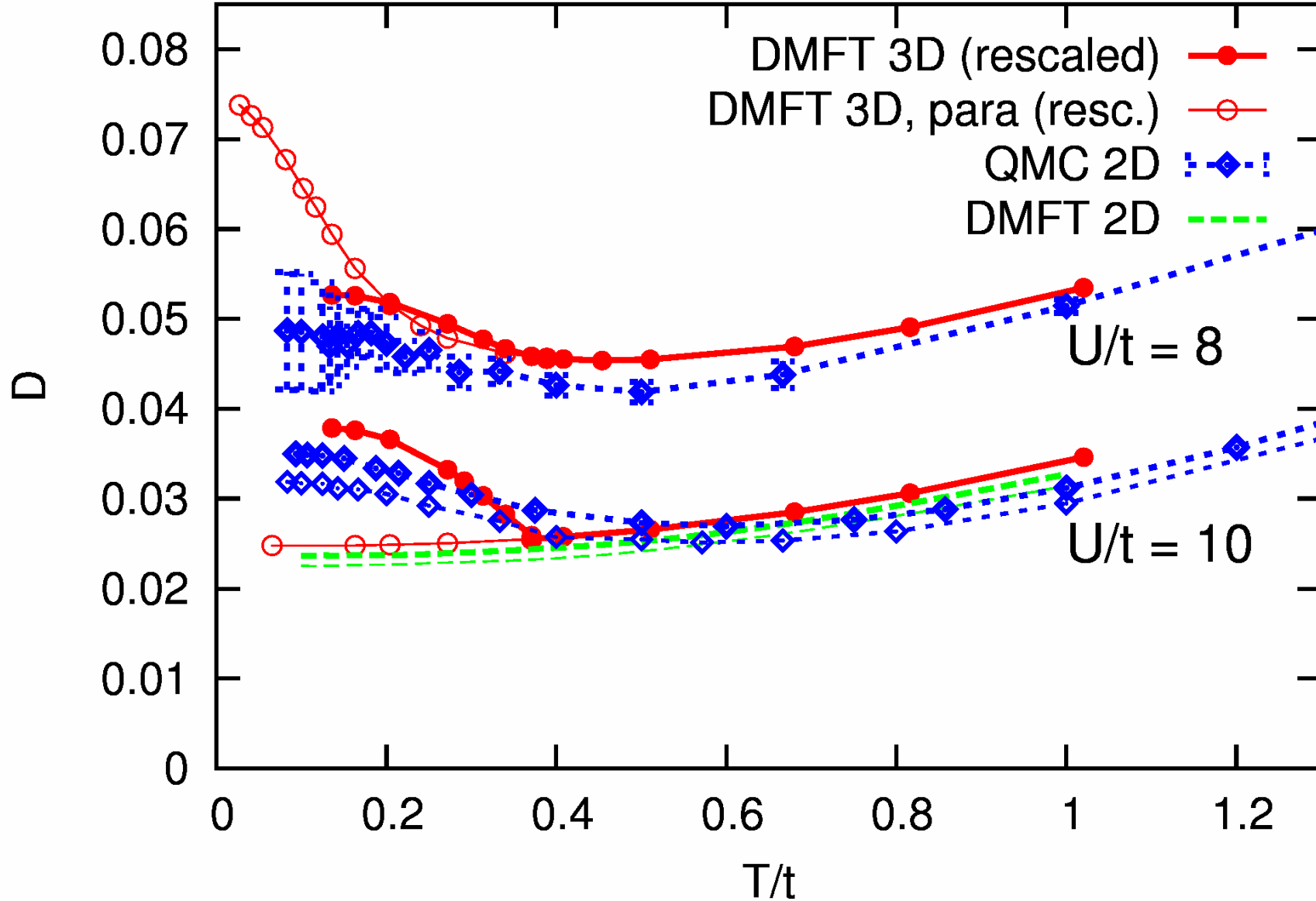
Comparison DMFT – direct QMC for the 2d square lattice

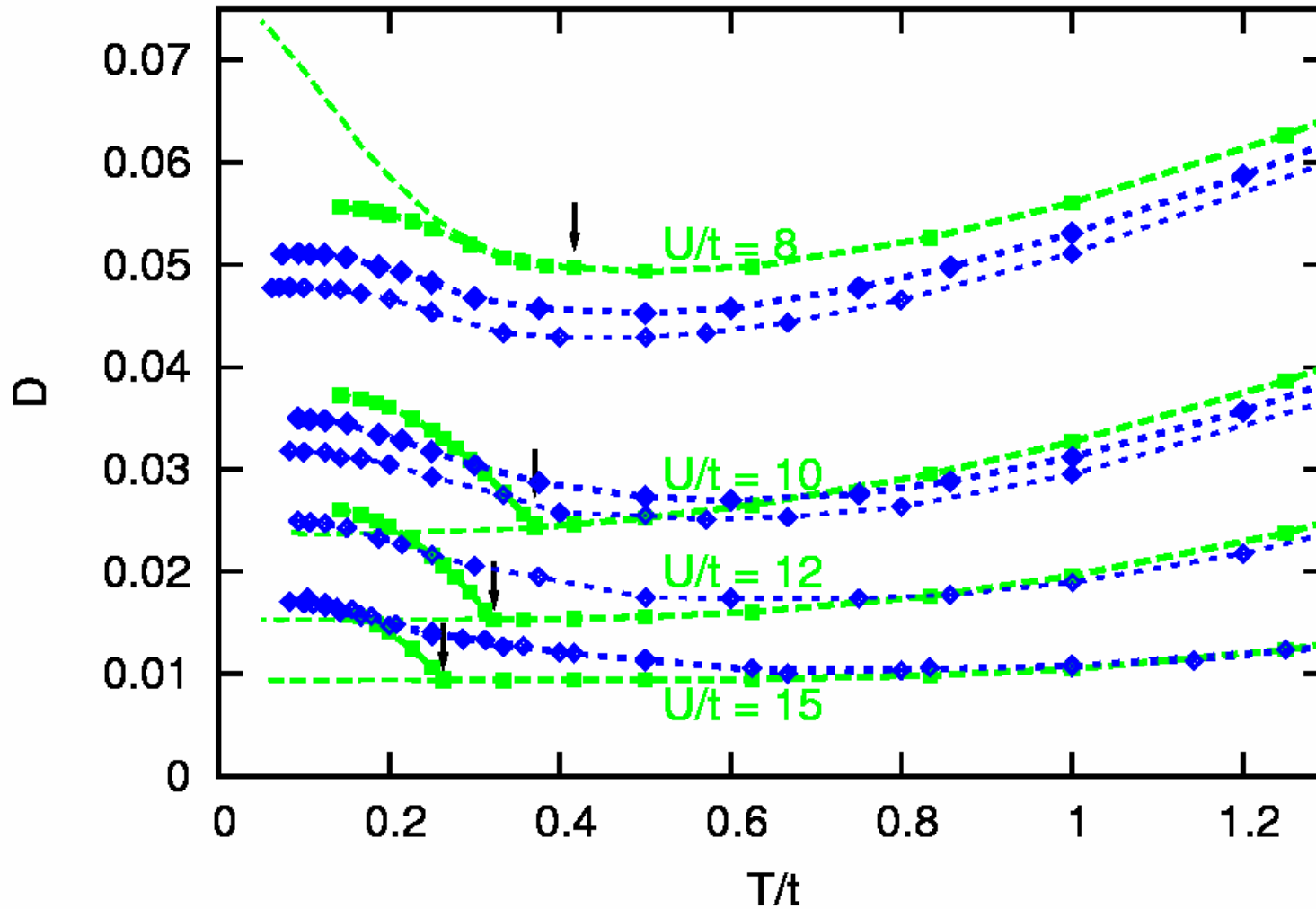


Comparison DMFT – direct QMC for the 2d square lattice



Comparison DMFT – direct QMC for the 2d square lattice

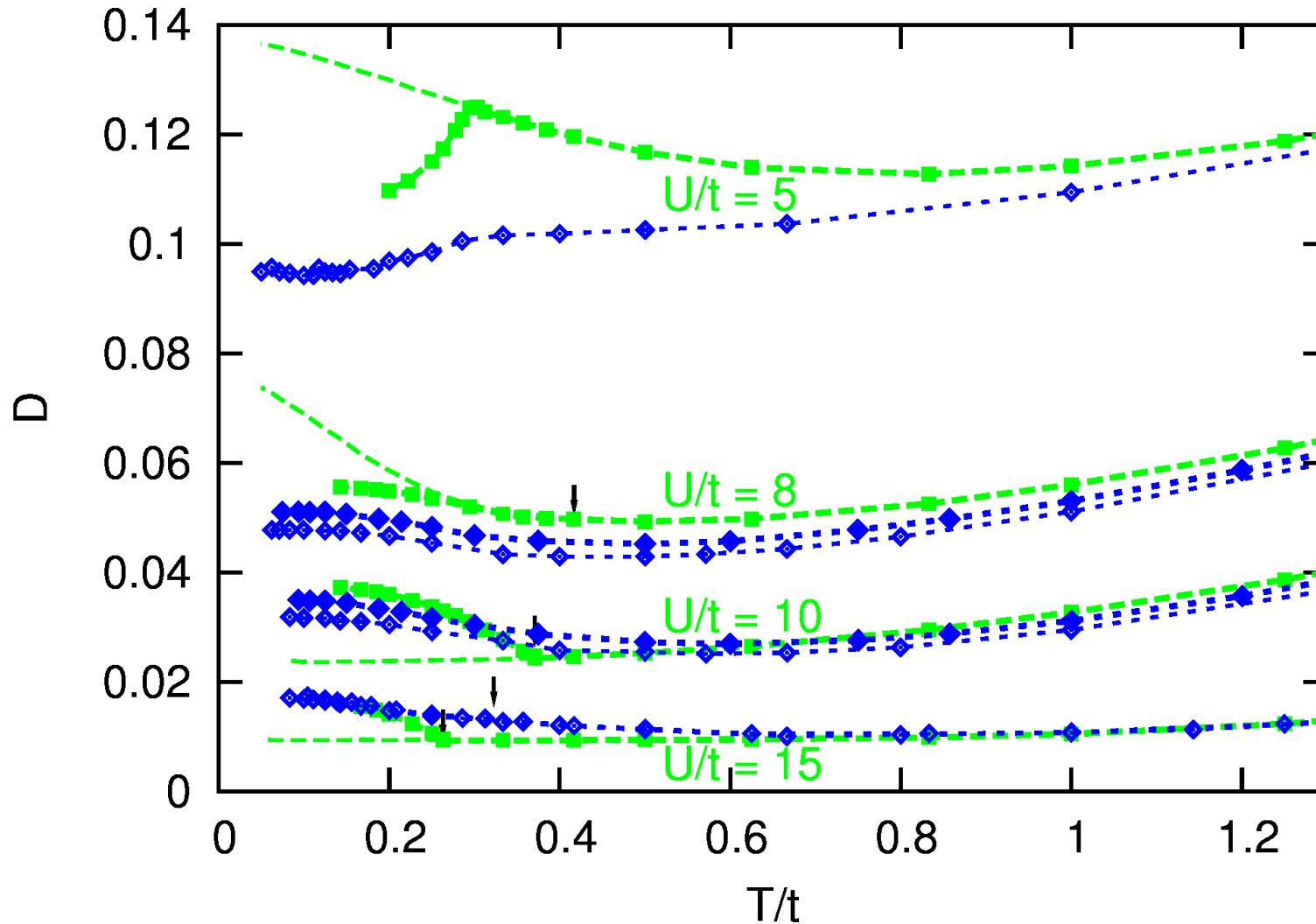




green: DMFT, blue: BSS-QMC (thicker lines: smaller $\Delta\tau$)

excellent agreement at $U = 8$; rounding off at $T \gtrsim T_N^{\text{DMFT}}$ for larger U

Even the low- T suppression of D at small U corresponds with direct QMC:

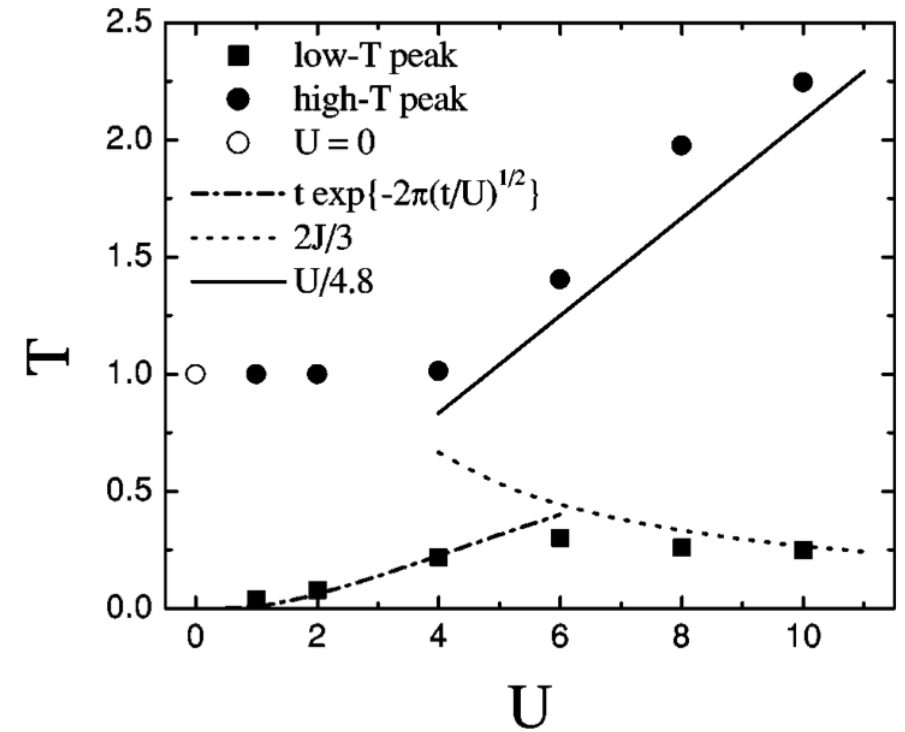
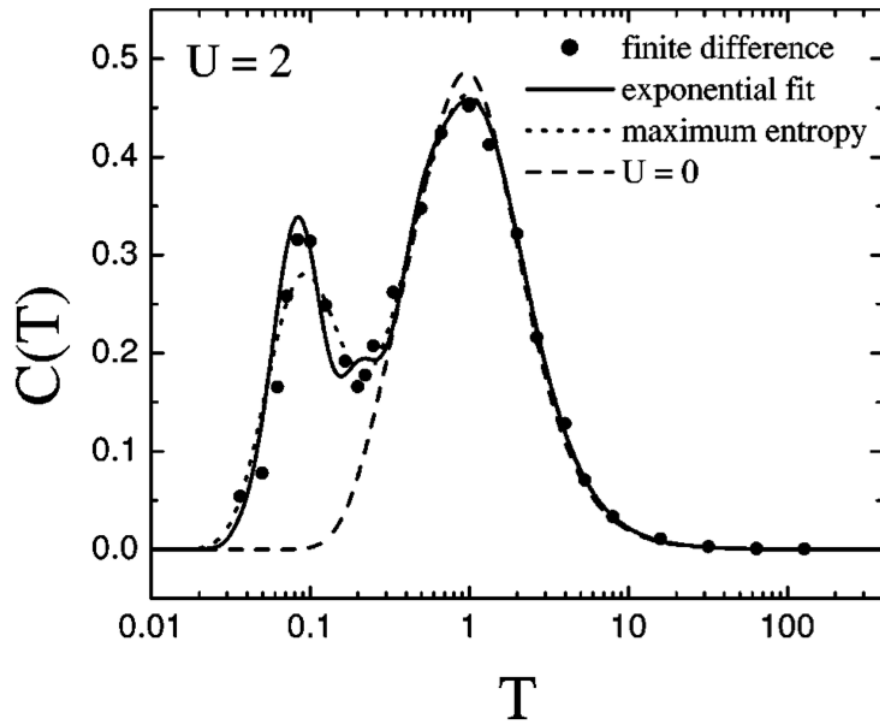


How is this possible? How much better is the agreement in 3 dimensions?

Spin crossover scale in 2 dimensions – definition?

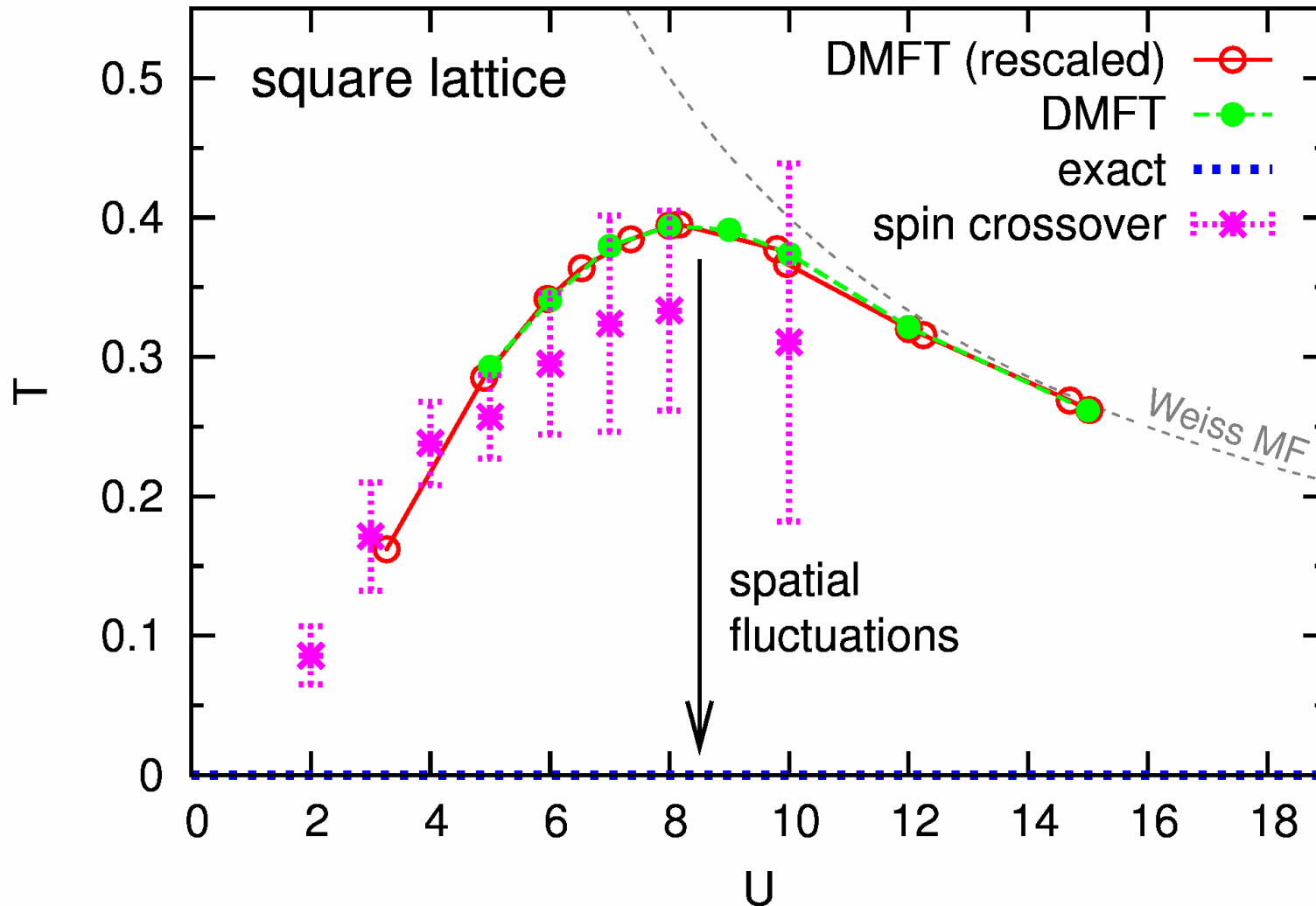
PAIVA, SCALETTAR, HUSCROFT, AND MCMAHAN

PHYSICAL REVIEW B **63** 125116



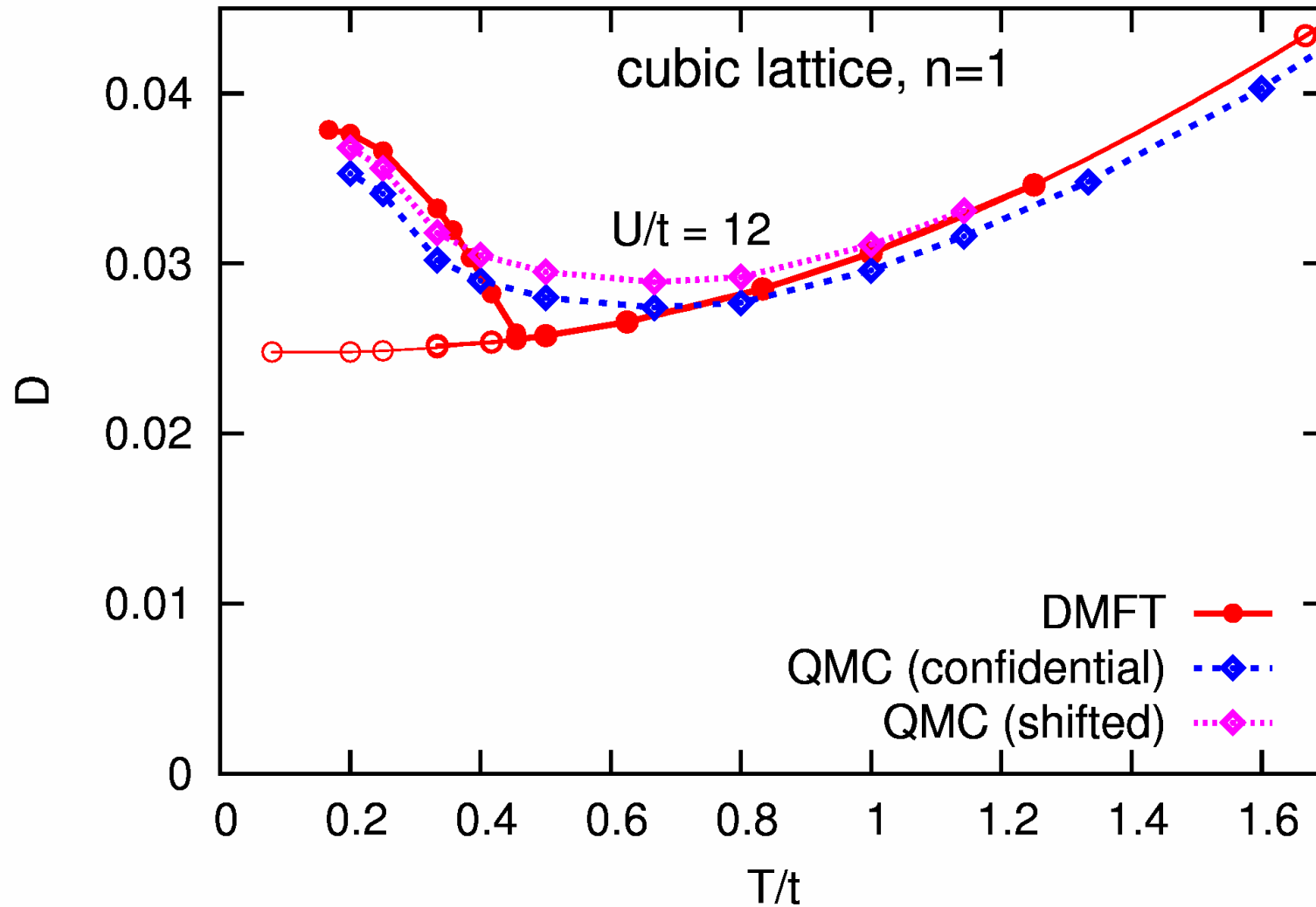
[Paiva, Scalettar, Huscroft, McMahan, PRB (2001)]

Comparison for square lattice: spin crossover temperature vs. T_N^{DMFT}



Nearly perfect agreement!!!

Comparison in 3 dimensions



Summary

Multigrid HF-QMC method: numerically exact (quasi CT) + efficient

Mott transition for 3 degenerate flavors in (U, T, μ) space

Novel semi-compressible phase, spectra, small lattice effects

[E. V. Gorelik, N. Blümer, *Phys. Rev. A* **80**, 051602(R) (2009)]

Real-space DMFT study of antiferromagnetism

Efficient and flexible RDMFT-QMC code

AF order at finite T signaled by enhanced D

Proximity effects important – LDA deficient

[E. V. Gorelik, I. Titvinidze, W. Hofstetter, M. Snoek, N. Blümer, *PRL* **105**, 065301 (2010)]

DMFT surprisingly accurate in low dimensions

Outlook

3D calculations for realistic trap parameters and system sizes

Inequivalent spins/flavors: OSMT-like physics, ordered phases

Multigrid HF-QMC for RDMFT; impact of higher Bloch bands

Outlook

3D calculations for **realistic trap parameters** and system sizes

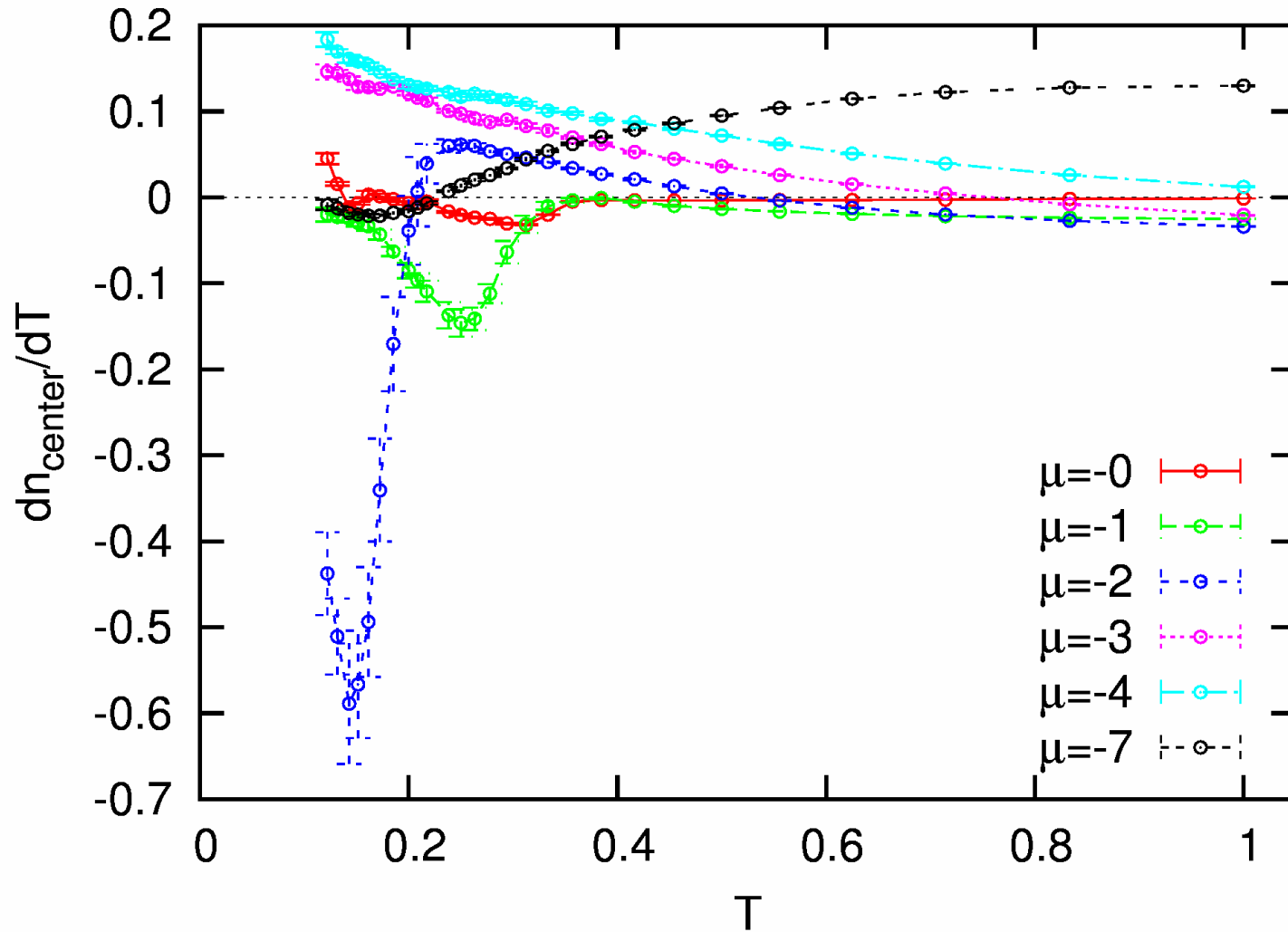
Inequivalent spins/flavors: **OSMT-like physics**, ordered phases

Multigrid HF-QMC for RDMFT; impact of **higher Bloch bands**

Spin-off: **solids with large unit cells** (distortions, surfaces, impurities, . . .)

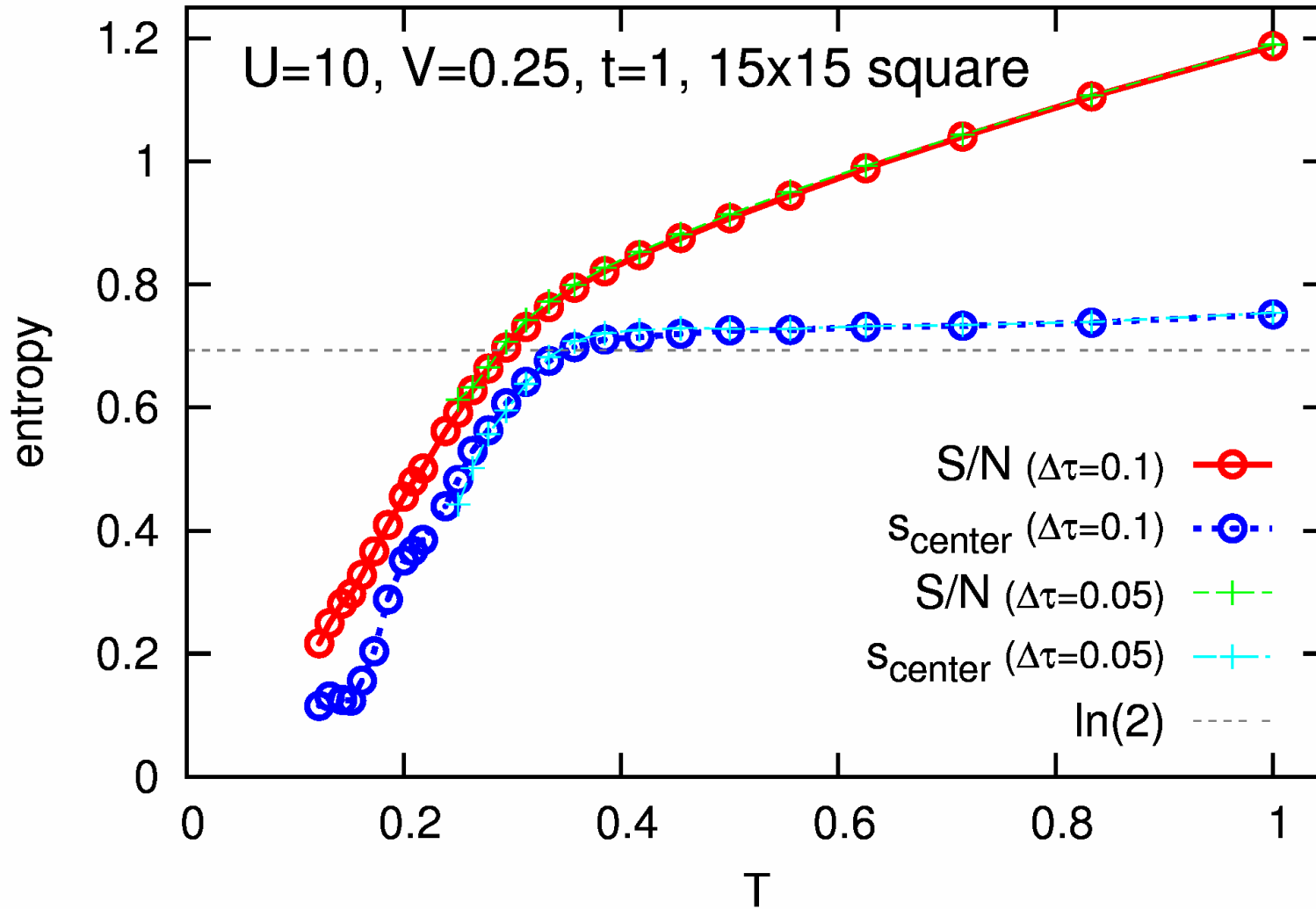
Thanks to: E. Gorelik, I. Titvinidze, W. Hofstetter, M. Snoek,
U. Schneider, I. Bloch, H. Moritz, L. Tarruell,
R. Scalettar, T. Paiva, and DFG (TR49)

Entropy: no direct computation, but from relations such as $dS/d\mu = dN/dT$



Example: derivative of central density (at $U/t = 10$, $V/t = 0.25$) for square lattice

Strong negative peak at Neel temperature (\rightsquigarrow need fine integration grid)



very small discretization dependence

Important: central entropy can be much smaller than average entropy!